Table of Contents

Wifi Access

Wifi will be available to all participants from Sunday March 17 until Saturday March 23 via the network “EPN Visitors”, within the entire EPN Campus.

Login: `ADD2019`
Password: `ADD2019C`

Do not use a proxy, choose Auto Proxy Discovery or equivalent.

Those having and account in the ILL Visitors club can also connect via the ILL Scientific Visitors network with their usual login and password.

Aim, Scope and Format

The ADD2019 School and Conference aim to deepen the understanding and to further the training of the various communities working on real-space data analysis with neutron and X-ray diffraction techniques. The Fourier transformation of diffraction data into real-space, historically used for the structural determination of liquids and glasses, has been in recent years more and more employed in the study of partially disordered crystalline powder samples, and most recently to characterize spin-spin correlations in disordered or frustrated magnetic systems.

The scientific scope of ADD2019 covers both X-ray and neutron diffraction techniques, and will again include single crystal diffuse scattering as an integral part of both the School and the Conference. The School proposes pedagogical lectures on real space data analysis techniques followed by 7 parallel sessions of hands on tutorials for training with various data-modelling software packages: **`DISCUS`**, **`PDFgui`**, **`DiffpyCMI`**, **`EPSR`**, **`Spinvert`**, **`RMCProfile`**, and **`Yell`**. The Conference proposes 8 invited, 16 additional oral contributions, and a poster session.

The Fourier transformation of diffraction data into real space produces a Pair Distribution Function (PDF) that provides a model-independent "snapshot" of the local structure within the sample. The PDF(r) thus probes both static and dynamic atomic correlations (and also magnetic spin-spin correlations in the case of neutron diffraction). PDF analysis techniques are therefore complementary to the well-known Rietveld method of refining diffraction data in Q-space to provide a space-time averaged picture of sample structure. PDF analysis now enjoys a wide range of applications, in particular to nano-structured materials.

Building on the success of our previous ADD workshops in Grenoble (ADD2013 of 18-22 March 2013, ADD2016 of 7-11 March 2016), the ADD2019 School+Conference will start Sunday evening 17 March 2019 and finish Friday afternoon 22 March, with a full 5-day programme that includes 2-1/2 days for the School followed by 2-1/2 days for the Conference, basically the same format as for ADD2016, but with a few additional features.

With respect to ADD2016, the 2019 edition includes 2 additional hands-on tutorials: (1) **`DiffPy-CMI`**: a more flexible and powerful command-line version of **`PDFgui`**. (2) **`Spinvert`**: a Reverse Monte-Carlo program for refining diffuse magnetic neutron scattering data from powdered samples and providing a spin-spin Pair Distribution Function or "magnetic PDF" for the magnetic species.

In addition, ADD2019 features new pedagogical lectures on data-reduction and data-correction techniques to analyse X-ray and neutron scattering from liquids/glasses, disordered crystals and for the analysis of single-crystal diffuse scattering.

Real space analysis of diffraction data deals with general structural concepts such as atomic/spin distribution functions and structural/magnetic correlation lengths, and now employs standard formulae common to neutron, X-ray and other scattering techniques. It therefore facilitates a synergetic convergence of hitherto largely disjoint communities: liquid/glass scattering, crystalline powder diffraction, single-crystal diffuse scattering and diffuse magnetic scattering.

Sponsors


ESRF
The European Synchrotron


NEUTRONS
FOR SOCIETY


Science & Technology Facilities Council
ISIS Neutron and Muon Source


ess
EUROPEAN
SPALLATION
SOURCE


Malvern
Panalytical
a spectris company


DECTRIS
detecting the future


SINE
2020

Programme

Sunday 17 March 2019			
18:00		Beginning of Registration for the School	
19:00		Welcome buffet dinner at the ILL	

Monday 18 March 2019 (School)			
8:00		Registration continues for the School	
		Chairperson	ADD organizer
8:30		**Mark Johnson**	Welcome (school)
8:45		ADD organizer	Introduction and Information
9:00	S01	**Phil Salmon**	PLENARY: Structure of Liquid and Amorphous Materials
10:00		Coffee break	
		Chairperson	ADD organizer
10:30	S02	**Simon Billinge**	PLENARY: Recent and future developments in PDF-land
11:30	S03	**Reinhard Neder**	PLENARY: Single-Crystal Diffuse scattering
12:30		Lunch at canteen	
		Chairperson	ADD organizer
14:00	S04	**Emil Bozin**	PDFgui – a small box modelling platform for nanoscale structure analysis
14:45	S05	**Pavol Juhas**	DiffPy-CMI - a software toolbox for real-space structure analysis and Complex Modeling
15:30		Coffee break	
		Chairperson	ADD organizer
16:00	S06	**Tucker / Playford**	RMCProfile: Local structure of crystalline to amorphous materials
16:45	S07	**Bowron / Youngs**	Empirical Potential Structure Refinement (EPSR): A method for structural modelling of liquids, glasses and complex nanoscale systems
17:30	S08	**Joseph Paddison**	Spinvert: Magnetic structure refinement for paramagnets
18:15		ADD organizer	Organizational information
19:00		Dinner at ESRF/ILL canteen	

Tuesday 19 March 2019 (School)			
8:30		School Registration still possible during the morning, outside the amphitheatre	
		Chairperson	ADD organizer
9:00	S09	**Reinhard Neder**	DISCUS: Simulation and refinement of disordered crystal structures
9:45	S10	**Arkadiy Simonov**	3D-ΔPDF: Pair distribution function analysis for single crystals.
10:30		Coffee break	
		Chairperson	ADD organizer
11:00	S11	**Brunelli/Vaughan**	XRD experimental procedure and data reduction
11:25	S12	**Fischer/Cuello/ISIS**	ND experimental procedure and data reduction
11:50	S13	**R. Neder/et al.**	SCD experimental procedure and data reduction
12:15	S14	**Gwilherm Nénert**	Correction of XRD data from a table-top x-ray source
12:30		Lunch at ESRF/ILL canteen	
14:00			Parallel hands-on tutorials
16:00		Coffee break	
16:30			Parallel hands-on tutorials
18:00		*(free time)*	
19:00		Dinner at ESRF/ILL canteen	

Wednesday 20 March 2019 (School in the morning, Conference in the afternoon)			
8:30			Parallel hands-on sessions tutorials
10:30		Coffee break and beginning of Registration for the Conference	
11:00			Parallel hands-on sessions tutorials
12:30		Lunch at canteen	
		Chairperson	ADD organizer
14:15		**Harald Reichert**	Welcome (conference)
14:30		ADD organizer	Introduction and Information
14:45	I01	**Werner Paulus**	INVITED: Short and long-range structural correlations in non-stoichiometric transition metal oxides, explored by in situ single crystal diffraction
15:30		Coffee break	
		Chairperson	ADD organizer
16:00	I02	**Joseph Paddison**	INVITED: Understanding spin liquids at the nanoscale
16:45	O01	**Philip Welch**	Magnetic diffuse scattering in the Gd-pyrochlore antiferromagnet - $Gd_2Pt_2O_7$
17:10	O02	**Nikolaj Roth**	Three-dimensional magnetic difference pair distribution function analysis of single crystal diffuse neutron scattering from frustrated magnets
17:35	O03	**Ella Mara Schmidt**	The interpretation of broad diffuse maxima using superspace crystallography
18:00		Poster session - Wine and Cheese buffet at the ILL	

Thursday 21 March 2019 (Conference)			
		Chairperson	ADD organizer
8:30	I03	**James Drewitt**	INVITED: Structure of glass-forming aluminate liquids under extreme conditions by neutron diffraction with isotope substitution
9:15	O04	**Stefano Checchia**	Highly polymerized carbonate glass at ultrahigh pressure: insights into the structure of carbonatitic melts at extreme conditions
9:40	O05	**Gaston Garbarino**	Structure of low Z liquids under extreme conditions using X-rays: from dream to reality
10:05	O06	**Anne Stunault**	D3 at the ILL: structural studies of hydrogenous liquid and amorphous systems using polarised neutrons
10:30		Coffee break	
		Chairperson	ADD organizer
10:55	I04	**Pierre Bordet**	INVITED: X-ray PDF investigations of complex metal-organic materials.
11:40	O07	**Emil Bozin**	Phase separation at the dimer-superconductor transition in $Ir_{1-x}Rh_xTe_2$
12:05	O08	**Jakub Drnec**	Wide angle x-ray scattering combined with pair distribution function analysis of pyrolyzed wood
12:30		Lunch at ESRF/ILL canteen	
		Chairperson	ADD organizer
13:55	I05	**Lionel Desgranges**	INVITED: A renewed approach of UO_2 nuclear fuel using PDF analysis
14:40	O09	**Ben Frandsen**	Nanoscale degeneracy lifting in triangular antiferromagnets studied by combined PDF + mPDF
15:05	O10	**Navid Qureshi**	Magnetic frustration in SrLn2O4 compounds studied via mPDF-analysis
15:30		Coffee break	
		Chairperson	ADD organizer
16:00	I06	**Anita Zeidler**	INVITED: The structure of water
16:45	O11	**Sabrina Thomä**	Solvent restructuring around iron oxide nanoparticles
17:10	O12	**Harry Geddes**	Quantitative Analysis of Complex Materials Using Non-Negative Matrix Factorisation of PDF Data
17:35		Poster session	
19:00		Bus to restaurant	
19:30		Conference dinner	

Friday 22 March 2019 (Conference)			
		Chairperson	ADD organizer
8:55	I07	**David Wragg**	INVITED: PDF Analysis of Batteries Using Diffraction Computed Tomography
9:40	O13	**Ann-Christin Dippel**	Grazing incidence PDF for real time studies of thin films
10:05	O14	**Olivier Masson**	Avoiding the Warren, Krutter and Morningstar approximation in PDF analysis
10:30		Coffee break	
		Chairperson	ADD organizer
11:00	I08	**Kirsten Jensen**	INVITED: New nanostructures from X-ray total scattering and PDF analysis
11:45	O15	**Mikkel Juelsholt**	Mechanisms for tungsten oxide nanoparticle formation in solvothermal synthesis: From polyoxometalates to crystalline materials
12:10	O16	**Archana Munirathnappa**	Average and Local Structure of $NaCe(WO_4)_2$ Nanophosphor: A Structure-Property Correlation
12:35		Lunch at ESRF/ILL canteen	
14:00		**Robert McGreevy**: To model or not to model – is that the question? *(College 6 seminar in Chadwick amphitheatre)*	
15:00		Final discussion and closing	
16:00		Visit of ILL instruments (if permitted by safety authorities)	

Lectures

Structure of Liquid and Amorphous Materials: An Approach using Pair-Distribution Functions

Philip S. Salmon[1]
[1]Department of Physics, University of Bath, Bath BA2 7AY

It is necessary to know the atomic-scale structure of a liquid or glass in order to understand its material properties. Liquids and glasses are, however, structurally disordered, i.e., there is an absence of translational periodicity that leads to Bragg peaks in the diffraction pattern for a crystal. Instead, the diffraction pattern for a liquid or glass is diffuse (Fig. 1), and it is a challenge to solve the structure.

In this talk I will outline the theory that is necessary to understand the X-ray and neutron diffraction patterns that are measured for structurally disordered materials, and show how they can be used to obtain real-space structural information in the form of partial pair-distribution functions $g_{\alpha\beta}(r)$ [1, 2]. Attention will be paid to multi-component systems, where overlap of the pair-correlation functions means that it is not possible to obtain all of the individual $g_{\alpha\beta}(r)$ from a single diffraction experiment.

In favourable cases, however, the individual $g_{\alpha\beta}(r)$ functions can be measured by using multi-pattern techniques that include (i) neutron diffraction with isotope substitution (NDIS), (ii) anomalous X-ray diffraction (AXD), and (iii) a combination of X-ray and neutron diffraction. These methods will be illustrated by case studies taken from recent work using instrumentation at central neutron and X-ray sources. It is necesary to perform these experiments with care in order to obtain reliable results.

Finally, I will introduce the ideas behind structural refinement techniques such as reverse Monte Carlo (RMC) and empirical potential structure refinement (EPSR), where measured diffraction patterns are used in the construction of atomistic models.

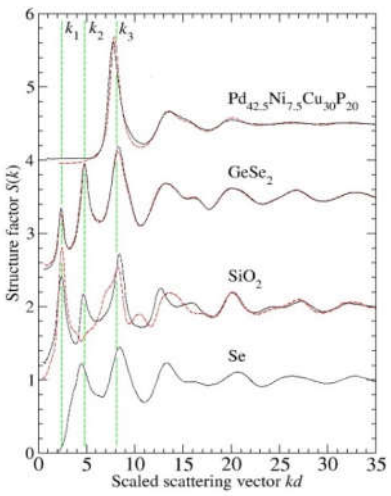

Figure 1: Representative structure factors $S(k)$ for metallic, network-forming and elemental glasses, plotted in terms of the scaled scattering vector kd, where d is the nearest-neighbour real-space distance. The functions were measured by using either neutron (solid curves) or X-ray (broken curves) diffraction. The peaks at k_1, k_2 and k_3 are associated with real-space ordering on different length scales [3].

[1] H. E. Fischer, A. C. Barnes and P. S. Salmon, *Rep. Prog. Phys.* **69** (2006), 233.
[2] P. S. Salmon and A. Zeidler, *J. Phys.: Condens. Matter* **27** (2015), 133201.
[3] A. Zeidler and P. S. Salmon, *Phys. Rev. B* **93** (2016), 214204

Corresponding author: p.s.salmon@bath.ac.uk

Recent and future developments in PDF-land

Simon J. L. Billinge[1,2]
[1]Department of Applied Physics and Applied Mathematics, Columbia University, New York, NY10027
[2]Condensed Matter Physics and Materials Science Department, Brookhaven National Laboratory, Upton, NY 11973

The atomic pair distribution function (PDF) method is becoming more widely used, and more widely known. There are recently emerging powerful experimental developments related to PDF and total-scattering studies. At this workshop you will learn in detail about carrying out and applying PDF to your own scientific research, and there will be excellent tutorial talks on this. Therefore, in this talk I will focus on recent technological and methodological developments, and some that are in the pipeline, that are allowing ever richer science to be done. These approaches can yield quantitative information such as thermodynamic parameters that help us to understand function even in working devices, as well as to study failure of the devices. These will include recent applications of PDF to scientific problems anabled by the new developments. I will also describe recent and upcoming developments in PDF analysis and modeling software that are under development in the group.

Corresponding author: sb2896@columbia.edu

Single Crystal Diffuse Scattering

R.B. Neder[1]
[1]Kristallographie und Strukturphysik, Friedrich-Alexander-Universität Erlangen-Nürnberg, Staudtstr. 3, 91058 Erlangen, Germany

Diffuse scattering has been observed for almost as long as any single crystal diffraction, see [1] for a recent review on the subject. Further reviews are found for example in [2-7] and references therein. Diffuse scattering is observed for all classes of crystalline materials, metal alloys, simple inorganic materials, quaiscrystals, molecular structures including protein crystals.

The intensity of the Bragg reflections describes the crystal structure very well with one important limitation. To the Bragg reflections all unit cells look alike. The Bragg reflections thus contain information on the average structure only. Any difference between the unit cells manifests itself in additional, usually weak diffuse scattering between the Bragg reflections. The diffuse scattering may be an almost featureless background or show a pattern of intricate complexity and may consist of streaks, layers, broad peaks or even curved distributions. The origin of the structural deviations may be due to dynamic effects such as the thermal movement of atoms or due to static effects. The first effect is commonly termed thermal diffuse scattering, while the second effect is referred to as disorder diffuse scattering.

The static deviations from the average structure can have many different reasons and may be present at different dimensions within the crystal. The deviations may be something as simple as a distribution of two or more atom types at a single site within the unit cell. Very often these local replacements cause a slight static shift of the surrounding atoms and these may be described as small clusters of slightly different structure. In a molecular structure the simplest defects might be a molecule in a slightly different conformation. From these simple defects one can consider a continuous and gradual change to larger objects such as domains with slightly different order or actual disolutions of a guest phase in the host crystal. Other defect types may disrupt the strict periodicity of the crystal on a larger scale such as stacking faults. Commonly the periodicity is maintained within the layers but the layer sequence deviates from a strictly periodic sequence.

Somewhat independent of the actual defect type, we need to consider the distribution of the defects throughout the host structure. Many times the defects are not randomly distributed and the correlations between neighboring defects introduce structure into the diffuse scattering.

In this lecture an overview of defect types, the arrangement of defects and the corresponding diffuse scattering is given. The lecture will describes current measurement, analysis and modelling techniques.

[1] T.R. Welberry, T. Weber, *Crystallography Reviews* **22** (2015).
[2] B.T.M. Willis, H. Jagodzinski, F. Frey, J.M. Cowley, J. Gjonnes, P.S. Pershan in *Int. Tables for Crystallography Vol B*, U. Shmueli (Ed.), IUCR (1993), 383.
[3] W. Schweika, *Disordered Alloys*, Springer (1998)
[4] V.M. Nield, D.A. Keen, *Diffuse Neutron Scattering from Crystalline Materials*, Oxford University Press (2001).
[5] T.R. Welberry, *Diffuse X-Ray Scattering and Moldes of Disorder*, Oxford University Press (2004)
[6] R.B. Neder, T. Proffen, *Diffuse Scattering and Defect Structure Simulation*, Oxford University Press (2008)
[7] T.R. Welberry, D.J. Goossens., *IUCr J.* **1** (2014) 550

Corresponding author: reinhard.neder@fau.de

PDFgui – a small box modelling platform for nanoscale structure analysis

Emil S. Bozin[1]
[1]Condensed Matter Physics and Materials Science Department, Brookhaven National Laboratory

PDFgui is a small box nanostructure modeling environment that has been used by the total scattering community for over a decade, both as an introductory tool for the novices in the field and as a workhorse of the PDF analysis, and in these regards has achieved a great success. It is a user friendly interface to PDFfit2 structure modeling software, used in analysis of X-ray and neutron powder diffraction based pair distribution function data of crystalline and nanocrystalline materials. PDFfit2 is a program as well as a library for real-space refinement of crystal structures. It is capable of fitting a theoretical three-dimensional (3D) structure to atomic pair distribution function data and is ideal for nanoscale investigations. The fit system accounts for lattice constants, atomic positions and anisotropic atomic displacement parameters, correlated atomic motion, and experimental factors that may affect the data. The atomic positions and thermal coefficients can be constrained to follow the symmetry requirements of an arbitrary space group. The PDFfit2 engine is written in C++ and is accessible via Python, allowing it to inter-operate with other Python programs. PDFgui is a graphical interface built on the PDFfit2 engine [1]. PDFgui organizes fits and simplifies many data analysis tasks, such as configuring and plotting multiple fits. PDFfit2 and PDFgui are freely available via the Internet [2]. This talk aims to illustrate the PDFgui characteristics and layout, as well as to provide an overview of its capabilities. The types of parameters, basic functionality, and predefined macros designed for targeted modeling strategies will be discussed. Both the advantages and the limitations will be addressed from the task complexity standpoint as encountered in typical nanostructure problems. Time permitting, central features and the simplicity of use will be demonstrated live on a standard material system example. During the followup tutoroal sessions dedicated to PDFgui operational details will be covered. The focus will be placed on participant‘s in-depth familiarization of the software capabilities through hands-on examples on systems chosen to highl specific aspects of the PDFgui functionality.

[1] C. L. Farrow, P. Juhás, J. W. Liu, D. Bryndin, E. S. Bozin, J. Bloch, Th. Proffen and S. J. L. Billinge, J. Phys.: Condens. Matter **19** (2007) 335219.
[2] PROGRAM is available on https://www.diffpy.org/products/pdfgui.html

Corresponding author: bozin@bnl.gov

DiffPy-CMI - a software toolbox for real-space structure analysis and Complex Modeling

P. Juhás[1], S. J. L. Billinge[2,3]
[1]Computational Science Initiative, Brookhaven National Laboratory, Upton, NY 11973, USA
[2]Condensed Matter Physics and Materials Sci. Department, Brookhaven National Laboratory, Upton, NY 11973, USA
[3]Department of Applied Physics and Applied Mathematics, Columbia University, New York, NY 10027, USA

This presentation and the associated hands-on tutorial will introduce DiffPy-CMI, a software for structure analysis from experimental atomic Pair Distribution Function (PDF) and for Complex Modeling [1, 2]. DiffPy-CMI (Complex Modeling Infrastructure) has been developed to handle ill-posed inverse problems, where diffraction experiments do not provide enough signal to determine complicated structures or nanostructures. To overcome this problem, we use Complex Modeling approach [3] which combines additional experimental or theoretical inputs and uses them all together in a common optimization routine. DiffPy-CMI provides a flexible and extensible software required for creating such models tailored for the specific knowledge about studied material. DiffPy-CMI runs on Linux and Mac operating systems and is primarily written in Python with computationally intense parts coded in C++. In a big picture DiffPy-CMI provides several ways of representing atomic structures, a set of forward calculators (e.g., PDF, bond valence sums, powder and single crystal diffraction), and finally a fit-manager to define and run multi-input refinements. The fits can be conducted with short Python scripts or within the Jupyter Notebook interactive environment. In addition to Complex Modeling, DiffPy-CMI also enables more subtle PDF refinements which are not possible in PDFgui [4] - for example PDF fits of non-periodic small clusters or of molecular crystals with rigid structure units. The software provides access to internal simulation routines, which can be tweaked or extended, and thus permits rapid implementation of new ideas and more accurate models. We will demonstrate the capabilities of DiffPy-CMI on a series of science cases, starting from simple forward calculations and following up with PDF fitting examples that go beyond PDFgui. The examples will also include multi-probe structure refinements, such as from PDF and bond valence sums data and from PDF and small angle scattering.

[1] P. Juhás, et al., *Acta Crystallogr. A* **71** (2015), 562-568.
[2] DiffPy-CMI is available at https://www.diffpy.org.
[3] S. J. L. Billinge, I. Levin, *Science* **316** (2007), 561-565.
[4] C. L. Farrow et al., *J. Phys: Condens. Mat.* **19** (2015), 335219.

Corresponding author: pjuhas@bnl.gov

RMCProfile: Local structure of crystalline to amorphous materials

M. G. Tucker[1] & H. Playford[2]
[1]Diffraction Group, Neutron Sciences Division, Oak Ridge National Laboratory, Tennessee, USA
[2]ISIS Facility, Rutherford Appleton Laboratory, Harwell Oxford, Didcot, Oxfordshire, OX11 0QX, U.K

Many of the useful materials that make modern life possible are crystalline. Quartz keeps our watches on time, perovskites are widely used in consumer electronics and solid oxide fuel cells may help to power the future.

The importance of local structure and disorder in crystalline materials is being recognised more and more as a key property of many functional materials. From negative thermal expansion to solid state amorphisation and the 'nanoscale' problem to improved fuel cell technology, a clear picture of the local atomic structure is essential to understanding these phenomena and solving the associated problems.

Total scattering, an extension of the powder diffraction method, is increasingly being used to study crystalline materials. The unique combination of Bragg and diffuse scattering can be used to determine both the average structure and the short-range fluctuations from this average within a single experiment. To maximise the structural information from such data, three-dimensional atomic models consistent with all aspects of the data are required.

RMCProfile [1] expands the reverse Monte Carlo (RMC) modelling technique [2] to take explicit account of the Bragg intensity profile from crystalline materials. Analysis of the RMCProfile-generated atomic models gives more detailed information than is available directly from the data alone. We will give several examples where RMCProfile has been used to successfully study the structure and disorder of crystalline materials to illustrate its potential. Also, since the original RMC technique was designed to study amorphous materials, we will give examples where RMCProfile has been used to model amorphous structures that derive from crystalline materials.

[1] see www.rmcprofile.org; M G Tucker, D A Keen, M T Dove, A L Goodwin and Q Hui, *J. Phys. Condens. Matter* **19** (2007) 335218
[2] R L McGreevy and L Pusztai, *Mol. Simul.* **1** (1988) 359

Corresponding authors: tuckermg@ornl.gov & helen.playford@stfc.ac.uk

Empirical Potential Structure Refinement (EPSR): A method for structural modelling of liquids, glasses and complex nanoscale systems

D.T.Bowron and T.G.A. Youngs
ISIS Neutron and Muon Facility, UKRI Science and Technology Facilities Council,
Rutherford Appleton Laboratory, Chilton, Didcot, OX11 0QX, UK

Empirical Potential Structure Refinement (EPSR) is a Monte Carlo computer simulation method which attempts to build, from X-ray and neutron scattering data, three-dimensional atomistic models of glasses, liquids, and disordered or partly crystalline heterogeneous systems [1-3]. The method uses a "reference potential" (RP), which can often be obtained from literature simulations of the material in question, or else can be invented by the user to incorporate prior information, such as dispersion forces, Coulomb forces, expected minimum atom overlap distances, etc. Typical moves include molecule translations and rotations, as well as individual atom moves and, where required, rotations of side-chains about specified bonds, within molecules. In the more recent versions of EPSR the latter rotations can be constrained against specified dihedral angles as required to preserve molecular conformation. Facilities are available within the program to build atomic and small molecule systems, long chain molecules such as polymers, as well as complex heterogeneous systems, such as molecular fluids confined in nanoporous crystalline or amorphous media. Models can scale from approximately a few thousand atoms to approximately one hundred thousand atoms. The method readily incorporates both neutron and X-ray scattering data, and has in the past been used, via the RP, to refine structures against EXAFS data. Examples of this work will be included in the talk.

It is important to realize that methods using Monte Carlo approaches to interpret diffraction data, frequently demonstrate that there is not always a single atomic structure which is compatible with a set of such data. This arises because in most instances, and even when different isotope and/or X-ray data are available as additional constraints, the number of site-site correlations needed to define the structure far outweighs the number of unique datasets available. In addition some site-site terms are strongly weighted in the data, while others may have only a weak weighting. Additionally, scattering data are never perfect: the process of measuring them inevitably involves some degree of approximation in correcting for backgrounds and other scattering contributions, as well as data normalisation. Finally, for molecular systems, a complete solution will never be possible, even in principle, because the scattering experiment necessarily cannot provide complete information on the orientational structure between pairs of molecules. Hence, rather than attempting to provide a single answer to the question "what is the structure of this material?", EPSR should be regarded as a vehicle for investigating the range of **possible** structures that are compatible with a set of scattering data. In EPSR the data are introduced into the simulation via an "empirical potential" (EP) which is derived from the difference between simulation and data. The weighting of different datasets in estimating this potential can be varied, as can its overall amplitude. These features, combined with the ability to tune the reference potential, give the user the opportunity to explore possible structures while retaining an acceptable degree of physicality in the outcome.

The latest version of EPSR (EPSR25) and associated GUI is available as a download from this website [4]. Windows, OS X, and Linux operating systems are all accommodated. For the latter two operating systems a working gfortran compiler is also required. Graphics are provided by the freely available Gnuplot suite, and Java is also required for some graphical capabilities.

[1] A. K. Soper, *Chem. Phys.* **202**, 295-306 (1996)
[2] A. K. Soper, *Physical Review B*, **72**, 104204 (2005)
[3] A. K. Soper *J. Phys. Condens. Matt.* **19**, 335206 (2007)
[4] https://www.isis.stfc.ac.uk/Pages/Empirical-Potential-Structure-Refinement.aspx

Corresponding author: daniel.bowron@stfc.ac.uk

Spinvert: Magnetic structure refinement for paramagnets

J. A. M. Paddison[1,2,3], J. R. Stewart[4], A. L. Goodwin[5]
[1]Churchill College, University of Cambridge, Cambridge CB3 0DS, UK
[2]Cavendish Laboratory, University of Cambridge, Cambridge CB3 0HE, UK
[3]School of Physics, Georgia Institute of Technology, Atlanta, GA, USA
[4]ISIS Neutron and Muon Source, STFC Rutherford Appleton Laboratory, Didcot, UK
[5]Department of Chemistry, University of Oxford, Oxford, UK

I introduce the program Spinvert [1], which uses a reverse Monte Carlo algorithm to refine spin configurations to the magnetic component of diffuse neutron-scattering data. Spinvert is designed to be useful for magnetically-disordered materials including frustrated magnets, spin liquids, and spin glasses. I present several examples to demonstrate the capabilities of the suite of programs included with Spinvert: fitting to powder and/or single-crystal diffuse-scattering datasets [2], predicting single-crystal diffuse-scattering patterns given powder data [3], and analysing refined spin configurations in real space, providing access to single-ion spin anisotropies and spin-pair correlation functions.

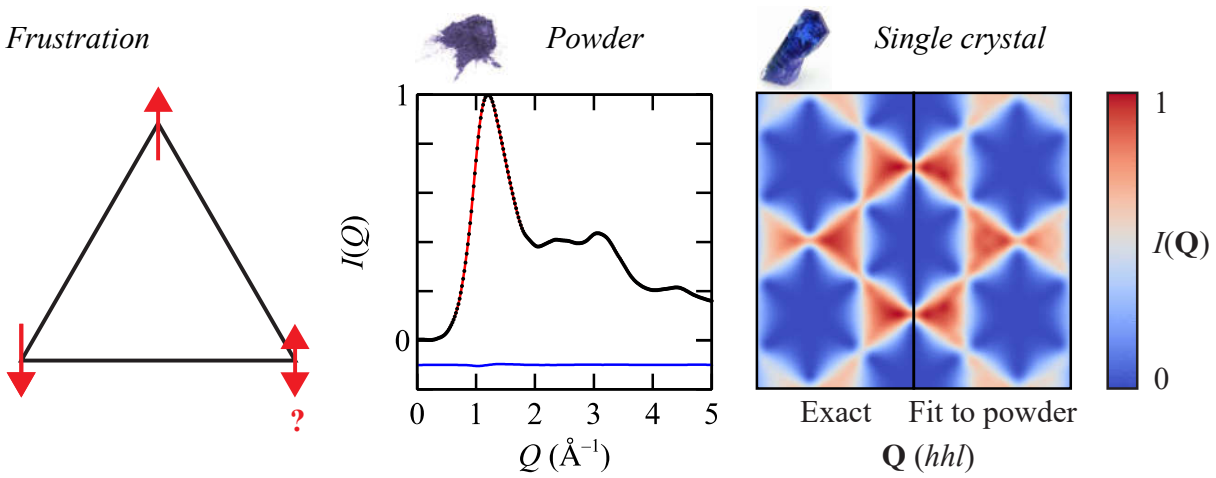

Figure 1: (Left) Example of magnetic frustration: three vectors on a triangle cannot be mutually opposite. (Right) Spinvert refinement to powder neutron-scattering data for a frustrated system allows the single-crystal magnetic scattering pattern to be reconstructed (figure based on Ref. 3).

[1] J. A. M. Paddison, J. R. Stewart and A. L. Goodwin, *J. Phys.: Condens. Matter* **25** (2013), 454220.
[2] J. A. M. Paddison, M. J. Gutmann, J. R. Stewart, *et al.*, *Phys. Rev. B* **97** (2018), 014429.
[3] J. A. M. Paddison and A. L. Goodwin, *Phys. Rev. Lett.* **108** (2012), 017204.

Corresponding author: jamp3@cam.ac.uk

DISCUS, Simulation and refinement of disordered crystal structures

R.B. Neder
Kristallographie und Strukturphysik, Friedrich-Alexander-Universität Erlangen-Nürnberg, Staudtstr. 3, 91058 Erlangen, Germany

DISCUS is a program that can simulate crystal structures and can calculate the corresponding diffraction pattern[1]. Its scope includes the possibility to simulate perfect crystal structures, as well as disordered structures. The program includes several toolboxes to introduce defects into the crystal structure. The strength of the program is the nearly unlimited flexibility that it offers to the user. One can use the program to simulate individual atoms, molecules, small clusters, finite sized nanoparticles or crystals that are essentially infinite in size. Into each of these structures many different defects can be introduced via a set of tools integrated into the program. By combining several of these tools, the final structure could be a crystal that still has an average periodic crystal structure, or a complex core/shell nanoparticles as well as a glass like structure without periodicity.

The tools to create disorder include basic options like the manipulation of individual atoms and extended tools to manipulate the crystal at large. These tools include short range order concepts to distribute different atom species or to distribute displacement correlations throughout the crystal. Empirical potential functions allow to introduce local distortions to the structure. Another tool builds stacking faults. These can be created as growth faults or use a short range order mechanism to build faults with more complex layer sequences. A new companion program allows the use of abstract generators to create essentially any stacking fault sequence. DISCUS uses an abstract domain concept to incorporate defects into a host structure. These defects might be anything from an individual atom, a small cluster, a guest crystal with regular or irregular internal host-guest surface or a set of molecules on top of a surface. The domains themselves may be subject to a short range order distribution. Finally, modulated structures can be simulated with the use of displacement or density waves. To build finite crystals, options exist to create crystals limited by a suitable surface.

DISCUS calculates single crystal diffraction pattern of as well as powder diffraction pattern and the pair distribution function (PDF).

The DISCUS program suite [2] includes a generic optimizer program DIFFEV. The DIFFEV program is used in combination with DISCUS to refine disordered crystal structures with respect to experimental data. All programs of the DISCUS suite are available for Linux, Mac and Windows. The DIFFEV programm includes an MPICH option to allow fast parallel refinement on multiple core architectures or supercomputer frames.

A set of interactive teaching pages is available to introduce disorder diffraction concepts [3].

Figure 1: Example of a gold nanoparticle simulated by DISCUS. The particle is shaped as cubeoctahedron and decorated by fluorinated thiooctane molecules [4].

[1] R.B. Neder, T. Proffen, *Diffuse Scattering and Defect Structure Simulation*, Oxford University Press (2008)
[2] DISCUS is available on https://github.com/tproffen/DiffuseCode
[7] DISCUS Teaching pages available on https://www.icsp.nat.fau.eu/neder-group/ (Under revision)
[4] K. Page, T.C. Hood, Th. Proffen, R.B. Neder, J. Appl. Cryst., **44**, (2011), 327.

Corresponding author: reinhard.neder@fau.de

3D-ΔPDF: Pair distribution function analysis for single crystals.

A. Simonov
Kristallographie, Institut für Geo- und Umweltnaturwissenschaften, University of Freiburg, Germany

In this tutorial we will present the method for analyzing diffuse scattering from single crystals. The method is an extension of the popular powder Pair Distribution Function method and allows to understand the local order in disordered single crystals. The analysis is simple and is performed in real space, it does not require explicit building of models like in the case Monte-Carlo methods.

During the course of this lecture I will present the basics of the three dimensional difference pair distribution function method (3D-ΔPDF), and introduce its application in the program YELL.

[1] T. Weber, A. Simonov *Z. Krist* 227.5 (2012): 238-247.
[2] PROGRAM is available on https://github.com/YellProgram/Yell/releases
[3] Visualization software is available on https://github.com/aglie/DensityViewer/releases

Corresponding author: arkadiy.simonov@krist.uni-freiburg.de

Invited Talks

Short and long-range structural correlations in non-stoichiometric transition metal oxides, explored by in situ single crystal diffraction

W. Paulus
Institut Charles Gerhardt, ICGM, UMR 5253, CNRS-UM-ENSCM, Univ. Montpellier, France,

Transition metal oxides are an important class of compounds showing interesting properties of academic and applied interest. Non-stoichiometric oxides present a special case, as they can undergo important variations of oxygen stoichiometry, enabling to tune physical and chemical properties. Combining neutron diffraction, inelastic neutron scattering and ab initio lattice dynamics calculations, we have recently evidenced the importance of lattice dynamics, i.e. soft phonon modes, triggering low temperature oxygen mobility in Brownmillerite type $(Ca/Sr)(Fe/Co)O_{2.5}$, as well as Ruddlesden Popper type oxides, e.g. $La_2CuO_{4.07}$ and $(Nd/Pr)_2NiO_{4+\delta}$ [1-3]. This new concept, explaining why oxygen ions can diffuse in stoichiometric quantities already at ambient temperature, has technological relevance e.g. for optimization of oxygen membranes and electrolytes for sensors or membranes in SOFCs.

Low temperature reactivity of solids may thus be used as a concept, to investigate the structural complexity in transition metal oxides. The reaction pathway to insert oxygen at low temperatures in solid oxides becomes a decisive parameter to tune correlations, leading to extremely complex phase relations as physical and structural properties are not only depending on the overall stoichiometry, but on the sample history. Taking these oxides as oxygen 'sponges' operating at low reaction temperatures down to ambient, structural and electronic correlation lengths could then be influenced by the reaction conditions and kinetics.

We discuss here solid-state reaction mechanisms, associated with complex oxygen and domain ordering phenomena during oxygen uptake or release reactions in non-stoichiometric oxides with Brownmillerite and K_2NiF_4 type frameworks, essentially explored in situ by neutron scattering and synchrotron radiation using single crystals [4-5]. Following up chemical solid-state reactions on single crystals presents a powerful tool, allowing to scan the whole reciprocal lattice and to obtain valuable information about diffuse scattering, weak superstructure reflections, as well as information about possible twin domains associated to changes in the symmetry during of different domains during the reaction, which are impossible to access by powder diffraction.

[1] Paulus, W., et al., Lattice Dynamics To Trigger Low Temperature Oxygen Mobility in Solid Oxide Ion Conductors. *J. Am. Chem. Soc, 2008.* ***130****(47): p. 16080-16085.*
[2] M. Ceretti et al. Low temperature oxygen diffusion mechanisms in $Nd_2NiO_{4+\delta}$ and $Pr_2NiO_{4+\delta}$ via large anharmonic displacements, explored by single crystal neutron diffraction, *J. Mater. Chem. A, 3, 42 (2015) p21140-48.*
[3] Perrichon, A., et al., Lattice Dynamics Modified by Excess Oxygen in Nd_2NiO_{4+d}: Triggering Low-Temperature Oxygen Diffusion, *J. Phys. Chem. C, 2015. 119(3): p. 1557-1564.*
[4] A. Maity et al., Solid-state reactivity explored in situ by synchrotron radiation on single crystals: from $SrFeO_{2.5}$ to $SrFeO_3$ via electrochemical oxygen intercalation, *J. Phys. D: Appl. Phys. 48 (2015)*
[5] M. Ceretti et al., $(Nd/Pr)_2NiO_{4+\delta}$: reaction intermediates and redox behavior explored by in situ neutron powder diffraction during electrochemical oxygen intercalation, *Inorganic Chemistry, 2018, 57 (8), pp.4657-4666.*

Corresponding author: werner.paulus@umontpellier.fr

Understanding spin liquids at the nanoscale

J. A. M. Paddison[1,2,3], Z. L. Dun[3,4], X. Bai[3], M. Daum[3], H. S. Ong[2], J. O. Hamp[2], P. Mukherjee[2], N. P. Butch[5], M. G. Tucker[6], Y. Liu[6], H. D. Zhou[4], C. Castelnovo[3], S. E. Dutton[3], A. L. Goodwin[7], M. Mourigal[2]

[1]Churchill College, University of Cambridge, Cambridge CB3 0DS, UK
[2]Cavendish Laboratory, University of Cambridge, Cambridge CB3 0HE, UK
[3]School of Physics, Georgia Institute of Technology, Atlanta, GA, USA
[4]Department of Physics and Astronomy, University of Tennessee, Knoxville, TN, USA
[5]NIST Center for Neutron Research, NIST, Gaithersburg, MD, USA
[6]Spallation Neutron Source, Oak Ridge National Laboratory, Oak Ridge, TN, USA
[7]Department of Chemistry, University of Oxford, Oxford, UK

Frustrated magnetic materials can host exotic states of matter known as spin liquids, which are disordered but strongly correlated at the nanoscale. The magnetic diffuse scattering measured in neutron-scattering experiments is highly sensitive to the local magnetic correlations in these states, but understanding these data is often challenging. In my talk, I will show how such data can be converted into meaningful models, even without advance knowledge of the underlying magnetic interactions, and when single-crystal samples are not available [1]. I will present two examples of the analysis of magnetic diffuse scattering in real materials. First, I will discuss the recently-synthesised material $Dy_3Mg_2Sb_3O_{14}$, in which kagome layers of corner-sharing triangles are occupied by Ising Dy^{3+} spins that point either "in" our "out" of the triangles [2,3]. I show that our neutron-scattering data can be explained by ordering of emergent magnetic charges – an emergent charge being the sum of "in" (+1) and "out" (–1) spins for a triangle of the kagome lattice [4]. In this state, a macroscopic degeneracy of spin arrangements coexists with an ordered component of the spin structure, so that the material contains both a spin liquid and a spin crystal simultaneously – an exotic phenomenon known as spin fragmentation [5]. Second, I will present recent results on the *quantum* spin-liquid candidate $YbMgGaO_4$, in which Yb^{3+} spins occupy a triangular lattice [6,7]. I will show how magnetic diffuse-scattering measurements can provide insight into bond-dependent interactions that are often difficult to determine using other approaches. I will conclude by discussing future directions in the diffuse-scattering study of spin liquids.

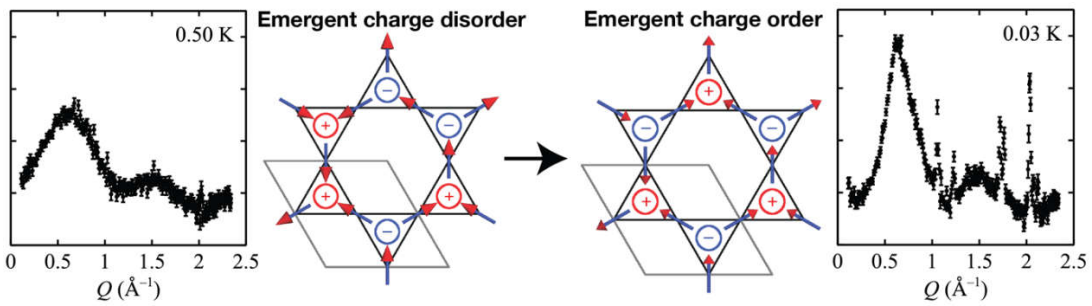

Figure 1: Magnetic phase transition from the correlated paramagnetic state (left) to the emergent charge-ordered state (right) in $Dy_3Mg_2Sb_3O_{14}$. Magnetic powder neutron-scattering data are shown far left and far right. Corresponding spin structures are shown centre left and centre right, where + emergent charges are shown in red, and – emergent charges in blue.

[1] J. A. M. Paddison and A. L. Goodwin, *Phys. Rev. Lett.* **108** (2012) , 017204.
[2] G. Möller and R. Moessner, *Phys. Rev. B* **80** (2009), 140409.
[3] G.-W. Chern, P. Mellado and O. Tchernyshyov, *Phys. Rev. Lett.* **106** (2011), 207202.
[4] J. A. M. Paddison, H. S. Ong, J. O. Hamp, *et al.*, *Nat. Commun.* **7** (2016), 13842.
[5] M. E. Brooks-Bartlett, S. T. Banks, L. D. C. Jaubert, *et al.*, *Phys. Rev. X* **4** (2014), 011007.
[6] Y. Li, G. Chen, W. Tong, et al., *Phys. Rev. Lett* **115** (2015), 167203.
[7] J. A. M. Paddison, M. Daum, Z. L. Dun, *et al.*, *Nat. Phys.* **13** (2017), 117.

Corresponding author: jamp3@cam.ac.uk

Structure of glass-forming aluminate liquids under extreme conditions by neutron diffraction with isotope substitution

J. W. E. Drewitt[1], L. Hennet[2], H. E. Fischer[3]
[1]School of Earth Sciences, University of Bristol, Queens Road, Bristol, BS8 1RJ
[2]Conditions Extrêmes et Matériaux : Haute Température et Irradiation, CEMHTI-CNRS, Université d'Orléans, 1d avenue de la Recherche Scientifique, 45071 Orléans cedex 2, France
[3]Institut Laue-Langevin, 71 avenue des Martyrs, CS 20156, 38042 Grenoble cedex 9, France

In contrast to pure silica, SiO_2, liquid alumina Al_2O_3 does not form a glass. This is in accordance with Zachiariasen's rules, since a significant fraction of aluminium atoms exhibit a coordination number of more than four and share edges [1]. However, the introduction of CaO increases the O:Al ratio, allowing the formation of corner-shared AlO_4 tetrahedra that facilitate glass formation. Using traditional methods, $(CaO)_x(Al_2O_3)_{1-x}$ melts can be vitrified in a narrow region centred around the eutectic at $x = 0.64$. Containerless processing suppresses heteorogeneous nucleation to promote deep undercooling and enables the extension of the glass-forming region to $0.37 \leq x \leq 0.75$ [2]. In this communication, I present neutron diffraction with isotope substitution (NDIS) measurements of aerodynamically levitated and laser-heated $CaAl_2O_4$ ($x = 0.5$) [3] and $Ca_3Al_2O_6$ ($x = 0.75$) [4] liquids in order to understand the structural characteristics that control glass formation. The results, including the direct measurement of the $g_{CaCa}(r)$ partial pair distribution function by double difference NDIS (fig. 1), were combined with molecular dynamics and reverse monte carlo simulations.

Although liquid $Ca_3Al_2O_6$ is largely composed of AlO_4 tetrahedra, ~ 10% unconnected AlO_4 monomers and Al_2O_7 dimers are present, representing a threshold after which the glass can no longer support the formation of an infinitely connected network. For $CaAl_2O_4$, the liquid undergoes a structural reorganisation on vitrification as over-coordinated AlO_5 polyhedra and oxygen triclusters breakdown to form a network of predominantly corner-shared AlO_4 tetrahedra. This is accompanied by the formation of branched chains of edge- and face-sharing Ca-centred Ca*O*x polyhedra.

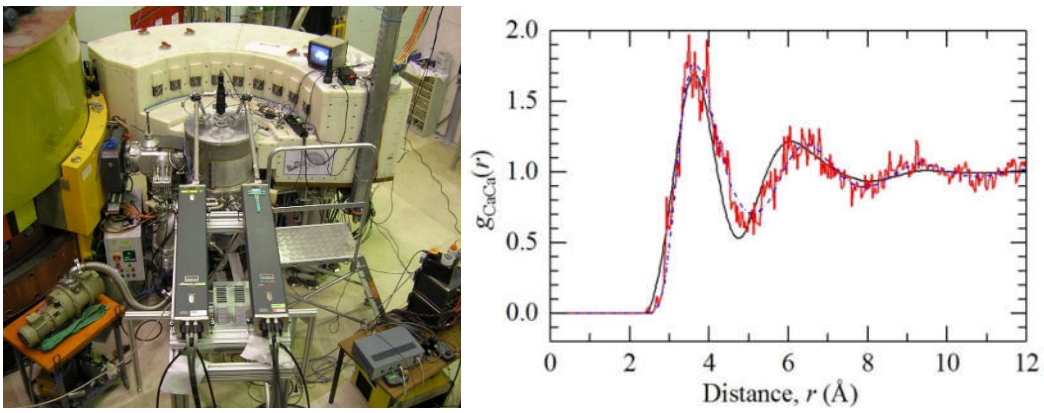

Figure 1: Left: aerodynamic levitation with laser-heating device installed at the instrument d4c (ILL). Right: the partial pair distribution function $g_{CaCa}(r)$ of liquid $Ca_3Al_2O_6$ obtained from double difference neutron diffraction with isotope substitution (black), molecular dynamics simulations (blue chain) and reverse monte carlo simulations (red) [4].

[1] L. B. Skinner et al., *Phys. Rev. B* **87** (2013), 024201.
[2] J. W. E. Drewitt et al., *J. Phys. : Condens. Matter.* **23** (2011), 155101
[3] J. W. E. Drewitt et al., *Phys. Rev. Lett.* **109** (2012), 235501.
[4] J. W. E. Drewitt et al., *Phys. Rev. B* **95** (2017), 064203.

Corresponding author: james.drewitt@bristol.ac.uk

X-ray PDF investigations of complex metal-organic materials.

P. Bordet
Univ. Grenoble Alpes, CNRS, Institut Néel, F-38000 Grenoble France

Pair Distribution Function (PDF) analysis of total scattering data is now a well established technique for the study of disordered or nanocrystalline inorganic materials. The *G(r)* PDF provides the probability of finding a pair of atoms separated by a distance *r*, whatever the crystalline or amorphous nature of the sample. However, for organic/molecular materials, the interpretation of the PDF becomes more complex due to the large number of atoms/parameters required to describe the structure and to the different natures of the chemical bonds involved. Since the widths of the PDF peaks are directly related to the strength of the interatomic interactions, strong intramolecular covalent bonds will yield sharp PDF peaks, while softer intermolecular van der Waals or hydrogen bonds will lead to a wider distribution of distances and much broader PDF oscillations. In the case of metal-organic compounds, an additional difficulty comes from the weak scattering power of the organic molecules relative to the inorganic part of the structure comprising much stronger scatterers.

Here we will present the results of two ongoing studies of metal-organic compounds using PDF analysis of x-ray total scattering data. In the first case, we investigate the conformation of a conducting polymer (PEDOT) inserted into the pores or the metal organic framework (MOF) MIL100Fe compound (cubic *Fd3m*, a = 73.3 Å) in order to enhance its metallic conductivity. In this compound, two types of mesoporous cages of ca. 25 and 29 Å aperture are accessible through microporous windows of ca. 5.5 and 8.6 Å [1]. The total scattering data were recorded at the CRISTAL-SOLEIL beamline by scanning a 2D pixel detector. The structure of MIL100Fe was confirmed by PDF refinement using the MolPDF software [2]. The large pore size allowed the polymer molecules to sit inside the pores without noticeable modification of the unit cell size. Thus, the PDF of the inserted polymer could be obtained by difference between the patterns of an inserted sample and a pristine one. Comparison with the PDF of the bulk polymer indicates that its structural arrangement and coherence length are mainly preserved inside the MOF, in agreement with the enhanced electrical performances.

In the second example, we investigate the local structure of a gold thiolate coordination polymer $[Au(SPh)]_n$ for which the crystalline phase is luminescent while the corresponding amorphous material obtained by heating is not, providing for switchable optical properties with potential applications [3]. Total scattering data were recorded at the ID22-ESRF beamline for the crystalline and amorphous phases. Their PDFs are largely dominated by the signal from Au and S atoms. However they could be refined including the organic part as rigid body using MolPDF, which allows one to apply distance/angle restraints as well as different atomic displacements parameters for different sets of bonds (e.g. intra- or intermolecular). Satisfactory refinements could be obtained in both cases and the results were in agreement with EXAFS data. The main structural effect upon amorphization is a small distortion of the Au-S double helix chains. The presence of defects decrease the coherence length along the chains, while interchain coherent interactions remain noticeable up to ~50 Å.

[1] P. Horcajada et al., *Chem. Commun.,* 2007, 2820–2822.
[2] MolPDF, J. Rodriguez-Carvajal and A. Bytchkov, ILL and ESRF, 2016
[3] C. Lavenn et al., *J. Mater. Chem. C*, 2015, 3, 4115

Corresponding author: pierre.bordet@neel.cnrs.fr

A renewed approach of UO_2 nuclear fuel using PDF analysis

L. Desgranges[1], G. Baldinozzi[2], D. Siméone[3], P. Garcia[1], H.E. Fischer[4]
[1]CEA-DEN C.E. Cadarache 13108 Saint-Paul lez Durance FRANCE
[2]Centralesupelec/SPMS/UMR-8085, 3 rue Joliot-Curie. 91192 Gif-sur-Yvette cedex
[3]CEA-DEN, Université Paris-Saclay, F-91191,
[4]Institut Laue-Langevin, 6 rue Jules Horowitz, B.P. 156, 38042 Grenoble cedex, France

Uranium dioxide is the main component of nuclear fuel, used worldwide. During irradiation, it is subject to irradiation damage and composition changes. These effects have been studied for more than 50 years and it is commonly admitted that the UO_2 crystalline structure is a rigid array with defined positions on which atoms can settle as a function of the irradiation [1]. However, some details of its crystalline structure are still under discussion because only a small number of experimental methods can give a precise crystallographic picture of a compound having a heavy cation, uranium, next to a small anion, oxygen.

We improved the description of UO_2 derived compounds by using neutron diffraction and Pair Distribution Function (PDF) analysis at the D4 neutron diffractometer (ILL), because these techniques provided an accurate description of the oxygen distribution. In this presentation, we will show on two examples that the commonly accepted picture of UO_2 does not apply. These examples are the incorporation of oxygen in UO_2, and UO_2 crystalline structure at high temperature.

In the case of UO_2 oxidation, oxygen atoms form clusters, named cuboctahedra. In these clusters, oxygen atoms are removed from their regular UO_2 positions and do not sit on the defined positions of an Fm-3m array [2]. They occupy the same positions as the interstitial atoms in order to form an oxygen polyhedron. PDF analysis as a function of temperature showed that the shape of this polyhedron changed during alpha-beta and beta-gamma phase transitions [3].

In the case of UO_2 behaviour at high temperature, the existence of a UO bond length, shorter than expected, was confirmed by both Rietveld and PDF analysis [4]. Moreover PDF analysis evidenced the existence of a local symmetry, Pa-3 instead of Fm-3m. The manner by which Pa-3 domains are arranged in order to give an average Fm-3m symmetry is discussed, and a structural model is proposed to describe UO_2 data at high temperature [5].

These two examples evidenced that UO_2 local order cannot be simply deduced from Fm-3m average symmetry, at least at high temperature. This realisation is a driving force not only to deepen the study of other UO_2 derived samples, for example doped with lanthanides, but also to test how the concept of local lower symmetry can apply to other fluorite type oxides [6].

[1] C. Gueneau et al. *J. Nucl. Mater.* **419** (2011) 145-167
[2] L. Desgranges, et al. *Inorg. Chem.* **50** (2011) 6146-6151
[3] L. Desgranges et al. *Inorg. Chem.* **55** (2016) 321-326
[4] L. Desgranges et al. *Inorg. Chem.* **56** (2017) 321-326
[5] L. Desgranges et al *Chem. Eur.* J. **24** (2018) 2085-2088
[6] D. Siméone et al. *Scientific Report* **7** (2017) 3727

Corresponding author: lionel.desgranges@cea.fr

The structure of water

A. Zeidler[1], P. S. Salmon[1]
[1]Physics Department, University of Bath, Bath, BA2 7AY, UK

Results on the structure of different phases of water obtained using the D4c diffractometer at the ILL reactor source will be presented. The method used is neutron diffraction with isotope substitution to obtain information on the partial structure factor level. Ambient water will be compared to the different phases of amorphous ice and crystallise ice Ih. Differences and similarities as well as the effect of the resolution function will be discussed.

Corresponding author: az207@bath.ac.uk

PDF Analysis of Batteries Using Diffraction Computed Tomography

D.S. Wragg[1], J. Sottmann[1,3], A. Ruud[1], Ø. Slagtern Fjellvåg[1], M. Di Michiel[2], G.B.M. Vaughan[2], H. Fjellvåg[1], O. Lebedev[3]

[1]Department of Chemistry, University of Oslo, 0315 Oslo, Norway

[2]The European Synchrotron, 71 avenue des Martyrs, 8043 Grenoble, France

[3]CNRS Crismat, 6 boulevard du Maréchal Juin, 14050 Caen, France

Energy storage is a crucial element of any renewable energy system. Balancing demand with supply from intermittent sources like wind and solar generation on a large scale and routine electrification of vehicles both require improved battery technology. Lithium batteries (LIBs) are a well-established technology and sodium ion batteries (SiBs), which have similar chemistry, are very promising for stationary storage applications at lower monetary and environmental cost than LIBs. Unfortunately, the standard anode for LIBs, graphite, has a poor capacity for sodium. The search for a high-capacity SIB anode which will maintain its capacity over many cycles and is safe, environmentally friendly and inexpensive, is an important focus in battery research.

To optimise SIB anode performance, we use operando methods to study the chemical mechanisms and structural composition of the materials. Since many of the materials we are interested in become amorphous during battery cycling, total scattering analysis has become an important tool alongside conventional XRD, X-ray spectroscopy and calculations. The multiple (and sometimes mobile) components of a battery stack make the background corrections required for PDF analysis of total scattering data difficult when working in typical transmission and reflection operando-XRD battery cells [1,2]. To address this problem, we have applied the pair distribution function computed tomography (PDF-CT) method to SIB anodes at ESRF beamline ID15. By reconstructing the scattering data from the anode using tomographic methods we can zoom in on specific parts of the battery and extract PDF data without further background subtractions. The method has been used to show, clearly and for the first time, the different structures which develop during cycling of sodium in a phosphorus alloying anode (figure 1) [3], and is now being applied in combination with XRD-CT to more complex SIB anode materials which combine alloying and conversion-type reactions.

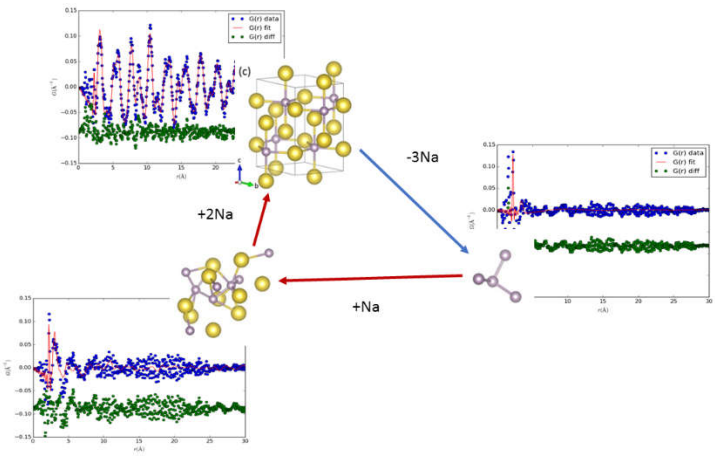

Figure 1. PDF-CT reveals the structures formed during sodium cycling in a phosphorus anode

[1] P. K. Allan, et al. *J. Am. Chem. Soc*. **138** (2016) 2352.
[2] O. J. Borkiewicz, et al. *J. Appl. Cryst.* **45 (**2012) 1261
[3] J. Sottmann, et al. Angew. Chem. Int. Ed. Engl. **56** (2017) 11385

Corresponding author: david.wragg@smn.uio.no

New nanostructures from x-ray total scattering and PDF analysis

Kirsten M. Ø. Jensen
Department of Chemistry and Nanoscience Center, University of Copenhagen

Nanomaterials have come to play a huge role in modern materials chemistry: By nanosizing the functional materials used in a range of different applications, the properties of the materials can be improved, and new applications can arise. This development has challenged the conventional techniques for material characterization. However, total scattering combined with Pair Distribution Function analysis allows us to look further into nanostructure and establish the structure-property relation for advanced functional materials.[1] Here, I will present recent work illustrating how we use x-ray total scattering to study atomic structure in advanced nanomaterials, with special focus on metal and metal oxide nanoparticles. [2] We observe that new structural motifs, unstable in the bulk form, become dominant in nanoscale materials. In molybdenum oxides, for example, we use PDF analysis coupled with HR-STEM to determine the structure of 3 nm MoO_2 particles, where rutile-based shear planes appear, changing the material properties.

Apart from studying the synthesized nanoparticles, I will also show how *in situ* x-ray total scattering allows following the formation of materials. Despite decades of research into nucleation processes, very little is known on how nanoparticle formation during solvothermal synthesis takes places on the atomic scale. We have developed methods which allows using *in situ* synchrotron X-ray Total Scattering and Pair Distribution Function analysis to follow nanoparticle nucleation and growth in situ.[3] In contrast to conventional crystallographic studies, PDF analysis gives structural information from non-crystalline species, allowing obtaining structural information on the atomic scale, all the way from precursor to the final nanoclusters during synthesis. Using x-ray total scattering, we deduce the *atomic structure* of prenucleation clusters, present in the processes just before the crystalline nanoparticles have formed. We show that the solvent and synthesis conditions have large influence on the nucleation pathway and the structure of the nano-scale clusters in the synthetic pathway.

[1] S. J. L. Billinge, I. Levin, *Science* **316**, 561-565, (2007).
[2] K. M. Ø. Jensen, P. Juhas, M. A. Tofanelli, C, K, Heinecke, G. Vaughan, C. Ackerson, S. J. L. Billinge, *Nature Communications* **7**, 11859, (2016).
[3] K. M. Ø. Jensen, C. Tyrsted, M. Bremholm, B. B. Iversen, *ChemSusChem* **7**, 1594-1611, (2014).

Corresponding author: kirsten@chem.ku.dk

Oral Contributions

Magnetic diffuse scattering in the Gd-pyrochlore antiferromagnet - $Gd_2Pt_2O_7$

Philip G Welch[1,2], Wei-Tin Chen[3], Jason S Gardner[3], Andrew R Wildes[4], Joseph A M Paddison[5], Andrew L Goodwin[1], and J Ross Stewart[2]

[1]Inorganic Chemistry Laboratory, University of Oxford, South Parks Road, Oxford, OX1 3QR

[2]ISIS Neutron and Muon Facility, Science and Technology Facilities Council, Rutherford Appleton Laboratory, Didcot, OX11 0QX, United Kingdom

[3]Centre for Condensed Matter Sciences, National Taiwan University, Taipei, 10617, Taiwan

[4]Institut Max von Laue-Paul Langevin, F-38042 Grenoble 9, France

[5]Churchill College, University of Cambridge, Storey's Way, Cambridge, CB3 0DS, United Kingdom

The pyrochlore ($A_2B_2O_7$) lattice of corner sharing tetrahedra has, over the past 20 years, been widely studied. Magnetic frustration, either due to competing antiferromagnetic (AF) interactions, or ferromagnetic (FM) interactions in the presence of strong easy-axis or XY anisotropy, leads to some fascinating ground states such as the spin-ice Coulomb phase, quantum-spin liquid phases, and novel magnetic order [1]. Our group - for many years - has been studying gadolinium-pyrochlore compounds with either titanium or tin on the B-site. The motivation for studying these pyrochlores is that they should be representative of a pure Heisenberg antiferromagnet on the pyrochlore lattice. The seminal work of Palmer and Chalker [2] showed that such a lattice, with only near-neighbour exchange and dipolar interactions, should (for certain ratios of J_{ex}/J_{dip}) order in a k=**0,** 4-sublattice, co-planar ground state, now known as the Palmer-Chalker state.

Both $Gd_2Ti_2O_7$ and $Gd_2Sn_2O_7$ exhibit long-range magnetic order at low temperatures, at around 1 K in both cases. Neutron diffraction studies of powder samples of $Gd_2Sn_2O_7$ [3, 4] show that, indeed, this forms the Palmer-Chalker ground state below 1 K. Very recent diffuse scattering measurements by our group on the paramagnetic scattering cross-section show that while 2nd or 3rd near neighbour exchange interactions may exist in $Gd_2Sn_2O_7$ they are on the 0.5% level compared to J_1 which we found to have a value of around 0.3 K (AFM) [5].

Recently, a new Gd-pyrochlore, $Gd_2Pt_2O_7$ was synthesised as reported by Hallas and co-workers [6]. In many respects, this new Gd-pyrochlore is reminiscent of $Gd_2Sn_2O_7$, exhibiting a massive first order anomaly in the heat capacity at a temperature of 1.6 K. This transition occurs at a much higher temperature than for $Gd_2Sn_2O_7$, which orders at 1 K. It is noteworthy that on integration of the heat capacity, the full Rln8 entropy associated with the S = 7/2 Gd spins is recovered, indicating that the magnetic ground state of $Gd_2Pt_2O_7$ contains little or no magnetic disorder.

We have performed a polarised neutron study of isotope enriched $^{160}Gd_2Pt_2O_7$ using the D7 diffuse scattering spectrometer at the ILL. Using a combination of mean-field fitting, direct Monte-Carlo modelling, and reverse Monte-Carlo refinement, we have investigated the correlated paramagnetic regime above the 1.6 K ordering temperature and have calculated the expected single-crystal diffuse magnetic scattering, and the spin-spin correlation functions along high-symmetry directions in real-space. Furthermore, we have determined that, similar to $Gd_2Sn_2O_7$, there is an ordering transition into the Palmer-Chalker state, at a temperature of 1.6 K. This ordering transition takes place at a significantly higher temperature than in $Gd_2Sn_2O_7$, which is attributed to the additional superexchange pathways created due to the empty platinum *5d* e_g orbitals.

[1] J. S. Gardner, M. J. P. Gingras, and J. E. Greedan, *Rev. Mod. Phys.*, **82**, (2010), 53.
[2] S. E. Palmer and J. T. Chalker, *Phys. Rev. B*, **62**, (2000), 488.
[3] A. S. Wills, et al., *J. Phys.: Condens. Matter*, **18**, (2006), L37.
[4] J. R. Stewart, et al., *Phys. Rev. B*, **78**, (2008), 132410.
[5] J. A. M. Paddison, et al., *J. Phys.: Condens. Matter*, **29**, (2017), 144001.
[6] A. M. Hallas, et al., *Phys. Rev. B*, **94**, (2016), 134417.

Three-dimensional magnetic difference pair distribution function analysis of single crystal diffuse neutron scattering from frustrated magnets

N. Roth[1], A. F. May[2] B. C. Chakoumakos[3], F. Ye[3], B. B. Iversen[1]
[1]Center for materials crystallography, Department of chemistry, Aarhus University, Denmark
[2]Materials Science and Technology Division, Oak Ridge National Laboratory, Oak Ridge, USA
[3]Neutron Scattering Division, Oak Ridge National Laboratory, Oak Ridge, USA

Magnetically frustrated materials are gaining a huge increase in interest due to exotic physical phenomena found in spin liquids and glasses. In order to obtain a better understanding of such magnetically disordered materials, magnetic diffuse neutron scattering can be measured and analyzed. For a long time, analysis mainly consisted of inspection of the wave-vector and temperature dependence of scattering, giving only limited information about the disorder. Recently, more advanced methods have been developed, such as modelling the scattering using reverse Monte-Carlo simulations for both powder and single-crystal data. Another recent approach has been to develop a magnetic pair distribution function analysis for powder neutron scattering. Such analysis gives a one-dimensional look at magnetic pairwise interactions, both ordered and disordered.

Here we show a new technique for single-crystal magnetic diffuse neutron scattering analysis[1]. The technique is analogous to the three-dimensional-difference pair distribution function (3D-ΔPDF) pioneered by Weber and Simonov for X-ray scattering [2], as it takes the Fourier transform of only the magnetic diffuse scattering. The resulting 3D-magnetic difference pair distribution function (3D-mΔPDF) gives a real-space view of the spin-spin correlation. As only the diffuse scattering is used, it is possible to get a view of the disordered part of the magnetic structure. This allows analysis of materials with an average magnetic structure containing some disorder without the ordered part dominating the result. In this way, it is possible to directly observe whether two magnetic moments tend to be more parallel or antiparallel aligned than the average structure.

We demonstrate the technique on the frustrated magnetic mineral Bixbyite, $FeMnO_3$. The scattering from Bixbyite is quite complex, as there is strong Bragg reflections, weak symmetry breaking reflections as well as both nuclear and magnetic diffuse scattering. We show how to separate out specifically the magnetic diffuse scattering in order to compute the 3D-magnetic difference-PDF. The analysis reveals that nearest neighbor metal atoms tend to prefer antiparallel alignment, next-nearest neighbors parallel alignment etc. and that correlations exist up to relatively long distances (> 15 Å).

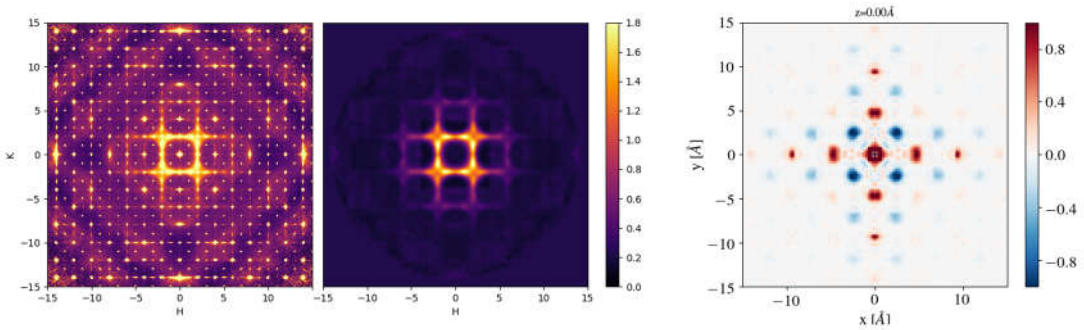

Figure 1: Left: HK0 plane of the total elastic neutron scattering from Bixbyite at 7K. Middle: Isolated magnetic diffuse neutron scattering. Left: 3D-magnetic difference pair distribution function in the z=0Å plane.

[1] N. Roth et al., *IUCRJ* **5** (2018) 410-416
[2] T. Weber, A. Simonov, *Z. Krist.* **227** (2012) 238-247

Corresponding author: nikolajroth@chem.au.dk

The interpretation of broad diffuse maxima using superspace crystallography

E. M. Schmidt, R. B. Neder
Institute for Crystallography and Structural Physics, Friedrich-Alexander Universität Erlangen Nürnberg

Single crystal diffuse scattering is generally interpreted using correlation parameters, such as the Warren-Cowley short range order parameters, that describe probabilities for certain configurations on a local scale [1]. If the diffuse maxima are at a general position in reciprocal space, many parameters are needed to simulate a short range ordered structure in direct space, which reproduces the observed diffuse maxima.

In the field of incommensurate crystallography a (3+d)-dimensional approach is taken to describe satellite reflections in reciprocal space, that cannot be indexed with integer (h,k,l) [2]. A 3-dimensional aperiodic crystal structure is periodic in (3+d)-dimensional superspace and the atomic positions and/or occupancies of the 3D structure are described by modulation functions.

A perfectly periodic superspace gives rise to satellite reflections with a FWHM identical to the main Bragg reflections. In order to describe broadened satellite reflections we introduce disorder into superspace. By introducing phase domains in the superspace structure we can generate structures that give rise to diffuse maxima at any position in reciprocal space with an arbitrary width. The only parameters needed to sufficiently describe the structure in (3+d)-dimensional space, are the position of the diffuse maxima and the width of the maxima. This approach allows a description of both, occupational and displacive disorder.

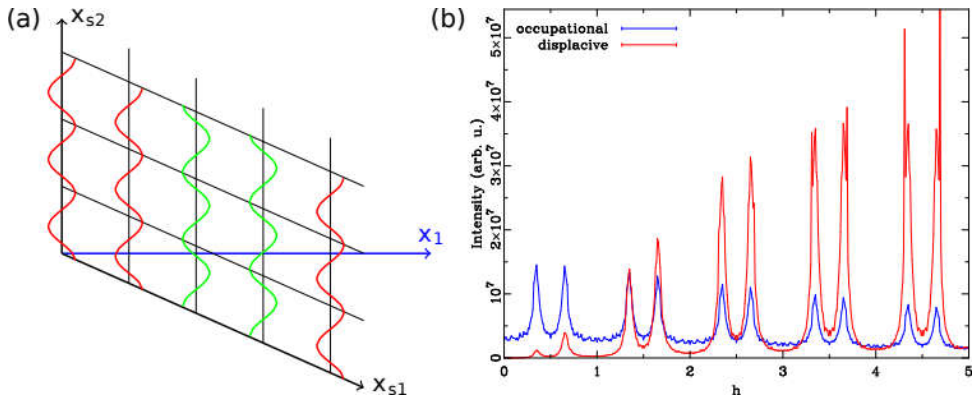

Figure 1: (a) Disordered superspace for a one dimensional crystal. The atomic surfaces are depicted as the cosine waves in superspace. The red and green waves are phase shifted by π, which is equivalent to multiplying the amplitude of the modulation function with −1. (b) Simulated diffraction pattern of (1+1)D disordered superspace models showing broadened satellite reflections. Blue: occupational disorder of an Ag:Au 1:1 crystal structure. Red: displacement disorder of a pure Ag crystal. In both cases the modulation vector is chosen as $q = \sqrt{3}/5$. Bragg reflections have been omitted.

[1] T. R. Welberry and T. Weber, *Crystallography Reviews* **22** (2016), 2.
[2] T. Janssen and A. Janner, *Acta Crystallographica* **B70** (2014), 617.

Corresponding author: ella.schmidt@fau.de

Highly polymerized carbonate glass at ultrahigh pressure: insights into the structure of carbonatitic melts at extreme conditions

V. Cerantola[1], C. Sahle[2], S. Petitgirard[3], C. Weiss[4], S. Checchia[2], M. Di Michiel[2], C. Cavallari[2], G.B.M. Vaughan[2], I. Collings[2], M. Hanfland[2], M. Wilke[5]
[1]European XFEL, 22869 Schenefeld, Germany
[2]ESRF-The European Synchrotron, 38000, Grenoble, France
[3]Institute of Geochemistry and Petrology, ETH, 8092 Zurich, Switzerland
[4]Facultät Physik/DELTA, Technische Universität Dortmund, 44227 Dortmund, Germany
[5]Institut für Erd- und Umweltwissenschaften, Universität Potsdam, 14476 Potsdam, Germany

Carbonatites, rare igneous rocks consisting mostly of carbonates, originate unambiguously in the mantle but the depth limit of their presence is not known. Due to their role as carbon reservoirs and movement vectors, the occurrence of carbonatites at depths near the core-mantle boundary (CMB) could be linked to key aspects of mantle geophysics [1-3]. Unlike well-understood silicates, the detection of carbonatitic melts at high pressure is problematic due to their low-viscous, amorphous nature and the difficult characterisation of low-Z amorphous samples in diamond anvil cells (DACs). We have been able to study these amorphous structures by PDF analysis at ultrahigh pressure, using optimised data collection and reduction methods by which we could extract the weak scattering from amorphous samples from the complex DAC background. Hence, DAC X-ray PDF combined with X-ray Raman scattering allowed the first study of the short-range structure of $K_2Mg(CO_3)_2$ glass at pressures up to 85 GPa. The trends of C-O, Mg-O and K-O bond lengths show that carbonatitic glasses and, by extension, carbonatitic melts undergo a gradual change in polymerization of the carbonate groups at depths (pressures) spanning from the mid-lower mantle down to the CMB. From this transition we can infer the change in coordination of the carbonate group, CO_3^{2-}, in favour of a new, three-dimensional *tetracarbonate* molecule, CO_4^{4-}. The validity of the method used for this PDF analysis of low-Z glasses in DAC opens new possibilites for characterising liquid and amorphous structures not only at extreme conditions, but generally embedded in a complex sample environments or even a complex matrix.

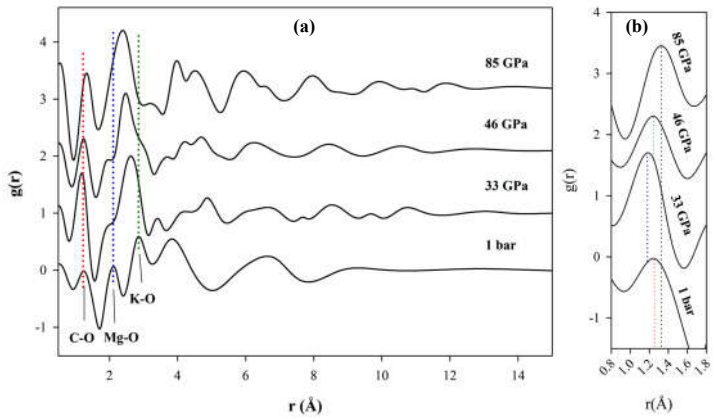

Figure 1: (a) Pair distribution functions $G(r)$ of $K_2Mg(CO_3)_2$ glass at selected pressures. (b) Close-up on the C-O bond distances at the corresponding pressures..

[1] F. Kaminsky, *Earth Sci. Rev.* **110** (2012), 127.
[2] B. O. Mysen, *Annu. Rev. Earth Planet. Sci.* **11** (1983), 75.
[3] A. P. Jones, M. Genge, L. Carmody, *Rev. Mineral Geochem.* **75** (2013), 289.

Corresponding author: valerio.cerantola@xfel.eu

Structure of low Z liquids under extreme conditions using X rays: from dream to reality

G. Garbarino[1], G. Weck[2], F. Datchi[3], S. Ninet[3], P. Loubeyre[2], M. Mezouar[3]
[1]European Synchrotron Radiation Facility, 71 Av. des Martyrs, 38000, Grenoble, France
[2]Département de Physique Théorique et Appliquée, CEA/DAM, 91297, Bruyères-le-Châtel, France
[3]Institut de Minéralogie, Physique des Matériaux et de Cosmochimie, Univ. Paris 6, Sorbonne Universités, 4 place Jussieu, 75252, Paris, France

The discovery of polymorphism in disordered (glassy, amorphous) solids and fluids have largely questioned our understanding of these states of matter. So far, however, the number of systems for which this phenomena has been evidenced by experiments remains limited, and the existence of a first-order transition in a homogenous isotropic melt has been only clearly established in the case of phosphorus [1]. First-order transitions between a molecular and a polymeric liquid have been recently predicted by first-principles calculations in liquid nitrogen at 88 GPa and 2000 K [2] and in liquid CO_2 at 45 GPa and 1850 K [3]. The only device presently capable of reaching these extreme conditions is the diamond anvil cell (DAC). However, the sample in the DAC is sandwiched between two diamond anvils of thickness 100 times larger. Consequently, the diffracted signal from the sample is very weak compared to the Compton signal of the anvils, and hardly measurable for pressures above 20 GPa. We will present here a newly developed experimental setup, installed at ESRF ID27 beamline, which drastically reduces the background signal and enables the measurement of the structure factor of low-Z simple fluids to higher pressures [4]. It is based on the adaptation of a multichannel collimator originally designed for angular-dispersive x-ray diffraction with large-volume presses [5]. Experimental results on fluid hydrogen [6], carbon dioxide [7], nitrogen [8] and light alkali metals [9] will serve as examples to show the large signal-to-noise improvement achieved with this setup, from which quantitative structure factors could be extracted.

[1] Katayama Y. et al. *Nature* **403** (2000) 170.
[2] Boates B. & Bonev S. A. *Phys. Rev. Lett.* **102** (2009) 015701.
[3] Boates B. el al. *Proc. Natl. Acad. Sci*. **107** (2010) 12799.
[4] Weck G. et al. *Rev. Sci. Ins.* **84** (2013) 063901.
[5] Yaoita K. et al. *Rev. Sci. Ins*. **68** (1997) 2106; Mezouar M. et al. *Rev. Sci. Ins.* **73** (2002) 3570
[6] Weck G. et al. *Phys. Rev. B* **91** (2015) 180204.
[7] Datchi F. et al. *Phys. Rev. B* **94** (2015) *014201*.
[8] Weck G. et al. *Phys. Rev. Lett* **119** (2018) 235701.
[9] G. Garbarino et al, *in prep.*

Corresponding author: gaston.garbarino@esrf.fr

D3 at the ILL: structural studies of hydrogenous liquid and amorphous systems using polarised neutrons

Anne Stunault[1], Sébastien Vial[1], Gabriel J. Cuello[1] and David Jullien[1]
[1]Institut Laue Langevin, CS 20156, F-38042 Grenoble Cedex, France

In diffraction, the structural information of materials is contained in the coherently scattered signal. Unfortunately, the determination of the coherent structure factor of hydrogenous liquid and amorphous systems is very difficult: X-rays are barely sensitive to hydrogen, while neutron results still lack accuracy due to the contamination of the scattering intensities by a huge spin-incoherent signal from 1H, in some cases reaching over 90 % of the total signal.
Using polarised neutrons with polarisation analysis, one can experimentally separate the coherent and incoherent contributions to the scattered intensity, since nuclear coherent scattering does not reverse the neutron spin while 2/3 of the spin-incoherent scattering do reverse it.
The D3 polarised hot neutron diffractometer at ILL, formerly devoted to magnetic studies on single crystals, has been upgraded and now offers a new setup for the studies of liquids over a wide Q-range using polarised neutrons [1]. Within the ILL endurance upgrade program, the capabilities of this new, fully operational, option are currently being enhanced by the implementation of a new detector assembly, including a wide angle 3He spin filter and a multidetector. We detail the principle of the method, giving special attention multiple scattering, which has a critical impact on the data quality.
Through several examples we demonstrate the power of the method and show the complementarity with what is currently achieved on other dedicated instruments (cold, polarised neutrons, and hot, non-polarised neutrons). Examples include molecular liquids (water, alcohols, sugars in solution) as well amorphous systems of industrial interest (cements, pharmaceutical industry). [2]
The improved accuracy of the data obtained using polarized neutrons will also have a high impact on the assessment of ab initio calculations, as shown e.g. by recent results in electrolytes.

[1] A. Stunault, S. Vial, L. Pusztai, G. J. Cuello and L. Temleitner, Journal of Physics: Conference Series 711, 012003 (2016), A. Stunault, S. Vial, D. Jullien, G. J. Cuello, Physica B, doi:10.1016/j.physb.2017.10.130 (2017)
[2] L.Temleitner,A.Stunault,G.J.Cuello,L.Pusztai,Phys.Rev.B92, 014201 (2015), L.A. Rodríguez Palomino, G.J. Cuello, J. Dawidowski, L. Temleitner, L. Pusztai, A. Stunault, J. Phys. Conf. Ser. 663, 012002 (2015)

Corresponding author: stunault@ill.fr

Phase separation at the dimer-superconductor transition in $Ir_{1-x}Rh_xTe_2$

R. Yu[1], S. Banerjee[2], H. Lei[1], M. Abeykoon[3], C. Petrovic[1], Z. Guguchia[1,4], and E. S. Bozin[1]
[1]Condensed Matter Physics and Materials Science Department, Brookhaven National Laboratory
[2]Department of Applied Physics and Applied Mathematics, Columbia University
[3]Photon Sciences Division, Brookhaven National Laboratory
[4]Department of Physics, Columbia University

The detailed evolution of the local atomic structure across the (x, T) phase diagram of transition metal dichalcogenide superconductor $Ir_{1-x}Rh_xTe_2$ ($0 \leq x \leq 0.3$, $10\ K \leq T \leq 300\ K$) is obtained from high-quality X-ray diffraction data using the atomic pair distribution function (PDF) method. The observed hysteretic thermal structural phase transition from a trigonal (P-3m1) to a triclinic (P-1) dimer phase for low Rh content emphasizes the intimate connection between the lattice and electronic properties. For superconducting samples away from the dimer/superconductor phase boundary, structural transition is absent, and the local structure remains trigonal down to 10 K [1]. In the narrow range of compositions close to the boundary, PDF analysis reveals structural phase separation [2], suggestive of weak first-order character of the Rh-doping induced dimer-superconductor quantum phase transition. Samples from this narrow range show weak anomalies in electronic transport and magnetization, hallmarks of the dimer phase, as well as superconductivity albeit with incomplete diamagnetic screening. The results suggest that the dimer and superconducting orders exist in the mutually exclusive spatial regions.

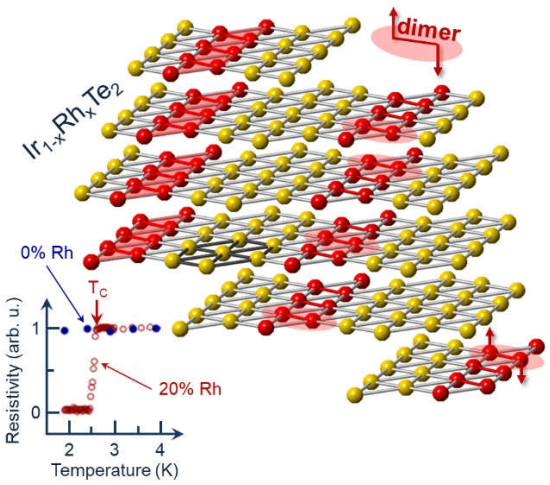

Figure 1: Atomic structure (iridium sublattice) of the low temperature phase of $IrTe_2$ featuring Ir^{4+} dimers (red) ordered on a triangular Ir network. Inset: low temperature electrical resistivity of pure and Rh-substituted $IrTe_2$.

[1] Runze Yu, Soham Banerjee, Hechang Lei, Ryan Sinclair, Milinda Abeykoon, Haidong Zhou, Cedomir Petrovic, Zurab Guguchia, and Emil S. Bozin, Phys. Rev. B **97** (2018) 174515
[2] Runze Yu, Soham Banerjee, Hechang Lei, Milinda Abeykoon, Cedomir Petrovic, Zurab Guguchia, and Emil S. Bozin, Phys. Rev. B **98** (2018) 134506.

* Total scattering X-ray PDF data were collected at 28-ID-2 (XPD) beamline of the National Synchrotron Light Source II at Brookhaven National Laboratory. Work at Brookhaven National Laboratory was supported by US DOE-BES under Contract No. DE-SC0012704.

Corresponding author: bozin@bnl.gov

Wide angle x-ray scattering combined with pair distribution function analysis of pyrolyzed wood

A. Poulain[1], C. Dupont[2], P. Martinez[1], Ch. Guizani[3] and J. Drnec[1]
[1]ESRF, Grenoble, France
[2]IHE Delft Institute for Water Education, Delft, The Netherlands
[3]University Grenoble Alpes, CNRS, Grenoble, France

Carbonaceous materials derived from residual biomass have been studied for a wide range of applications, including environmental, catalytic, industrial, electronic and agricultural purposes , because this material is abundant, cheap and environmentally-friendly. The applications depend on specific microstructures, leading to distinct macroscopic properties, such as electrical conductivity, surface area or stiffness.

Biomass pyrolysis (devolatilization), is the thermal decomposition of material without reactive gas atmosphere. Its mechanism remains neither well-understood or mastered due to the complexity of the initial materials. The process gives rise to variable amounts of i) volatile matter (CO, CO2 or CH4), ii) condensable species including water and a large number of organic species gathered as tar and of iii) a carbon-rich solid residue called char. The relative ratio of these products depends on various pyrolysis parameters and therefore high level of process control is needed in order to tailor the final product for the need.

The objective of this contribution is to compare the models of hard carbon obtained from the two complementary X-ray scattering techniques: Wide Angle X-ray Scattering and Pair Distribution Function analysis, using CarbX [1,2] and PDFgui [3] programs, respectively. These models allow characterization of lignocellulosic biomass samples – beech wood and apricot tree pruning - and the structural changes occurring during their thermal degradation under different temperatures and heating rates.

CarbX provides unique information about the arrangement of graphene layers described by intralayer, interlayer, disorder and dispersion structural parameters. Pair distribution function modeling in PDFgui reveals imperfections in single graphene sheets, such as bond shortening and curvature, when refinement is performed in different r-ranges. The concentration of inorganic species, along with heating rate influences the final structure of pyrolysis products. The heating rate was more important than sample composition for an increase in extent of single graphene layer and average chord length, while the average graphene coherent stack height depended on both composition and heating rate. Higher fractions of inorganic material increased the average interlayer spacing and number of graphene layers per stack.

[1] W. Ruland, B.M. Smarsly, *J.App.Cryst* **35** (2002), 624-633.
[2] T. Pfaff, M. Simmermacher,B.M. Smarsly, *J.Appl.Cryst.* **51** (2018), 219-229.
[3] C.L. Farrow et al., *J. Phys.: Condens. Matter* **19** (2007), 335219.
[4] A. Poulain et al., *J.Appl.Cryst.*, accepted (2018)

Corresponding author: drnec@esrf.fr

Nanoscale degeneracy lifting in triangular antiferromagnets studied by combined PDF + mPDF

Benjamin A. Frandsen[1], Emil S. Bozin[2], Alexandros Lappas[3]
[1]Department of Physics and Astronomy, Brigham Young University, Utah, USA
[2]Condensed Matter Physics and Materials Science Department, Brookhaven National Laboratory, New York, USA
[3]Institute of Electronic Structure and Laser, Foundation for Research and Technology—Hellas, Heraklion, Greece

Antiferromagnetically coupled magnetic moments decorating triangular structural motifs form the basic building block for many types of geometrically frustrated magnets. Due to an inability to satisfy competing interactions simultaneously, frustrated magnets often display unusual behavior such as strongly suppressed magnetic ordering temperatures, exotic magnetic excitations, and extreme sensitivity to weak perturbations. Here, we examine the antiferromagnetic transitions in $CuMnO_2$ and $NaMnO_2$, both of which realize an anisotropic triangular lattice of $S = 2$ spins. Through combined atomic and magnetic pair distribution function analysis, we reveal an intricate connection between local structural distortions of the lattice and short-range magnetic correlations well above the transition temperature. We also establish an unconventional transition mechanism in $NaMnO_2$ by which a short-range distortion of the local atomic structure lifts the magnetic degeneracy on the nanoscale, triggering a long-range transition to antiferromagnetic order.

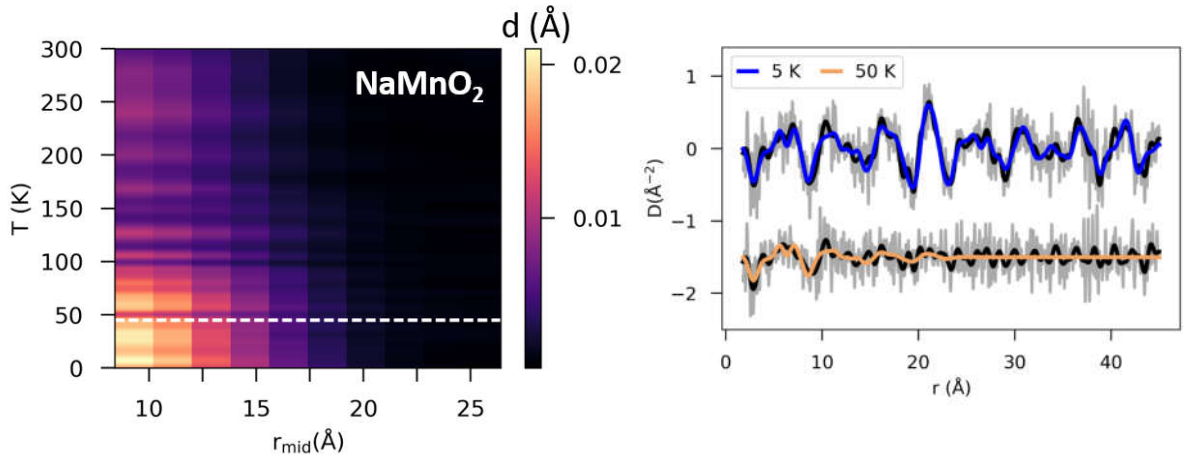

Left: Color map showing the magnitude of the local structural distortion in $NaMnO_2$ as a function of temperature and fitting range. Right: Magnetic PDF fits at 5 K and 50 K.

Corresponding author: benfrandsen@byu.edu

Magnetic frustration in $SrLn_2O_4$ compounds studied via mPDF-analysis

Simon Riberolles[1,2], Navid Qureshi[2], Oleg A. Petrenko[1], Henry E. Fischer[2]
[1]Department of Physics, University of Warwick, Coventry CV4 7AL, U.K.
[2]Institut Laue-Langevin, 71 avenue des Martyrs, CS 20156, 38042 Grenoble cedex 9, France

The Ln^{3+} magnetic ions in $SrLn_2O_4$ compounds reside on 2 sites (distinguished by their slightly different crystallographic environments) within distorted hexagonal planes that are connected perpendicularly via 1D chains and triangular ladders. Geometric frustration between next-nearest neighbors results in complex magnetic structures containing a certain degree of local spin disorder, thus leading to diffuse magnetic scattering of neutrons. The total magnetic scattering (both Bragg and diffuse) can be isolated from the neutron diffraction pattern and Fourier transformed to produce a magnetic Pair-Distribution Function or mPDF(r) [1], a real-space function of relative distance between magnetic ions (here only Ln^{3+}) that exhibits positive or negative peaks for ferro- or antiferro-magnetic alignment between spins, respectively. The local quasi-instantaneous magnetic structure reported by the mPDF(r) is complementary to the space+time averaged structure gained through Rietveld refinement of elastic magnetic scattering at Bragg peak positions, and has an additional advantage of revealing not only static spin-spin correlations below T_N, but also dynamic spin-spin correlations above T_N.

In the case of Ln = Gd, the temperature dependence of the mPDF(r) shows that the 1D chains order first and progressively as T decreases towards T_N = 2.7 K, followed by ordering between chains and within the hexagonal sheets once T_N is reached (see figures below). The positive slope in the mPDF(r) between 0 and 2.5 Å corresponds to the *collinear* ferromagnetic ordering within the 1D chains. The short range of the dynamic spin-spin correlations above T_N is immediately visible.

In the case of Ln = Nd (data not shown), the mPDF(r) exhibits both below and above T_N = 2.3 K a clear negative peak at 3.55 Å that corresponds to the *transverse* antiferromagnetic ordering along the 1D chains. As expected, a positive peak occurs at twice this distance, *i.e.* 7.1 Å, whose spin-spin correlations are however weaker above T_N due to the finite magnetic correlation length. In addition, a negative peak at 6.1 Å below T_N attests to the antiferromagnetic inter-ladder ordering of the long-range ordered magnetic phase whose two possible spin assignments were also distinguished, but with greater difficulty, using standard Rietveld refinement techniques.

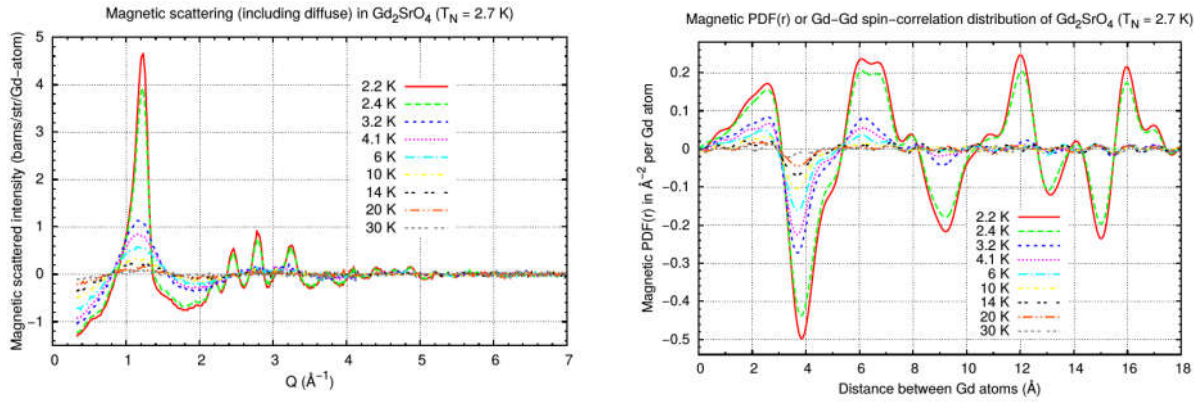

Figure 1: (Left) Magnetic Bragg peaks and magnetic diffuse scattering measured from a powder sample of $SrGd_2O_4$ with the D4c neutron diffractometer (wavelength = 0.5 Å) at the Institut Laue-Langevin. (Right) The corresponding magnetic Pair-Distribution Function or mPDF(r) obtained via Fourier transformation.

[1] B.A. Frandsen, X. Yang and S.J.L. Billinge, *Acta Cryst.* (2014) **A70**, 3-11.

Corresponding author: fischer@ill.fr

Solvent restructuring around iron oxide nanoparticles

S.L.J. Thomä[1], J. Brunner[2], B.Maier[2], E. V. Sturm (née Rosseeva)[2], M. Zobel[1]
[1]University of Bayreuth, Germany
[2]University of Konstanz, Germany

Recently, the existence of solvation shells around nanoparticles (NP) dispersed in liquid media was given proof by pair distribution function analysis (PDF).[1] The ability to build solvation shells was found to be an universal phenomenon widely independent of NP's capping agent, solvent polarity and particle size. However, a systematic study on how the single parameters influence the restructuring of solvent molecules around NPs is still lacking.
We performed a synchrotron X-ray study on oleic acid capped iron oxide nanocubes of two sizes and different degree of truncation dispersed in cyclohexane and THF and corresponding dried powder. The NPs were synthesized via the established thermal decomposition of an iron oleate precursor in solution, which yields highly monodisperse truncated cubic nanocrystals. [2]
By substracting both the solvent background as well as the NP contribution from the PDF of the NP dispersion, information on the local molecular ordering of the solvent molecules at the NP interfaces is obtained. Hereby, we detected different restructuring behavior for the investigated organic solvents relating to the extent of ordering and the layer spacing. A correlation of interfacial ordering and self-assembly behavior of the iron oxide NPs to structural features of assembled mesocrystals seems at hand. Finally, we will elucidate the formation mechanism and structuration principle of the mesocrystals, which is not understood so far. [3]

[1] M. Zobel, R. B. Neder, S. A. J. Kimber, *Science* **347** (2015), 292.
[2] J. Brunner et al.; *Adv. Mater. Interfaces* **4** (2017), 1600431
[3] E. V. Sturm, H. Cölfen, *Chem. Soc. Rev*. **45** (2016), 5821

Corresponding author: mirijam.zobel@uni-bayreuth.de

Quantitative Analysis of Complex Materials Using Non-Negative Matrix Factorisation of PDF Data

H.S. Geddes[1], H. Blade[2], L.P. Hughes[2], A.L. Goodwin[1]
[1]Inorganic Chemistry Laboratory, University of Oxford, UK
[2]AstraZeneca, Macclesfield, UK

Poor water-solubility of some crystalline drugs can result in drug formulations failing to achieve the required bioavailability. As a result, conventional pharmaceutical design methods using crystalline drug forms are sometimes insufficient in the development of effective pharmaceutical compounds. Increasingly popular alternatives include formulations in which the active pharmaceutical ingredient (API) is in an amorphous form. An important class of amorphous formulation are amorphous solid dispersions (ASDs), whereby the amorphous drug is stabilised in a water-soluble polymer binder.[1,2] ASDs are complex systems as neither component exhibits long-range structural order. Yet understanding and controlling the structural integrity of ASDs is a key challenge in pharmaceutical science because crystallisation of the drug component is a common cause of formulation degradation.[2] Recrystallisation is thought to be seeded by small nuclei that can be difficult to detect experimentally. So there is a strong need for new experimental and analytical techniques for characterising the degree of crystallinity and/or propensity for API recrystallisation in ASDs

This presentation will outline our methodology for extracting and quantifying the separate contributions to the collective Pair distribution function (PDF) of complex pharmaceutical formulations.[3] Our key result is to show that by measuring the PDFs for a series of ASDs with different API loading fractions and by interpreting these PDFs by employing a non-negative matrix factorisation (NMF) approach,[5] we are able to extract the PDFs of the component elements (including amorphous API) and the relative contributions to each formulation. Interpretation of our results allows us to determine meaningful quantities and infer conformational differences between the crystalline and amorphous forms of the API.

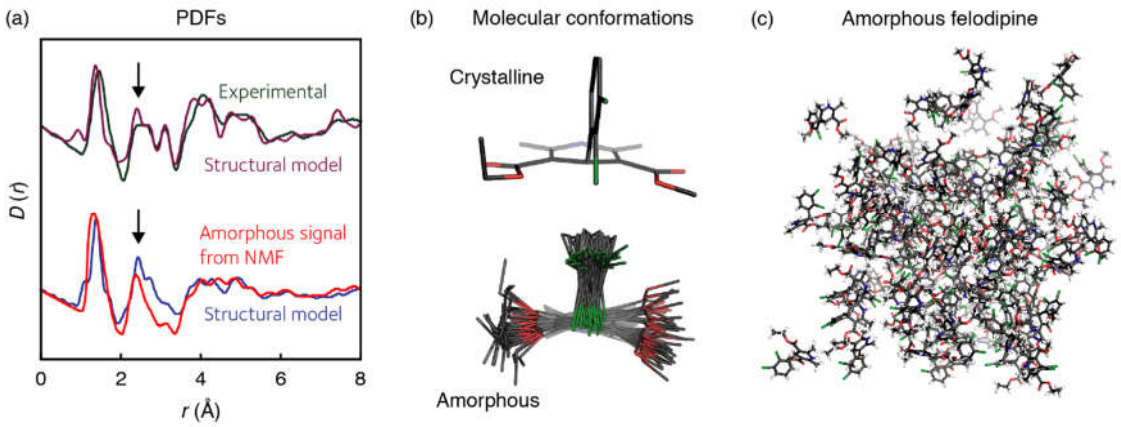

Figure 1: Comparison of the amorphous felodipine PDF extracted using NMF analysis with the PDF of crystalline felodipine (a) and corresponding superposition of felodipine molecules for crystalline (top) and amorphous felodipine (bottom) (b). (c) MD configuration for amorphous felodipine.

[1] M. Mureşan-Pop, et al., *J. Mol. Struct.* **1141** (2017), 607–614.
[2] C. L.-N. Vo, C. Park, B.-J. Lee, *Eur. J. Pharm. Biopharm.* **85** (2013), 799–813.
[3] C. A. Young, A. L. Goodwin, *J. Mater. Chem.* **21** (2011), 6464–6476.

Corresponding author: harold.geddes@chem.ox.ac.uk

Grazing incidence PDF for real time studies of thin films

A.-C. Dippel[1], M. Roelsgaard[2], Bo B. Iversen[2], O. Gutowski[1], U. Ruett[3]
[1]Deutsches Elektronen-Synchrotron DESY, Hamburg, Germany
[2]Department of Chemistry, Aarhus University, Denmark
[3]Advanced Photon Source, Argonne National Laboratory, USA

Pair distribution function (PDF) analysis has become a widely used and most effective tool to study the local structure of materials that comprise some degree of disorder. So far, it has routinely been applied to bulk samples such as powders, solid bodies, or nanoparticle dispersions. More recently, the PDF technique has more and more been utilized in the investigation of thin films. The particular difficulty to obtain high quality total scattering data from thin films lies in the small amount of sample being spread out in two dimensions but confined to typically below 1 µm in the third dimension. In addition, this layer is deposited on a substrate that is usually thicker by a factor of at least 1000. Different approaches to thin film PDF have been applied, including the exfoliation of the film from the substrate to grind it up into a powder [1] sample, as well as measuring the film on the substrate in transmission under normal incidence on the surface [2]. While both of these methods are technically similar to bulk measurements with respect to the data collection and evaluation, they have drawbacks in that they may lose film-specific structural features such as texture, or provide unfavorable signal to background ratio due to the substrate contribution. On the other hand, surface diffraction type measurements under grazing incidence yield enhanced surface sensitivity of the film regardless of the thickness of the substrate. In this presentation, we demonstrate the advantages of grazing incidence PDF to quantitatively analyse thin films with thicknesses down to a few nanometers [3]. In contrast to previous thin film PDF studies, we use microfocused high energy X-rays (>60 keV) and a large, fast area detector in rapid acquisition PDF mode. Thus, we obtain high quality PDF data on the time scale of seconds which enables *in situ* and *operando* studies of thin films in real time.

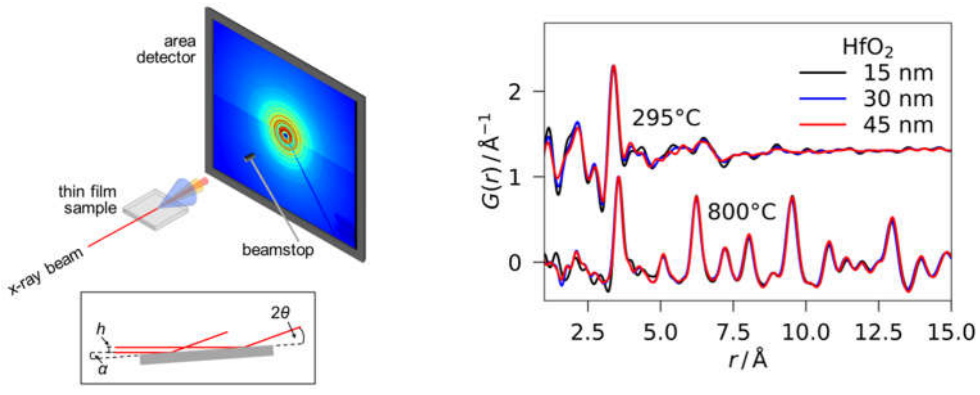

Figure 1: (left) Schematic illustration of the grazing incidence geometry, experimental setup and illumination of the sample by the x-ray beam (inset, with beam height h, incidence angle α, and scattering angle 2θ); (right) PDFs of spin-coated HfO_2 thin films heat-treated at different temperatures to form amorphous (295 °C) and crystalline (800 °C) layers, demonstrating similar data quality for the varying thicknesses.

[1] S. R. Bauers *et al.*, *J. Am. Chem. Soc.* **137** (2015), 9652.
[2] K. M. Ø. Jensen *et al, IUCrJ* **2** (2015), 481.
[3] A.-C. Dippel et al., *IUCrJ* (2019), in press.
[4] K. Stone *et al.*, *APL Mater.* **4** (2016), 076103.

Corresponding author: ann-christin.dippel@desy.de

Avoiding the Warren, Krutter and Morningstar approximation in PDF analysis

O. Masson, P. Thomas
Institut de Recherche sur les Céramiques (IRCER) – UMR CNRS 7315, Université de Limoges, Centre Européen de la Céramique, 12 rue Atlantis, 87068 Limoges Cedex, France

The atomic Pair Distribution Function (PDF) of samples containing different types of atoms, i.e. multi-component systems, is related not only to the density of atom pairs in the material but also to the chemical composition and the type of radiation used for the experiment. In the case of neutron scattering, the PDF is just a weighted linear combination of partial PDFs [1]. In the X-rays case, however, no such a simple and exact relation can be given. This comes from the fact that the Q dependence of the atomic scattering factors differs from one kind of atoms to another. This shortcoming has been noticed for a long time and was first partly overcome in 1936 by Warren, Krutter and Morningstar (WKM) [2] by using a mean form factor with effective number of electrons per atom. This approximation is still in use nowadays, more than 80 years later, and is implemented in popular software (e.g. PDFgui software [3]) dealing with periodic structure models, i.e. for which PDF is calculated as a real-space summation of peak profiles. Although simple and useful, the WKM approximation has however three major drawbacks: (i) it is not defined in a unique way, (ii) its accuracy is unknown and (iii) it can introduce significant errors for common materials combining both heavy and light elements [4]. We have recently shown than PDF is exactly expressed as a weighted linear combination of modified partial functions, which allows it to be efficiently calculated with any structure models [5].

In this presentation, we describe the effects of the WKM approximation on PDF analysis, in particular the effects on peak profile shape and refined structural parameters. We also present how PDF can be simply and exactly calculated using expression given in [5]. Finally, we demonstrate with the example of a functional material combining both heavy and light elements that only exact calculations enable subtle structural features to be extracted from X-ray PDF analysis. This example is drawn from a recent study of the local structure of apatite-type lanthanum silicates, a promising class of oxide-ion conductors [6]. It is shown that coupling X-ray PDF exact calculations and accurate structure models constructed using density functional theory enabled elucidation of the nature of their conduction mechanism, in particular the presence of oxide-ion interstitial located within the conduction channel.

[1] T. Egami and S. J. L. Billinge in *Underneath the Bragg Peaks: Structural Analysis of Complex Materials*, Pergamon Materials Series (2012).
[2] B. E. Warren, H. Krutter, O. Morningstar, *J. Am. Ceram. Soc.* **19** (1936), 202.
[3] C. L. Farrow et al., *J. Phys.: Condens. Mat.* **19** (2007), 335219.
[4] V. I. Korsunskiy, R. B. Neder, *J. Appl. Cryst.* **38** (2005), 1020.
[5] O. Masson, P. Thomas, *J. Appl. Cryst.* **46** (2013), 461.
[6] O. Masson et al., *Sci. Technol. Adv. Mater.* **18** (2017), 645.

Corresponding author: olivier.masson@unilim.fr

Mechanisms for tungsten oxide nanoparticle formation in solvothermal synthesis: From polyoxometalates to crystalline materials

Mikkel Juelsholt[1], Troels Lindahl Christiansen[1] and Kirsten M. Ø. Jensen[1]
[1]Department of Chemistry & Nanoscience Centre, University of Copenhagen

Nanoparticles of tungsten oxides have a range of important applications in e.g. gas-sensing, catalysis and in supercapacitors. Tungsten oxides show rich structural chemistry due to rich redox chemistry and a range of stable crystal structures[1]. The properties are highly dependent on the size and structure of the material, and in order to obtain a 'tailor-made' material, it is crucial to understand the mechanisms that dictate the formation of the material during synthesis. X-ray total scattering with Pair Distribution Function (PDF) analysis allows following the structural changes that take place all the way from precursor cluster over nucleation clusters to the final crystalline particles[2].

We here present a study of $(NH_4)_{0.25}WO_3$ nanostructures formed in a solvothermal synthesis by thermal decomposition of ammonium metatungstate hydrate in water and oleylamine. Using *in situ* X-ray Total Scattering and Pair Distribution Function analysis, we observe how the solvents influence the precursor and induce two distinct crystallisation pathways. We show how the reaction pathway is crucial for the defects formed in the crystalline nanoparticles. Additionally, we also show how the solvents influences the size and structure of the nanoparticles. By modifying the precursor structure, we prove that the reaction mechanism of tungsten oxide nanoparticles is directly related to the molecular structure present just before crystallisation.

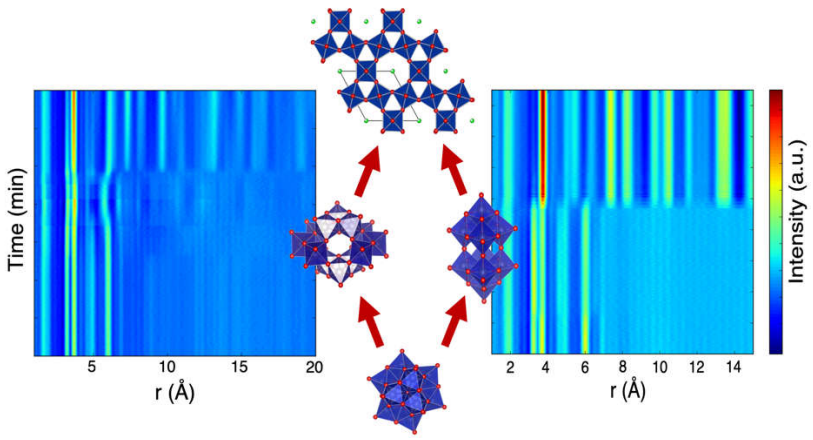

Figure 1: The two different reactions pathways to $(NH_4)_{0.25}WO_3$ nanostructures in oleylamine (left) and water (right). While both solvent result in the same crystal structure, the defects and intermediate structures formed are completely dependent on the solvent.

[1] Zheng, H., et al. *Advanced Functional Materials* **21**(2011): 2175-2196.
[2] Jensen, K. M. Ø., et al. *ChemSusChem* **7**(2014): 1594-1611.

Corresponding author: mikkel.juelsholt@chem.ku.dk

Average and Local Structure of $NaCe(WO_4)_2$ Nanophosphor: A Structure-Property Correlation

Archana K. Munirathnappa[1], Joerg C. Neuefeind[2], Premakumar Yanda[3], A. Sundaresan[3], and Nalini G. Sundaram[1]

[1]Functional Energy Nanomaterials Group, Materials Science Division, Poornaprajna Institute of Scientific Research, Bidalur, Near Devanahalli-562110, Bengaluru, Karnataka, India.

[†]Manipal Academy of Higher Education, Manipal, Karnataka, India-576104

[2]Chemical and Engineering Materials Division, ORNL, Oak Ridge, Tennsssee 37831, United States.

[3]Chemistry and Physics of Materials Unit, New Chemistry Unit and School of Advanced Materials, Jawaharlal Nehru Centre for Advanced Scientific Research, P.O Bengaluru-560064, Karnataka, India.

Rare earth activated $ARE(WO_4)_2$ materials where A=alkali metal ion and *RE*=Rare earths are multifunctional disordered materials generally applied for solid state display systems and optoelectronics owing to their unique optical properties due to the 4*f* and 4*f*-5*d* transitions [1, 2]. Among these, $NaRE(WO_4)_2$ is found to adopt Scheelite like structure [3, 4] where, the substitution of pair of Na^+ and RE^{3+} in A site of AWO_4, leads to crystallographic changes such as structural distortion, phase transformation and local structure distortions, which could affect optical properties[5]. Hence structural elucidation is of great interest to understand the importance of luminescent host lattice and its local structural distortions on the observed luminescence properties. In this context, phase pure nanoparticles of $NaCe(WO_4)_2$ are synthesized by an efficient template free solvothermal method using two different solvents (NaCeW-a) in water and (NaCeW-b) in ethylene glycol as reaction solvent under optimized reaction conditions. Insights in to surface morphology of NaCeW-a and NaCeW-b clearly show distinct difference with respect to the solvent. In addition Rietveld refinements on powder neutron diffraction (NPD) data of both the samples confirms that the $NaCe(WO_4)_2$ crystallized in Scheelite like tetragonal system with $I4_1/a$ space group. Interestingly, the local structure analysis via total scattering (PDF) refinements revealed that $NaCe(WO_4)_2$ adopts the non-centrosymmetric $I\bar{4}$ space group in the shorter 'r' range (1.5 to 10 Å). Furthermore, PDF analysis showed that the Na/CeO_8 polyhedra is slightly distorted and distributed in 2b and 2d Wyckoff sites. Additionally, high resolution XPS measurements indicated that the valence state of cerium ion is preserved to be +3 in $NaCe(WO_4)_2$ and is corroborated by VSM measurements. Both materials exhibited bright narrow green emission up on UV excitation with slight variation in emission intensity. Thus our study summarize the structure-property studies of $NaCe(WO_4)_2$ material which could be a potential candidate as green phosphor finds its application in solid state display systems.

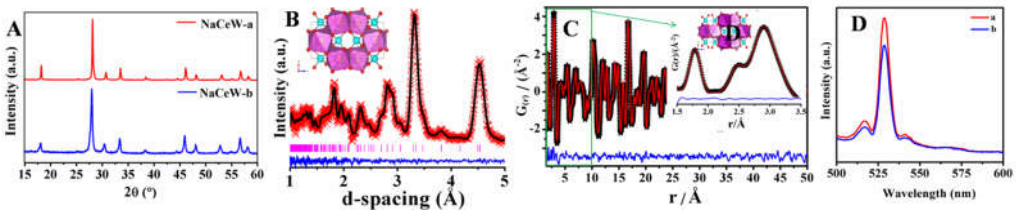

Figure A) Powder XRD patterns of NaCeW-a and NaCeW-b Figure B) Observed (red cross) calculated (black line), difference (blue) and (hkl) planes in pink obtained by the Rietveld refinements NaCeW-a and inset illustrating the crystal structure representation in *b*-direction. Figure C) PDF fit in the range from 1-50 Å, Inset shows the improved PDF fit <3.5 Å using non centrosymmetric I $\bar{4}$ space group. Figure D) Fluorescence emission spectra of NaCeW-a and NaCeW-b under UV excitation.

[1] Munirathnappa, A.K., et al., *Crystal Growth & Design*, **18,** (2017),253-263.
[2] Bhat, S.S., et al., *Phys Chem Chem Phys*, **16,** (2014),18772-80.
[3] Dirany, N., et al., *CrystEngComm*, **18**, (2016), 6579-6593.
[4] Shimemura, T., et al., *Journal of the Ceramic Society of Japan*, **124**, (2016), 938-942.
[5] Bhat, S.S.M., et al.,*Crystal Growth & Design*, **14**, (2014), 835-843.

Corresponding author: nalini@poornaprajna.org

Posters

Impact of Average, Local and Electronic Structure on Visible Light Photocatalysis in Novel $BiREWO_6$ (RE = Eu & Tb) Nanomaterials

Pradeep P. Shanbogh[1], Rajamani Raghunathan[2], Mikhail Feygenson[3], ,Joerg Neuefeind[3], Jasper Plaisier[4] and Nalini G. Sundaram[1]

[1]Functional Energy Nanomaterials Group, Materials Sciences Division, Poornaprajna Institute of Scientific Research, Bengaluru 572064, India.

[2]UGC-DAE Consortium for Scientific Research, DAVV Campus, Khandwa Road, Indore – 452001

[3]Chemical and Engineering Materials Division, Oak Ridge National Laboratory, Oak Ridge, Tennessee 37831, United States

[4]MCX Beamline, Elettra - Sincrotrone Trieste S.C.p.A., ss 14 km 163,5, 34149 Basovizza, Trieste, Italy

Bi_2WO_6, the simplest member of Aurivillius phase (n = 1) is a wide band gap (E_g =2.8 eV) semiconductor photocatalyst and can harvest light below 440 nm[1]. Generally doping alters the band gap and electronic structure of the oxide materials. Particularly[2], rare earth (RE) ions with 4*f* electronic configuration can absorb light from UV, Visible and IR which are associated with the f-f transitions[3,4], thus possibility of tuning material for wide spectrum responsive photocatalyst. This work describes the crystal structure of hydrothermally synthesized $BiEuWO_6$ and $BiTbWO_6$ nanomaterials is deduced for the first time by combined Rietveld refinement of Neutron and Synchrotron data using the ordered and disorder models available in literature. The ordered model is validated for the average structure of these nanomaterials and it is further supported by the local structure analysis using neutron pair distribution function. Rare earth substituted nanomaterials are found to be efficient photocatalysts over the parent Bi_2WO_6 under visible light irradiation for Congo-red dye degradation. The difference in the observed photocatalytic activity of these nanomaterials is also explored through detailed comparison of crystal structure and electronic structure calculated through DFT method.

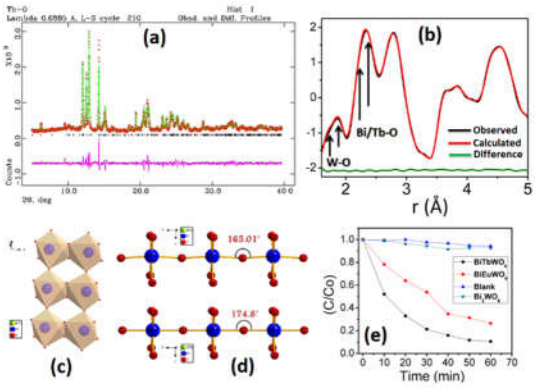

Figure 1: Observed, calculated and difference plots of $BiTbWO_6$ (a) Average structure refinement from Rietveld method (b) Local structure refinement from PDF method. (c) WO6 octahedral arrangement in BiTbWO6. (d). Corner linked W-O-W bond angle of $BiEuWO_6$ (above) and $BiTbWO_6$ (below). (e) Photocatalytic Dye degradation plots of $BiEuWO_6$ and $BiTbWO_6$.

[1] Fu, H.; Pan, C.; Yao, W.; Zhu, *J. Phys. Chem. B* **2005,** *109* (47), 22432-22439

[2] Wang, F.; Li, W.; Gu, S.; Li, H.; Wu, X.; Liu, X. *Chem. - Eur. J.* **2016,** *22* (36), 12859-12867.

[3] Tian, N.; Zhang, Y.; Huang, H.; He, Y.; Guo, Y. *J. Phys. Chem. C* **2014,** *118* (29), 15640-15648.

[4] Shanbogh, P. P.; Swain, D.; Narayana, C.; Rao, A.; Sundaram, N. G. *Cryst. Growth Des.* **2018,** *18* (4), 1935-1939.

This work is published here: Shanbogh, P. P et al., *ACS Appl. Mater. Interfaces*, **2018**, *10* (42), pp 35876–35887

Corresponding author: nalini@poornaprajna.org

Crystal structure and luminescence studies of zinc aluminate nanoparticles

Megha Jain[1,2], Manju[2,3], Ankush Vij[3], Anup Thakur[1]
[1]Advanced Materials Research Lab, Department of Basic and Applied Sciences, Punjabi University Patiala, Punjab, India-147 002
[2]Department of Physics, Punjabi University Patiala, Punjab, India-147 002
[3]Nanophosphors Lab, Department of Applied Physics, Amity University Haryana, Gurgaon, Haryana, India-122 413

$ZnAl_2O_4$ has been an attractive material due to its robust luminescence properties and promising applicability such as in solid state lighting, optoelectronic devices, catalysis, ceramics etc. [1-5]. Significant efforts have been made by researchers to explore the luminescence in doped $ZnAl_2O_4$ system. However, luminescence in its undoped state can be tuned by choosing appropriate synthesis method, temperature conditions, creation of defects and cationic vacancies [6-7]. The formation of defects enhances its properties to a significant level. In our study, solid combustion method is employed to synthesize $ZnAl_2O_4$ nanocrystals. Fuel blend approach has been utilized using two fuels urea (CH_4N_2O) and monoethanolamine (MEA) (C_2H_7NO). Luminescence behaviour is correlated with the crystal structure changes observed by varying fuel ratio. It is observed by X-ray diffraction (XRD) studies that sample prepared using urea as a fuel results in formation of a minor secondary phase corresponding to α-Al_2O_3. Rietveld refinement of XRD patterns indicates the formation of defects such as antisite defects, anion and cation vacancies etc. and yielded crystallographic information about nanocrystals. Energy band gap and Urbach energy values are indicative of band tailing and hence presence of shallow defects to different extents in all samples. Emission in blue region and near infrared (NIR) region probed by photoluminescence spectroscopy, revealed presence of various types of defects such as oxygen vacancies, cation antisite defects, cationic vacancies and interstitials. X-ray absorption near edge spectroscopy also confirmed the presence of multiple defects in all samples. Versatile applications of prepared samples in LEDs are predicted from colorimetric parameters.

[1] T. Gholami, M. Salavati-Niasari, M. Sabet, J. Clean Prod. 178 (2018) 14–21.
[2] S. B. Roshni, M. T. Sebastian, K. P. Surendran, Sci. Rep. 7 (2017) 40839.
[3] P. Loiko, A. Belyaev, O. Dymshits, I. Evdokimov, V. Vitkin, K. Volkova, M. Tsenter, A. Volokitina, M. Baranov, E. Vilejshikova, A. Baranova, A. Zhilind, J. Alloys Compd. 725 (2017) 998–1005.
[4] A. Fern´andez-Osorio, C. Rivera, A. V´azquez-Olmos, J. Ch´avez, Dyes Pigm. 119 (2015) 22–29.
[5] R. Ianos¸, S. Borc˘anescu, R. Laz˘au, Chem. Eng. J. 240 (2014) 260–263.
[6] S. T. Aruna, A. S. Mukasyan, Curr. Opin. Solid ST M. 12 (2008) 44–50.
[7] W. Wen, J.-M. Wu, RSC Adv. 4 (2014) 58090–58100.

Corresponding author: dranupthakur@gmail.com

The crystal structure of $CaSiH_{\approx 4/3}$ revisited

H. Auer, H. Kohlmann
Leipzig University, Department of Inorganic Chemistry, Johannisallee 29, 04317 Leipzig,

$CaSiH_{\approx 4/3}$ was the first Zintl phase hydride showing a polyanionic backbone of group 14 elements with an element-hydrogen contact. After its discovery and the initial claim of a covalent silicon-hydrogen interaction by DFT calculations [1], the bonding character was questioned again based on neutron diffraction and neutron vibrational spectroscopy data [2]. Until now, the bonding situation was not clear for this fundamental compound.

$CaSiH_{\approx 4/3}$ is a Zintl phase hydride. One hydrogen atom per formula unit is located in tetrahedral Ca_4-voids. The remaining hydrogen atoms coordinate silicon atoms leading to an idealised formula $CaHSi_{2/3}(SiH)_{1/3}$. The silicon binding hydrogen site is always underoccupied (≈ 50%) leading to an actual composition of $CaSiH_{1.2}$.

We did a thorough reinvestigation of $CaSiH_{\approx 4/3}$ using laboratory X-ray and neutron diffraction of the corresponding deuteride. We used ^{2}H-NMR to determine the quadrupolar coupling (C_Q) of the silicon coordinating deuterium site and interpreted these data under the aid of density functional theory calculations. Finally, we collected neutron total scattering data to directly measure the deuterium-silicon distance.

Powder diffraction patterns of $CaSiD_{\approx 4/3}$ show anisotropically broadened reflections. Depending on the parametrisation, the Si-D bond lengths strongly change. Therefore, we chose a local approach using ^{2}H-NMR and total scattering. The silicon bound deuterium site shows a quadrupole interaction of C_Q = 58(2) kHz corresponding to a structural model with a bond length of 1.56(1) Å [3]. We can now substantiate this result by a pdf-analysis (see figure). The first peak corresponds to the Si-D distance and is located at 1.54 Å. Therefore, our data allow a conclusive interpretation of the bonding situation as a covalent interaction with a Si-D bond length of 1.54 Å.

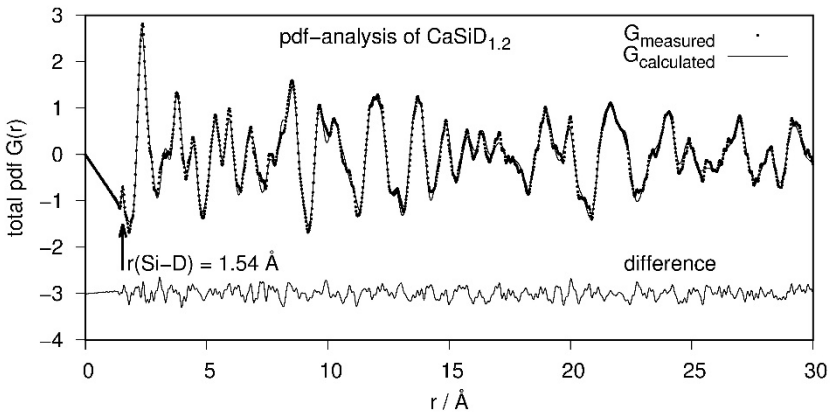

Figure. 1 Pair distribution function (pdf)-analysis of $CaSiD_{1.2}$ based on neutron total scattering data.

[1] N. Ohba, M. Aoki, T. Noritake, K. Miwa, S. Towata, *Phys. Rev. B* **72** (2005), 75104.
[2] H. Wu, W. Zhou, T. J. Udovic, J. J. Rush, T. Yildirim, *Phys. Rev. B* **74** (2006), 224101.
[3] H. Auer, R. Guehne, M. Bertmer, J. Haase, H. Kohlmann, *Z Krsitallogr. Suppl.* **38** (2018), 11.

Corresponding author: henry.auer@gmx.de

Structural evidence of multiferroicity in polycrystalline $TbMnO_3$ multiferroic

Harshit Agarwal[1], J. A. Alonso[2], N. P. Lalla[3], M. A. Shaz[1]
[1]Department of Physics, Banaras Hindu University, Varanasi, India
[2]Instituto de Ciencia de Materiales de Madrid, CSIC, Cantoblanco, E-28049 Madrid, Spain
[3]LTXRD Lab, UGC DAE CSR, Indore, India

$RMnO_3$ perovskite plays crucial role in field of multiferroics for which the structural behavior is important to understand. In case of manganites, the octahedral tilting plays important role to originate the multiferroicity. Such type of structural evidence of multiferroicity has been observed in polycrystalline $TbMnO_3$ using the study of X-ray diffraction and Neutron diffraction. The XRD pattern for polycrystalline $TbMnO_3$ has been observed at room temperature and low temperature @ 2K with zero and 7 Tesla magnetic field. The structural transition in $TbMnO_3$ has been observed at 2K and after applying the magnetic field. It was found that MnO6 octahedron in $TbMnO_3$ at 2K is much distorted than the octahedron at room temperature which is the origin of ferroelectricity in $TbMnO_3$ below 26K. Neutron diffraction study confirms that $TbMnO_3$ has an orthorhombic crystal structure (space group: Pnma, crystal symmetry: mmm) undergoing three magnetic phase transitions: first one from paramagnetic to an incommensurate antiferromagnetic ordering transition at T_N (41- 42 K) due to sinusoidal ordering of Mn^{3+}; the second one is an incommensurate-commensurate transition into a multiferroic cycloid type spin spiral transition at T_{lock} (25-27 K) and finally the antiferromagnetic ordering of Tb^{3+} moments at 7 K.

Corresponding author: harshit.agarwal@bhu.ac.in

SpecSwap-RMC: A Generalized RMC Approach to Structure, Combining Scattering and Spectroscopic Data

Lars G. M. Pettersson
Department of Physics, AlbaNova University Center, Stockholm University, SE-106 91 Stockholm, Sweden

Structure determination using Reverse Monte Carlo (RMC) typically relies on atomistic moves in a simulation model where, after each move, the property in question is computed and compared to experiment. The move is accepted if improving the agreement and accepted only with a probability related to the increased deviation if not. Since of the order a few hundred million moves need to be performed, this requires very rapid evaluation of the property in question. Typical applications include X-ray and neutron scattering and EXAFS in single-scattering mode.

RMC provides a range of maximally disordered solutions that are in agreement with the data in terms of the acceptance criterion. However, when applied to X-ray and neutron scattering on liquid water and simultaneously maximizing or minimizing the number of H-bonds, we find the fraction of tetrahedral molecules to range between 80% and 20% [1]. Different experimental probes are sensitive to different structural aspects and it can thus be advantageous to combine with, *e.g.*, spectroscopic data to narrow down the range of solutions.

To this end we have developed SpecSwap-RMC [2-4] which performs RMC on a large library of potential structures with precomputed scattering and spectroscopic signals associated with each structure. A subset of structures is selected and all properties are then built from the selected structures and compared to the experimental data. The RMC is then performed by exchanging structures instead of moving atoms. A set of weights is then generated based on how often each structure is found in the sample set when probed. These SpecSwap-RMC weights can then be used to reweigh the library, to extract an average structure that is consistent simultaneously with all the supplied data.

I will give examples of applications to liquid water, where we combine X-ray diffraction (XRD) and multiple-scattering EXAFS [3], to ice where we use SpecSwap-RMC to analyse what structures have actually been measured in XAS on various samples [5], and from ongoing work, where we combine XRD, NMR, XAS and XES [6] data on liquid water to find structures that are simultaneously consistent with all four experimental datasets.

[1] M. Leetmaa et al., *J. Chem. Phys*. **129** (2008), 084502.
[2] M. Leetmaa, K.T. Wikfeldt, L.G.M. Pettersson, *J. Phys.: Cond. Mat*. **22** (2010), 135001.
[3] K.T. Wikfeldt et al., *J. Chem. Phys*. **132** (2010), 104513.
[4] PROGRAM is available on https://github.com/leetmaa/SpecSwap-RMC.
[5] I. Zhovtobriukh, P. Norman, L.G.M. Pettersson, *J. Chem. Phys.* **150** (2019), 034501.
[6] I. Zhovtobriukh et al., work in progress.

Corresponding author: Lars.Pettersson@fysik.su.se

Direct determination of solution structure of lanthanide(III) complexes

Patrick R. Nawrocki, Nicolaj Kofod, Kirsten M. Ø. Jensen, Thomas Just Sørensen
Nano-Science Center and Department of Chemistry, University of Copenhagen, Denmark

Understanding the structure of f-block elements in solution is essential to improve upon current methods in elemental separation of lanthanides and to exploit their properties as luminescent probes [1,2]. The immediate coordination environment experienced by the lanthanides governs the ligand field parameters that split the J-coupled energy levels of the ion. Therefore, it is vital to determine the solution structure of lanthanide(III) complexes and thus determine the ligand field symmetry imposed on the trivalent lanthanide ion by the coordination sphere.

For this purpose, a total X-ray scattering approach can be used to obtain pair distribution functions, PDF, of the interatomic distances of the coordination complex [3]. Here, PDF has been used to investigate europium(III) 2,7-pyridinecarboxylate complexes. The PDF data as a function of stoichiometry is shown in Figure 1a. Optical spectroscopy was used to support the scattering data, to track the evolution of level splitting as the geometry changes. By establishing a link between the instantaneous coordination environment's point group symmetry with the luminescent fingerprint of the same system, the point group symmetry should eventually be determined by the luminescence spectra alone [4].

By investigating a titration series of europium(III) complexes with the tridentate ligand, we can determine that europium assumes a tricapped trigonal prism when fully complexes in solution.

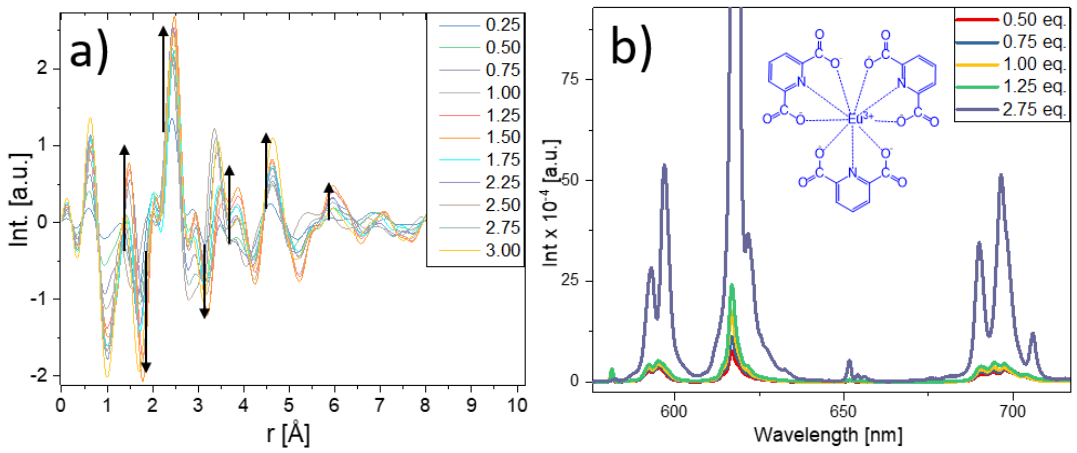

Figure 1: a) PDF data of the Eu:2,7-pyridinecarboxylate in a stoichiometry from 1:0.25 to 1:3.00 revealing how certain bond distances change through the series. b) Emission spectra at selected Eu: 2,7-pyridinecarboxylate ratios, showing the evolution of the transition band intensity and crystal-field splitting. Insert: Representation of the complex structure at a ratio of 1:3.

[1] B. J. Mincher, G. Modolo and S. P. Mezyk, *Solvent Extraction and Ion Exchange*, **27** (2009), 579-606.
[2] P. Caravan, *Chemical Reviews*, **99** (1999), 2293-2352.
[3] K. M. Ø. Jensen et al., *Journal of the American Chemical Society*, **134** (2012), 6785-6792.
[4] P. A. Tanner, *Springer Ser. Fluoresc.,* **7** (2011), 183-234.

Corresponding author: Patrick.anb@gmail.com

Bridging solid state [Ln(DOTA)]$^-$ structures with solution properties

Maria Storm Thomsen, Thomas Just Sørensen
Nano-Science Center & Department of Chemistry, University of Copenhagen, Universitetsparken 5, 2100 København Ø, Denmark

The correlation between structure and properties in molecular chemistry is indisputable [1]. While the solid state structure can be easily obtained with single-crystal X-ray diffraction[2], determining the dynamic solution structure is – particularly for f-elements–less straight forward [3]. Advances in solution phase total scattering are being made constantly [4]. There is, however, a pressing need for a way of directly connecting solution structure and observed solution properties. Our approach incorporates a study of molecular structures from single-crystal X-ray diffraction, as well as doped structures with isolated distinctive properties, to individual molecules in solution. Extensive research has been done on the kinetically inert Ln[DOTA]$^-$ complexes, primarily as a direct consequence of the use of Gd(III) complexes in magnetic resonance imaging [3a5]. Despite the rigid nature, Ln[DOTA]$^-$ complexes in solution exists as four structural ligand forms [1,3a], which gives rise to different physicochemical properties [6]. By employing solid state structures to map distinct structure-property relations, we aim to understand dynamic structures and averaged properties in solution. Solid state and solution state are bridged by dilute solid state structures of Ln[DOTA]$^-$ complexes (Figure 1). This makes it possible to isolate physicochemical properties coming from a specific form in the solid state and relate that to what is observed in solution.

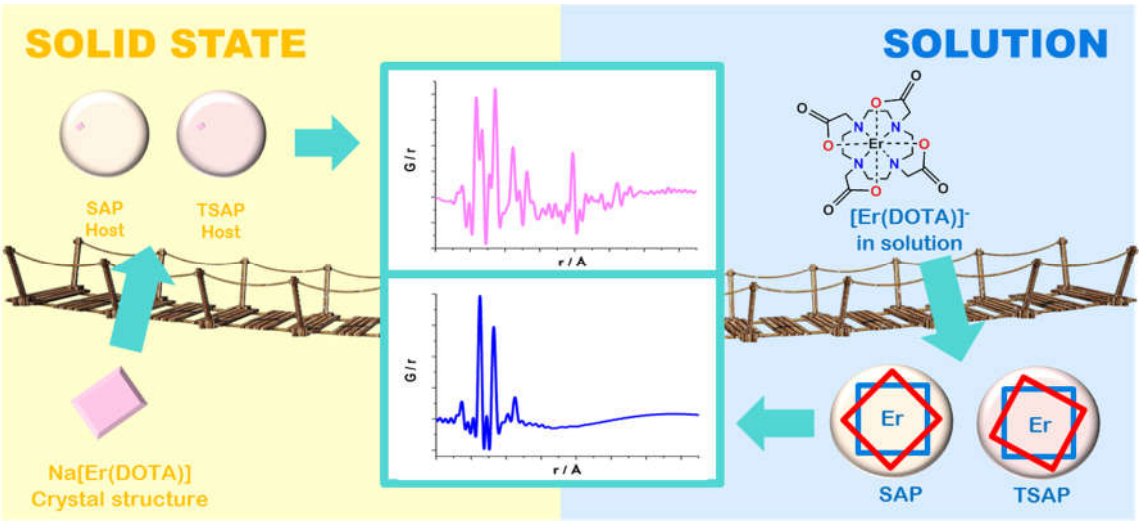

Figure 1: Understanding solution structure through PDF analysis and solid state structure.

[1] L. G. Nielsen, A. K. R. Junker and T. J. Sørensen, *Dalton Transactions*, 2018, **47**, 10360-10376.
[2] M. E. Boulon, G. Cucinotta, J. Luzon, C. Degl'Innocenti, M. Perfetti, K. Bernot, G. Calvez, A. Caneschi and R. Sessoli, *Angewandte Chemie*, 2013, **52**, 350-354.
[3] a) P. Caravan, J. J. Ellison, T. J. McMurry and R. B. Lauffer, *Chemical Reviews*, 1999, **99**, 2293-2352. b) T. J. Sørensen and S. Faulkner, *Acc Chem Res*, 2018, **51**, 2493-2501.
[4] Kirsten M. Ø. Jensen, *et al.*, *Journal of the American Chemical Society,* **2012,** *134* (15), 6785-6792
[5] a) E. M. Gale, P. Caravan, A. G. Rao, R. J. McDonald, M. Winfeld, R. J. Fleck and M. S. Gee, *Pediatric Radiology*, 2017, **47**, 507-521.
[6] a) Silvio Aime, Mauro Botta, and Giuseppe Ermondi, *Inorganic Chemistry,* 1992**,** ***31*** (21), 4291-4299. b) D. Parker, *et al., Chemical Reviews*, 2002, **102**, 1977-2010.

Corresponding author: mst@chem.ku.dk

Modified microstructure assisted gamma double prime peaks analysis in neutron diffraction

R.Y. Zhang[1], H.L. Qin[2], Z.N. Bi[2], T.L. Lee[3], J. Li[1], H.B. Dong[1]

[1]Department of Engineering, University of Leicester, University Road, Leicester LE1 7RH, UK

[2]High Temperature Materials Research Division, Central Iron and Steel Research Institute, No. 76 Xueyuannanlu, Haidian, Beijing, 100081, China

[3]ISIS Neutron Source, Rutherford Appleton Laboratory, Harwell Science and Innovation Campus, Chilton, Oxfordshire, OX11 0QX, UK

Mechanical properties of gamma prime (γ′) strengthened Ni-base superalloys can be studied using in-situ neutron diffraction technique by analysing diffraction peak shifts of both the matrix phase and strengthening phase [1]. However, this method is not available to gamma double prime (γ″) strengthened Ni-base superalloys such as Inconel 718 due to difficulties in obtaining γ″ diffraction peaks with satisfying intensity for quantitative analysis. As shown in Fig. 1a, the two γ″ variants contribute to {200} γ″ peak and {004} γ″ peak, respectively. {200} γ″ peak overlaps with {200} γ peak, while {004} γ″ peak shows low intensity. In this study, we propose a variant selection method to increase the γ″ peaks intensity so that quantitative analysis becomes possible. A bar shape Inconel 718 sample was subjected to aging heat treatment under a tensile stress along the axial axis. The applied stress differs the free energy in different γ″ variants during aging [2]. The amount of variants with more energy reduction is increased at the expense of the variants with less energy reduction in a grain. As shown in Fig 1b, the variant contributes to {004} γ″ peak is enhanced, resulting in a larger intensity of {004} γ″ peak, allowing the Pawley refinement and single peak fitting to be achieved. The lattice parameters of γ″ and γ phases are determined with fitting uncertainties less than 150 microstrains. The proposed variant selection method shows a promising potential in the studies of mechanical properties of γ″-strengthened Ni-base superalloys.

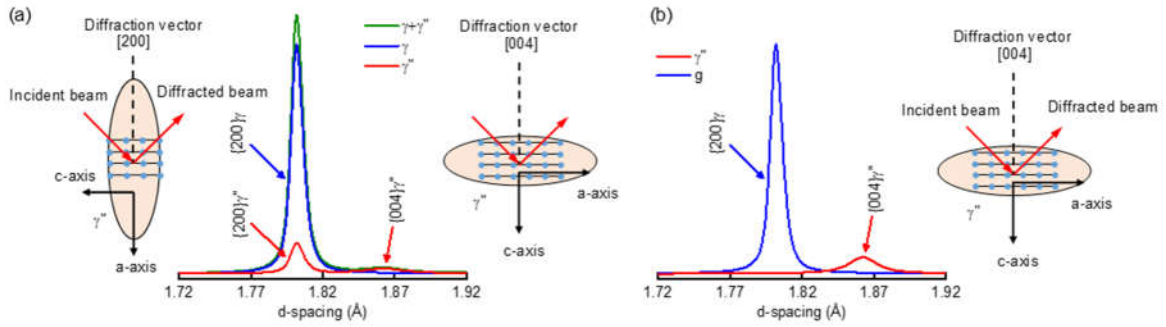

Figure. 1 Simulated neutron diffraction peaks from a material consisting of γ and γ" phase with volume fraction 87% and 13%, respectively. The γ" particle is set to be uniaxial shape with 70 nm in diameter and 15 nm in thickness. Lattice parameters are set to be $a_{\gamma"}=a_{\gamma}$=3.6 Å, and $c_{\gamma"}$=7.44 Å. (a) three γ" variants exist, (b) the amount of variant contributing to {004} γ" peak is enhanced at the expense of other variants. The intensity of {004} γ" peak from the variant selected material is enhanced with a larger height-to-background ratio

[1] E.M. Francis, B.M.B. Grant, J.Q.d. Fonseca, P.J. Phillips, M.J. Mills, M.R. Daymond, M. Preuss, Acta Mater., 74 (2014) 18-29.

[2] M. Gao, D.G. Harlow, R.P. Wei, S. Chen, Metall. Mater. Trans. A, 27 (1996) 3391-3398.

Corresponding author. Email address: hd38@le.ac.uk.

Temperature induced changes in the hydrogen-bond network of water-isopropanol mixtures at low isopropanol concentration range

Sz. Pothoczki[1], I. Bakó[2], L. Pusztai[1]
[1]Institute for Solid State Physics and Opics, Wigner RCP of the H.A.S. H-1121, Budapest, Konkoly Thege út 29-33, Hungary
[2]Institute of Organic Chemistry Research Centre for Natural Sciences, Hungarian Academy of Sciences, Magyar Tudósok körútja 2, P.O. Box 286, Budapest, Hungary

Isopropanol-water mixtures have attracted a continuous interest thanks to their anomalous behaviour in many aspects (thermodynamic and transport properties, diffusion coefficient, compressibility, viscosity). These features are reflected their non-trivial liquid-phase diagram as well. In these systems, hydrogen bonds play a fundamental role. By means of monitoring of their changes as a function of temperature can elucidate the freezing process at the molecular level.

For this purpose, we have performed a series of Molecular Dynamics simulations for isopropanol-water mixtures with 5, 10 and 20 mol% isopropanol content for reproducing X-ray diffraction data [1] at the available temperatures: 298 K and 268 K (for x=0.05); 298 K, 268 K and 263 K (for x=0.1); 298 K, 268 K, 263 K and 258 K (for x=0.2). For isopropanol the All-Atom Optimized Potential for Liquid Simulations (OPLS-AA) [2] has been used in each calculation. In order to find the potentials that provide the best agreement with experimental total scattering X-ray structure factors [1] we have applied two different water force field, the Extended Simple Point Charge model (SPC/E) [3] and the improved Transferable Intermolecular Potential with four Particles (TIP4P-2005) [4].

The resulting MD trajectories have been analysed to reveal the hydrogen-bond network. Two molecules are considered to be hydrogen-bonded to each other if they are found at a distance r(O···H) < 2.5 Å, and the interaction energy is smaller than -12 kJ/mol. [5]

Average number of hydrogen bonds/molecule as a function of composition and temperature has been calculated. Fractions of ethanol molecules as H-acceptors and as H-donors in the H-bonds have been identified. Observable trends on varying the temperature have been revealed in terms of size distributions of cyclic entities. [6] Furthermore, dynamical properties have been investigated. [7]

[1] T. Takamuku, K. Saisho, S. Nozawa, T. Yamaguchi, J. Mol. Liq. **119** (2005), 133.
[2] W.L. Jorgensen; D. Maxwell, S. Tirado-Rives, J. Am. Chem. Soc. **118** (1996), 11225.
[3] H. J. C. Berendsen, J. R. Grigera, T. P. Straatsma, J. Phys. Chem. **91** (1987), 6269.
[4] J. L. F. Abascal, C. Vega, J. Chem. Phys. **123** (2005), 234505.
[5] I. Bakó, J. Oláh, A. Lábas, Sz. Bálint, L. Pusztai, M.C. Bellissent Funel, J. Mol. Liq. **228** (2017), 25.
[6] Sz. Pothoczki. L. Pusztai, I. Bakó, J. Phys. Chem. B **122** (2018), 6790.
[7] Sz. Pothoczki, L. Pusztai, I. Bakó, J. Mol. Liq. **271** (2018), 571.

Corresponding author: pothoczki.szilvia@wigner.mta.hu

Formation mechanisms of tungsten oxide nanoparticles: Automated treatment of *in situ* PDF data for structural analysis

Emil T. S. Kjær, Mikkel Juelsholt, Troels L. Christiansen, Kirsten M. Ø. Jensen
Nanoscience Center and Department of Chemistry, University of Copenhagen, Denmark

In order to tailor make materials with specific properties, it is crucial to be able to control the material structure. To probe the structural changes happening during synthesis, we here apply *in situ* x-ray total scattering to the synthesis of tungsten oxide nanoparticles in alcohols. Using Pair Distribution Function (PDF) analysis, the structural development of precursors to nanoparticles can be followed in real time, allowing to deduce atomic scale mechanisms for material formation [1].
To extract all structural information out of large sets of time resolved, *in situ* PDF data, it is crucial for the data to be treated automatically and correctly. In particular, robust background subtraction and validation methods of the resulting PDFs are needed to systematically obtain the best possible PDFs. We here present a batch script written in python which automize several steps and makes it possible to treat data all the way from instrument calibration to initial structure characterization in one step. Through Pearson correlation, hundreds of known structures can rapidly be compared to the obtained, time resolved PDFs. By generating a PDF from a CIF and comparing it with the experimental data a linear correlation value from -1 to 1 can be calculated, hence discarding or saving structural models for further analysis. To decrease computation power while treating large data sets the Nyquist-Shannon sampling theorem has been implemented, reducing the number of datapoint without removing any structural information given in the PDF [2]. Calibration, integration and fitting are compatible/implemented through software libraries such as Fit2D, PyFAI [3] and DiffPy. Here the methodology is presented through a demonstration of synthesis of tungsten oxide nanoparticles in alcohols [4].

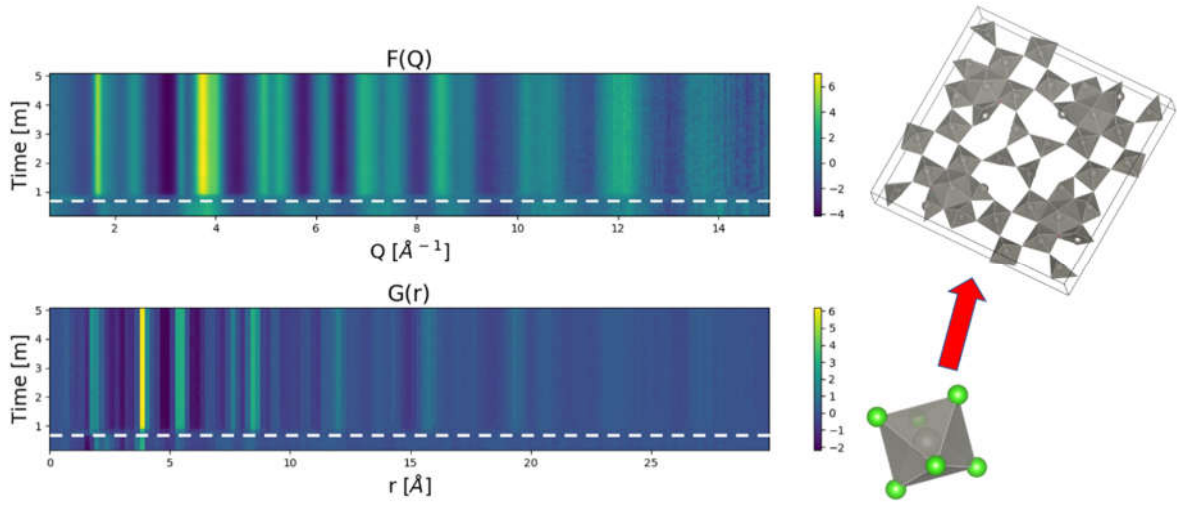

Figure 1: *In situ* PDF of WCl_6 in propanol heated at 310ºC. White dotted line indicated when the sampled was heated.

[1] Jensen, K.M.Ø., et al. ChemSusChem. **6** (2014): p. 1594-1611.
[2] Farrow, C.L., et al. *Phys. Rev. B* **84** (2011).
[3] Kieffer J. and Wright J. P. *Powder Diffraction, **28*** (2013), S339-S350
[4] Polleux, J., M. Antonietti, and M. Niederberger, *Journal of Materials Chemistry*. **16** (2006): p. 3969-3975.

Corresponding author: rsz113@alumni.ku.dk

Deconvolved intrinsic and extrinsic contributions to electrostrain in high performance (1-*x*)Ba($Zr_{0.2}Ti_{0.8}$)O_3-*x*($Ba_{0.7}Ca_{0.3}$)TiO_3 piezoceramics

Alicia Manjón-Sanz[1,2], Charles M. Culbertson[1], Dong Hou[3,4], Jacob L. Jones[4], Michelle R. Dolgos[1,5]
[1]Department of Chemistry, Oregon State University, Corvallis, Oregon, 97331, USA
[2]CELLS-ALBA Synchrotron Light Facility, Cerdanyola del Vallés, 08290 Barcelona, Spain
[3]Department of Materials Science and Engineering, Faculty of Natural Sciences, Norwegian University of Science and Technology, 7491 Trondheim, Norway
[4]Department of Materials Science and Engineering, North Carolina State University, Raleigh, North Carolina,27695, USA
[5]Department of Chemistry, University of Calgary, Calgary, Alberta, Canada T2N 1N4, Canada

The piezoceramic (1-*x*)Ba($Zr_{0.2}Ti_{0.8}$)O_3-*x*($Ba_{0.7}Ca_{0.3}$)TiO_3 (BZT-*x*BCT) has emerged as a leading lead-free candidate to replace $Pb(Zr_{1-x}Ti_x)O_3$ (PZT) for certain applications, adopting both the perovskite structure ABO_3. However, the structural response of BZT-*x*BCT to an electric field is not well understood, particularly how the local structure responds to varying electric fields. In this study, *in situ* synchrotron X-ray diffraction and total scattering measurements were performed on BZT-*x*BCT from *x* = 0.45 to 0.60 by using the set-up shown in Figure 1a. The lattice distortions were quantified from the unit cell parameters for the compositions in the orthorhombic (O) region (*x* = 0.45 to 0.50) and tetragonal (T) region (*x* = 0.51 to 0.60). It was found that the lattice distortion is minimized in compositions that exhibit the largest effective piezoelectric effect, particularly at the *x* = 0.45 composition (between the rhombohedral (R) and O regions), and at the morphotropic phase boundary (MPB) composition *x* = 0.50 (between O and T regions) (Figure 1b) where the physical properties are maximized. The degree of domain wall motion was quantified, and the results indicate that as the MPB is approached, the degree of domain wall motion increases dramatically. The increase in domain wall motion also coincides with the minimization of the lattice distortion. The pair distribution functions (PDFs) were calculated from the Fourier transform of the total scattering data. Analysis of the PDF peak shifts with electric field shows nonlinear lattice strains across all compositions, which indicates a deviation from classical piezoelectric behavior. We conclude that the strong piezoelectric properties in the BZT-*x*BCT system are attributed to an increased degree of domain wall reorientation that is facilitated by a decreased lattice distortion.

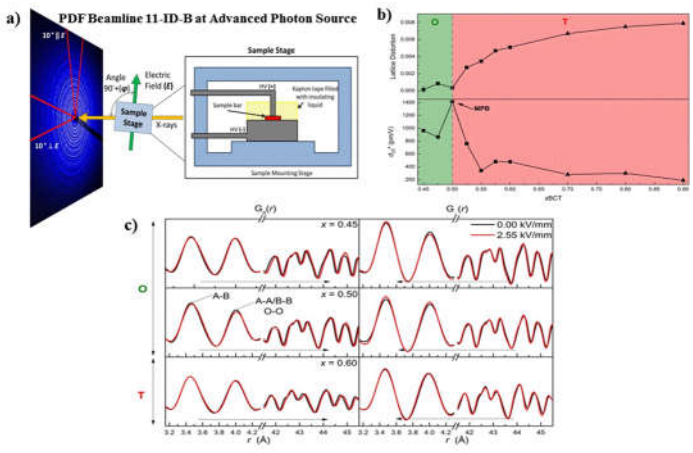

Figure 1: a) Schematic illustrating the experimental setup for synchrotron X-ray total scattering and diffraction measurements where φ = 4-8°. b) For BZT-*x*BCT ceramics as a function of composition (*x*): at the top, lattice distortion of the perovskite structure, and at the bottom, effective piezoelectric coefficient d_{33}^*. c) Low-*r* and high-*r* *G*(*r*) for *E* = 0.00 and *E* = 2.55 kV/mm for $G_{||}(r)$ and $G_{\perp}(r)$ for *x* = 0.45, 0.50 in the orthorhombic (O) range, and 0.60 in the tetragonal (T) range. Black arrows indicate that peaks shift to higher and lower *r* for $G_{||}(r)$ and $G_{\perp}(r)$, respectively.

Corresponding author: amanjon@cells.es

Characterization of the formation of metal oxido clusters by complex modelling of PDF and SAXS

Andy S. Anker[1], Troels Lindahl Christiansen[1], Marcus Weber[2], Martin Schmiele[3], Erik Brok[3], Emil T. S. Kjær[1], Pavol Juhás[4], Rico Thomas[2], Michael Mehring[2] and Kirsten M. Ø. Jensen[1]
[1]Nanoscience Center and Department of Chemistry, University of Copenhagen
[2]Institute of Chemistry, Chemnitz
[3]Niels Bohr Institute, University of Copenhagen, Nanoscience Center, University of Copenhagen
[4]Computational Science Initiative, Brookhaven National Laboratory

Metal oxides of bismuth and its oxido clusters in solution have attracted much attention with potential applications ranging from antibacterial agents to photocatalysis. In order to improve the photocatalytic activity of β-Bi_2O_3, it has been shown that easily accessible $\{Bi_{38}O_{45}\}$-based clusters represent well suited molecular precursors [1]. However, the chemical processes involved in the cluster formation are not well understood: While the molecular structures of various clusters have been solved by single crystal diffraction, it is much more challenging to study structures of such clusters directly in solution.

Bismuth oxido clusters exist in a range of sizes, most of them built up by simple or edge-sharing octahedral $\{Bi_6Ox\}$ units, but studies on their conversion processes are restricted to electrospray mass spectrometry. Here, we use *in situ* X-ray total scattering with PDF analysis to study the formation of a $\{Bi_{38}O_{45}\}$ cluster starting from $[Bi_6O_5(OH)_3(NO_3)_5]\cdot(H_2O)_3$ crystals dissolved in DMSO. The PDF analysis gives unique insight into the structural rearrangements on the atomic scale. By combining with Small Angle X-ray Scattering, SAXS, we furthermore investigate the size, morphology and size dispersion of the clusters taking place in the process. These two techniques complement each other, allowing us to follow the cluster chemistry as it takes place.

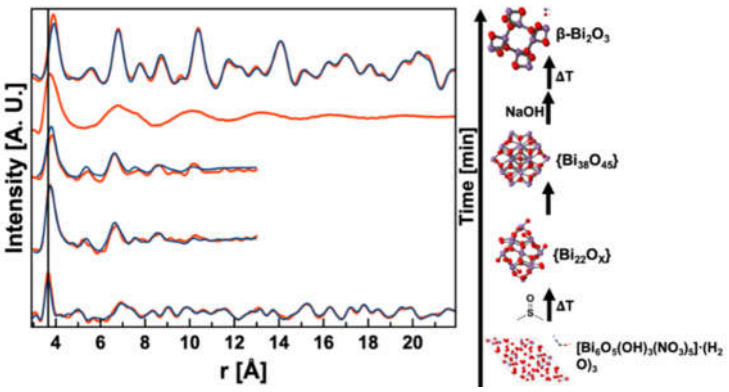

Figure 1: The chemical process from $[Bi_6O_5(OH)_3(NO_3)_5]\cdot(H_2O)_3$ crystals dissolved in DMSO through an bismuth oxido growth process and an amorphous phase, before nucleation of β-Bi_2O_3 crystals**.** The structure of the amorphous phase has not yet been characterized. A line about r = 3.8 Å is inserted to guide the eye in order to observe increasing Bi – Bi distances.

[1] M. Schlesinger, et. al, *Dalton T* **42** (2013), 1047-1056
[2] M. Mehring in *Metal Oxido Clusters of Group 13–15 Elements*, in *Clusters – Contemporary Insight in Structure and Bonding*, Editor S. Dehnen, Springer International Publishing: Cham. (2017), p. 201-268.
[3] C. Falaise et. Al, *J Am Chem Soc,* **135**(42): (2013) ,15678-81.
[4] K. J. Mitchell, K.A. Abboud, and G. Christou, *Nat Commun.,* **8**(1) (2017), 1445.
[5] L. Söderholm et. al., *Angew. Chem. Int. Ed. Engl*., **47**(2) (2008), 298-302.

Corresponding author: andy@nano.ku.dk

Chiral smectic phases of 3F4X$_1$PhX$_2$ (X$_1$, X$_2$ = H, F) compounds studied by X-ray diffraction combined with molecular modeling

A. Deptuch[1], M. Dziurka[2], J. Hooper[2], M. Srebro-Hooper[2], T. Jaworska-Gołąb[1], M. Marzec[1], D. Pociecha[3], M. Urbańska[4], M. Tykarska[4]

[1]M. Smoluchowski Institute of Physics, Jagiellonian University, Cracow, Poland
[2]Faculty of Chemistry, Jagiellonian University, Cracow, Poland
[3]Faculty of Chemistry, University of Warsaw, Warsaw, Poland
[4]Institute of Chemistry, Military University of Technology, Warsaw, Poland

Three chiral liquid crystalline compounds denoted as 3F4HPhH, 3F4HPhF and 3F4FPhF [1] with 0, 1 and 2 fluorine atoms in one aromatic ring, respectively (Figure 1a) were studied by X-ray diffraction (XRD) and theoretical calculations based on the density functional theory (DFT). XRD patterns were collected for polycrystalline samples in capillaries on Empyrean 2 diffractometer (PANalytical; CuKα, Debye-Scherrer geometry) with Cryostream 700 Plus (Oxford Cryosystems) temperature attachment and for flat samples deposited on Si wafers on D8 Discover diffractometer (Bruker; CuKα, θ/2θ scan) with Anton Paar DC350 temperature attachment. DFT calculations were performed in Gaussian 09 [2]. Molecules were optimised in four extended conformations with different orientations of the $C_3F_7CH_2OC_mH_{2m}O$- and -$COOC^*HCH_3C_6H_{13}$ chains [3].

XRD patterns were used to obtain the temperature dependence of the structural parameters of ferroelectric smectic C* (SmC*) and antiferroelectric smectic C_A* (SmC_A*) phases, namely: layer thickness *D*, the average distance *d* between molecules within layers and the correlation length ξ of the short-range order (Figure 1b). Despite similar values of *D* and *d* for the studied compounds, a decrease of ξ with increasing number of F atoms in the aromatic core was observed. Finally, the tilt angle values (the average angle that molecules make with the normal to the smectic plane) were calculated basing on the layer thickness and using the molecular length and shape-related correction [4] from DFT calculations. The values are compared with the tilt angles measured by the standard electro-optic method [3].

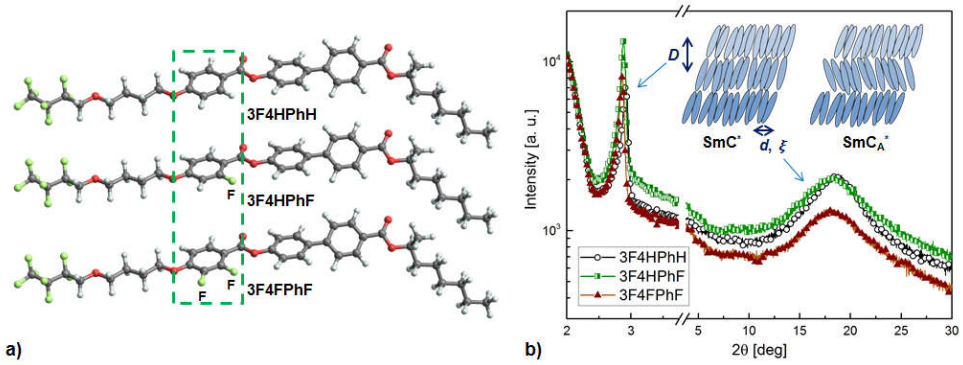

Figure 1: Molecules of 3F4X$_1$PhX$_2$ (X$_1$, X$_2$ = H, F) optimised with the DFT method, with the fluorinated ring marked by the rectangle (a) and XRD patterns of the samples in the SmC* phase collected about 110°C (b). The inset in (b) shows schematically the arrangement of molecules in the SmC* and SmC_A* phases.

[1] M. Żurowska et al. *J. Mater. Chem.*, **21** (2011), 2144-2153.
[2] Gaussian 09, Revision D.01. M.J. Frisch et al. Gaussian, Inc., Wallingford CT, 2013.
[3] A. Deptuch et al., *Liq. Cryst.*, submitted.
[4] A. Deptuch et al., *Phase Trans.*, **91** (2018), 186-198.

Corresponding author: aleksandra.deptuch@doctoral.uj.edu.pl

Resolving structures of Eu(III) nitrates in solution supported by Pair Distribution Function

Nicolaj Kofod, Patrick R. Nawrocki, Mikkel Juelsholt, Troels Lindahl Christiansen, Kirsten M.Ø. Jensen, Thomas Just Sørensen
Department of Chemistry and Nano-Science Center, Univeristy of Copenhagen, Universitetsparken 5, 2100 København Ø, Denmark

The rare earth elements are indispensable in modern technology as their unique properties are used in optical sensors, high performance magnets and as MR-contrast agents. In order to keep up with ever increasing demands for these elements, the techniques for rare earth extraction and separation must be improved. However, this requires a deeper insight into the solution chemistry of the trivalent ions, which is not well understood. The Laporte forbidden *f-f* transitions of these ions are strongly dependent to the crystal field symmetry and quenching from solvent molecules [1]. Furthermore, it has been shown that total x-ray scattering is an effective tool for investigating the solution structure of heavy elements [2,3]. In this study, we have studied the coordination chemistry of Eu(III) in methanol as the solvate as well as the complexes formed with nitrate by using a combination of total scattering, steady state, and time-resolved optical spectroscopy. By using spectroscopy, we can study the coordination geometry, the number of coordinated solvent molecules (q) [4], and the crystal field symmetry. This information we can correlate to total x-ray scattering data and probe the structure of the Eu(III) complexes in solution.

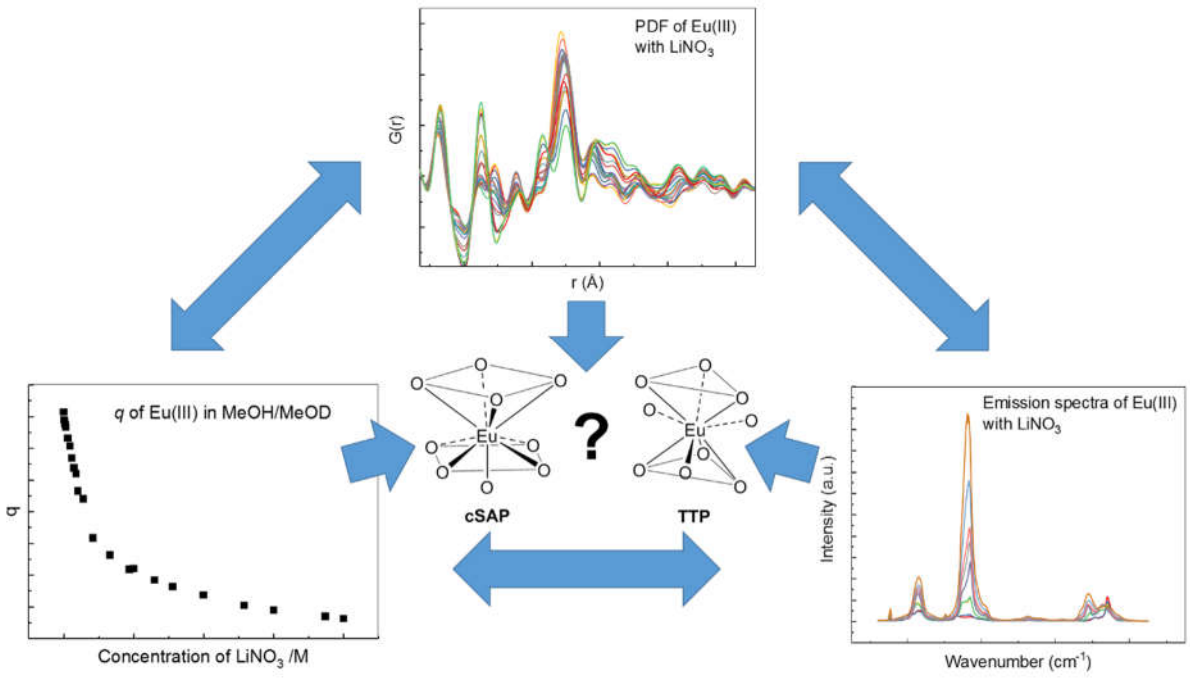

Figure 1: Total X-ray scattering (top) number of solvent molecules (q) (left) and emission spectra (right) of Eu(III) in methanol with different concentrations of $LiNO_3$

[1] M. Tropiano et. al., Journal of Luminescence, **2015**, 167, 296-304
[2] A. Habenschuss, F. H. Spedding, The Journal of Chemical Physics, **1979**, 70 (6), 2797-2806
[3] L. Soderholm, Analytical and Bioanalytical Chemistry, **2005**, 383 (1), 48-55
[4] A. Beeby et al., Journal of the Chemical Society, Perkin Transactions 2, **1999**, (3), 493-504

Corresponding author: nicolaj.kofod@chem.ku.dk

Nickel(II) cyanide as a classical realisation of the quantum S=1/2 XX chain

E. H. Wolpert, A. Simonov, A. L. Goodwin
Department of Chemistry, University of Oxford, Inorganic Chemistry Laboratory, South Parks Road, Oxford OX1 3QR, United Kingdom

One-dimensional statistical mechanical models continue to assume a particular importance in contemporary condensed-matter physics. Much of the focus within the field thus far has been on systems with one-dimensional electronic or magnetic behaviour, yet, it has long been known that the one-dimensional Ising model is also relevant to the structural behaviour of some surprisingly simple bulk phases [1,2]. These mappings have been used to interpret otherwise unexpected physical properties of some fundamentally important systems.
In our work we consider the problem of structural disorder in the layered inorganic material nickel(II) cyanide and demonstrate its relevance to a simple one-dimensional model of interacting anisotropic quaternions. The continuous degrees of freedom in the model are related to those of the S=1/2 particle. Our more general interest is in establishing meaningful correspondences between complex structural states and exotic magnetic and/or electronic phases in order to develop physical realisations of the latter for detailed study or exploitation.

We show that the relative positions of the square planar layers of nickel cyanide can be mapped onto a unit quaternion (Fig. 1). The nature of the interactions between the sheets, which is dominated by electrostatics, is then transformed into a dot product between neighbouring quaternions, leading to a 1D anisotropic chain of quaternions. From Monte Carlo simulations of the one-dimensional chain, we show that the simulated X-ray diffraction pattern reproduce the features of the experimental data remarkably well (Fig. 1) [3]. Thus we are able to show that nickel (II) cyanide is a physical realization of the anisotropic 1D quaternion chain. Hence finding a link between S=1/2 particle behavior and classical systems.

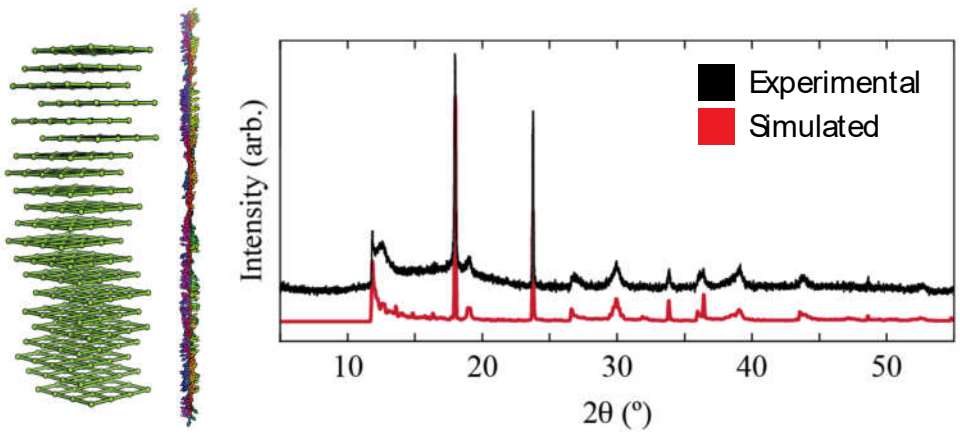

Figure 1: Mapping of nickel cyanide displacements such that the positions of the layers can be represented as quaternions projecting in four-dimensional space. Experimental (black) and simulated (red) X-ray diffraction patterns of nickel cyanide.

[1] S. Ramasesha and C. N. R. Rao, *Philos. Mag.* **34** (1977), 827-833.
[2] M. K. Uppal, S. Ramasesha and C. N. R. Rao. *Acta Cryst. A* **36** (1980), 356-361.
[3] A. L. Goodwin et al., *Phys. Rev. B* **80**, (2009), 054101

Corresponding author: emma.wolpert@chem.ox.ac.uk

^{36}Argon hydrate: an isotopic substitution study of the structure-II clathrate hydrate by neutron diffraction

P. H. B. Brant Carvalho[1], U. Häussermann[1], O. Andersson[2], C. Tulk[3], J. Molaison[3]
[1]Department of Materials and Environmental Chemistry, Stockholm University, Stockholm, Sweden
[2]Department of Physics, Umeå University, Umeå, Sweden
[3]Chemical and Engineering Materials Division, Oak Ridge National Laboratory, Oak Ridge-TN, USA

Clathrate hydrates (CHs) are crystalline inclusion compounds in which water forms a host with polyhedral cages that enclose small concentrations of guest molecules or noble gas atoms. There are two major clathrate structures, both cubic, often denoted as "CS-I" and "CS-II" [1]. Argon is a very weakly interacting guest. However, CS-II structured Ar CH forms when ice is exposed to slightly pressurized Ar (150 bar) with ice at low temperatures (below 250 K). Ar CH amorphizes near 1.2 GPa on pressurization at 95 K in close similarity to the pressure induced amorphization (PIA) of ice, which produces high-density amorphous ice (HDA) [1-4]. Of particular interest are the structural properties of the Ar CH: before and after PIA, after isobarically heating the PIA form to high temperature (ca. 160 K) above 1 GPa, potentially forming a very HDA type of state, and after subsequent isothermal reduction of pressure to ca. 0.1 GPa at about 135 K, potentially forming a low-density amorphous type of state. Ar-CH is peculiar because isotope substitution (Ar and ^{36}Ar) will allow (indirectly) the separation of water – water correlations and thus enable more accurate calculation of the amorphous water structure, without the contributions from the Ar – Ar, Ar – D, or Ar – O correlations. This is because the difference in scattering lengths of naturally occurring Ar and the isotope ^{36}Ar is among the largest of any isotope. Performing an isotope substitution and subtraction experiment with two samples containing natural Ar and ^{36}Ar under identical conditions will enable removal of the water – water correlations and result in the Ar – X correlations remaining. Isotopically substituted Ar CH can be also studied on its crystalline form for a better interpretation of its guest positional disorder [5]. Comparison with amorphous forms of ice will answer the question whether CHs are true proxies of amorphous water ice and will shed new light into origin and nature of the amorphous states of water.

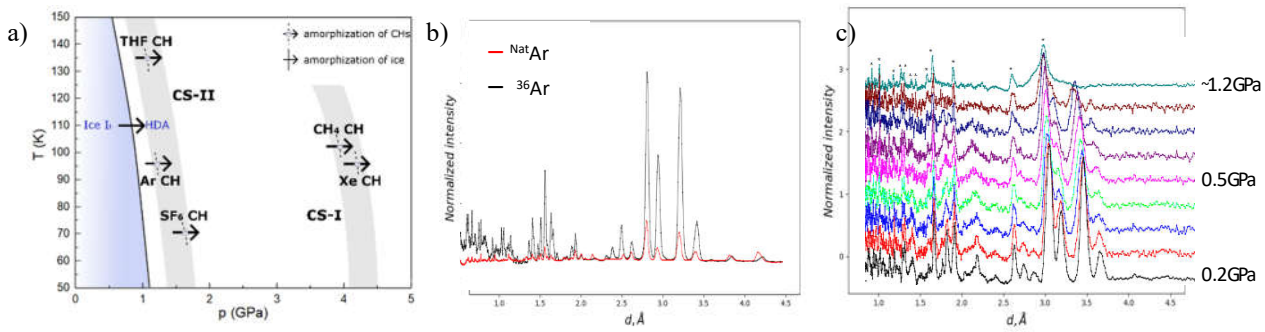

Figure 1: a) p-T diagram of ice and several CHs (data from different published [1-4] and unpublished work) showing their PIA. Grey areas highlight a tendency among CS-I and CS-II CHs. b) Difference between ^{Nat}Ar and ^{36}Ar CH neutron powder diffraction due to the 13 times stronger scattering length of ^{36}Ar. c) in situ neutron diffraction patterns following the step-wise pressurization of ^{36}Ar CH. Data collected at the SNAP beamline at SNS, ORNL.

[1] J. S. Loveday, R. J. Nelmes, Phys. Chem. Chem. Phys. 2008, 10, 937.
[2] O. Andersson, A. Inaba, J. Phys. Chem. Lett. 2012, 3, 1951−1955.
[3] O. Andersson, Y. Nakazawa, J. Phys. Chem. B 2015, 119, 3846.
[4] C. A. Tulk et al., Phys. Rev. B. 2012, 86, 054110; Y. P. Handa, J. S. Tse et al., J. Chem. Phys. 94 (1) 1991.
[5] L. Yang, C. A. Tulk, et al., Chem. Phys. Lett. 2010, 485, 104-109.

Corresponding author: paulo.barros@mmk.su.se

Local structure and big box modelling of Sn-doped BCZT lead-free piezoelectrics

F. Marlton[1], A. Pramanick[2], M. Jørgensen[1,3]
[1]Center for Materials Crystallography, iNano & Department of Chemistry, Aarhus University, Aarhus, Denmark
[2]Department of Physics and Materials Science, City University of Hong Kong Kowloon, Hong Kong SAR
[3]MAX IV Laboratory, Lund University, SE-221 00 Lund, Sweden

Piezoelectrics are highly functional materials due to their ability to couple electrical and mechanical energy. The piezoelectrics market is dominated by lead-based materials and hence, due to environmental concerns, there have been global efforts to find lead-free alternatives. This study is aimed at developing an understanding of the structure of these materials with regard to their electromechanical properties for future rational design.

Focus has been placed on relaxor based piezoelectrics as they tend to show local scale structural disorder and large electric field induced strain. However, their mechanisms are still highly debated. The materials focused upon here are derivatives from the BCZT ($(Ba_x\text{-}Ca_{1-x})(Zr_y\text{-}Ti_{1-y})O_3$) lead-free system, where compositions have shown promise for lead-free materials. Sn doping has been used to modify the cation displacements on the A and B sites of the perovskite structure.

X-ray and Neutron Pair Distribution Function (PDF) data has been used to assess the local structural features present and their deviations from the average structure. This has been analysed with small-box refinements and Reverse Monte Carlo (RMC) big-box modelling to understand the atomic displacements and correlations.

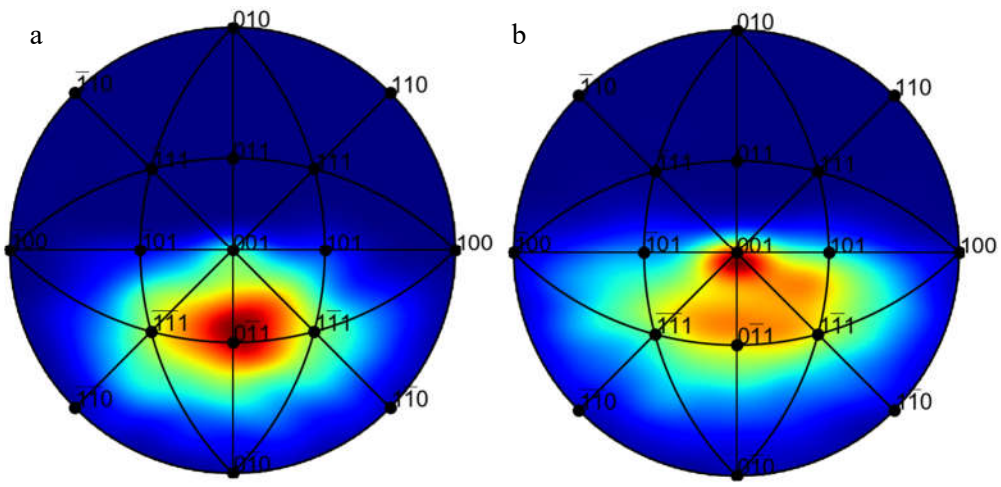

Figure 1: B-site atomic displacements in Sn-doped BCZT ceramics at a) 300K and b) 400K. Stereographic projections are based upon the perovskite pseudo-cubic structure. The colour intensity corresponds to the number of displacements weighted by the magnitude of the displacement.

Corresponding author: fredm@inano.au.dk

Structure of functionalised amorphous geopolymers

Monica Dapiaggi[1], Andrea Bernasconi[2], Mattia Nazzaro[3], Hermes Farina[3], Marco Cantaluppi[1] & Giorgia Confalonieri[4]

[1]Dipartimento di Scienze della Terra, Università degli Studi di Milano, Italia

[2]Ideal Standard International, Italia

[3]Dipartimento di Chimica, Università degli Studi di Milano, Italia

[4]Dipartimento di Scienze della Terra, Università degli Studi di Torino, Italia

Geopolymers are amorphous analogue of crystalline natural tectosilicates (like zeolites, for example), and have received a lot of attention in the recent years, due to their technological properties, such as low weight, mechanical resistance, and extreme versatility.

Silico-aluminate raw materials are used for a polycondensation reaction, with the aid of basic solutions containing cations such as Na, Ca, and/or K. They have an amorphous or semi-crystalline structure, which strongly depends on the synthesis conditions (type and amount of activator, pH and calcination temperature). Various geopolymers were produced, with different Si/Al ratios, and different cations (K or Na). In order to produce hybrid geopolymers, the starting source of silica was APTES ((3-aminopropyl)triethoxysilane) instead of the usual TEOS (tetraethyl orthosilicate). Different amounts of functionalised silicon were tried (from 0 to 100% wt), with Na^+ and K^+ as the balancing cation for Al/Si substitution.

Due to their amorphous nature, geopolymers are usually studied by means of solid state NMR, which provides the very local structure. However, more details about the relationship between the local and the medium range structure may be necessary, in order to understand their properties. Total scattering measurements, analysed by means of the EPSR (Empirical Potential Structure Refinement [1], and references therein) approach may then be used. So far, there are only a few papers in the literature using the total scattering approach (see [2] and references within), mainly studying geopolymers local structure as a function of temperature, concentrating mainly on the onset of crystallisation and on the fully crystallised sample. The samples were analysed by means of high-energy X-ray total scattering (at the beamline ID11@ESRF in Grenoble), and the corresponding Pair Distribution Functions (PDF) were produced. The data were modelled with EPSR, and produced very interesting results. EPSR modeling showed a strong dependence of the Si-O bond length (and bond length distribution) as a function of the amount of functionalized silicon; Al-O bond results more disordered than Si-O one, while Na and K really behave as charge-compensating cations. This preliminary work allowed to better understand how the organic substitution influences the local and medium-range structure of the geopolymer, with the aim of using this knowledge to produce tailored hybrid geopolymers.

[1] Soper, AK, *J. Phys.: Condens. Matter*, **19** (2007), 415108.

[2] White, CE, Provis, JL, Bloomer, B, Henson, NJ, Page, K, *Physical Chemistry Chemical Physics,* **15** (2013), 8573.

Corresponding author: monica.dapiaggi@unimi.it

Ba(Ti, Ce)O_3 solid solution: the relationship between composition, grain size, and structural properties

Giorgia Confalonieri[1], Vincenzo Buscaglia[2], Giovanna Canu[2], Maria Teresa Buscaglia[2] & Monica Dapiaggi[3]

[1]Dipartimento di Scienze della Terra, Università degli Studi di Torino, Italia

[2]Istituto di Chimica della Materia Condensata e di Tecnologie per l'Energia, Consiglio Nazionale delle Ricerche, Italia

[3]Dipartimento di Scienze della Terra, Università degli Studi di Milano, Italia

$BaTiO_3$ perovskite and its solid solutions are nowadays the most used ferroelectric materials, being them environmental friendly and with excellent properties. Among the various possible solid solutions with homovalent substitution at Ti site ($BaTi_{1-x}M^{IV}_xO_3$), only $BaTi_{1-x}Zr_xO_3$ was studied extensively from the structural point of view [1]. Other substitutions can be interesting: in particular, the one with cerium, $BaCe_xTi_{1-x}O_3$ (BCT), which presents a large difference in size between Ti and Ce ions. Therefore, in this work, BCT with different Ce amount (*x=0.02-0.20*) and various particle sizes (from 80-160 nm to 5 μm) was deeply explored both on the average and on the local structure by means of traditional Rietveld method and Pair Distribution Function. BCT in its ceramic form (grain size: 1 to 5 μm) presents a polar behaviour variation from conventional ferroelectric to relaxor via diffuse phase transition (DPT) [2, 3]. As the particle size is reduced, the so called "size effect" takes over, with larger variations in the electric properties with composition.

It is well known that ferroelectricity is related to titanium displacement within the octahedra, and our Rietveld analysis results find a good agreement between measured material properties and titanium off-center values in the ceramic materials. The progressive suppression of the spontaneous polarization with *x* and the cubic phase stabilization is related to the disruption of the correlated Ti displacements engendered by the large Ce^{4+} incorporated at the octahedral site [4], and a complex model must be used for the local structure. All the described effects are generally more pronounced when the material presents a reduced particle size, as cerium content and reduced size cooperate in the extension of the cubic structure stability field, with respect to the corresponding micrometric materials. The distortions at the local level are therefore confirmed to be largely responsible for the ferroelectric properties of the $BaCe_xTi_{1-x}O_3$ perovskite, either in the micrometric or in the reduced size samples.

[1] V. Buscaglia, S. Tripathi, V. Petkov, M. Dapiaggi, M. Deluca, A. Gajovic, Y. Ren, *J. Phys. Condens. Matter* **26** (2014), 065901.

[2] V.V. Shvartsman, D.C. Lupascu, *J. Am. Ceram. Soc.* **95** (2012), 1.

[3] G. Canu, G. Confalonieri, M. Deluca, L. Curecheriu, M.T. Buscaglia, M. Asandulesa, N. Horchidan, M. Dapiaggi, L. Mitoseriu, V. Buscaglia, *Acta Mater.* **152** (2018), 258.

[4] G. Confalonieri, V. Buscaglia, G. Capitani, G. Canu, N. Rotiroti, A. Bernasconi, A. Pavese & M. Dapiaggi, *J. Appl. Cryst* **51** (2018), 1283.

Corresponding author: monica.dapiaggi@unimi.it

Application of pair distribution function studies to bone mineral for bone quality assessment

E. L. Arnold[1], C. Greenwood[2], D.S. Keeble[3], K.D. Rogers[1]
[1]Cranfield University, Shrivenham, UK
[2]University of Keele, Keele, UK
[3]Diamond Light Source, Didcot, UK

The composition of diseased bone (such as osteoporosis, OP) is the subject of much debate. Our recent work demonstrates the amount of carbonate substitution within the lattice of osteoporotic mineral is significantly modified compared to non-diseased tissue. Increasing carbonate (CO_3^{2-}) substitution increases dissolution rate, decreases average crystallite size and alters crystal morphology, which could result in greater rates of bone loss observed in OP. CO_3^{2-} occupies two non-equivalent sites within biological hydroxyapatite (HA) through substitution of phosphate ions (B-type) and hydroxyl ions (A-type). Previous work is heavily reliant on IR studies which exploit lattice site degeneracy of the $v_2CO_3^{2-}$ absorption band. However, the significant overlapping of bands (from carbonate moieties) at this wavenumber produces equivocal quantification of carbonate that is not mitigated by peak fitting algorithms. The effect of carbonate substitution on crystallite size was investigated, as measured with both conventional X-ray diffraction (XRD) techniques, including Williamson-Hall analysis, and pair distribution function (PDF) studies, through use of the Mineralisation Ratio (MR) [1]:

$$MR = \frac{\sqrt{\sum_{r=15}^{25} G(r_n)^2/n}}{\sqrt{\sum_{r=1}^{7} G(r_n)^2/n}}. \qquad (1)$$

Samples including standard reference materials, synthetic HA with a range of CO_3^{2-} substitution levels, and biological HA taken from four species with varying known physicochemical properties (such as crystallite size and CO_3^{2-} substitution) were measured. PDFs were produced using GudrunX [2], then compared with those in literature (previously collected to lower Q resolution [1,3]). Previously MR has been seen to have a negative correlation with CO_3^{2-} substitution for synthetic HA [3]. This research has seen a similar trend in synthetic HA ($p<0.05$) as well as an opposing trend in biological HA ($p<0.1$) as shown in Figure 1a. This conflicting behaviour suggests synthetic HA may be a problematic model for studying biological HA with regards to CO_3^{2-} substitution. Additionally, a significant trend ($p<0.05$) has been seen between size (determined by XRD) and MR (Figure 1b) for both synthetic and biological HA, reinforcing the use of modern PDF techniques to analyse HA physicochemical properties.

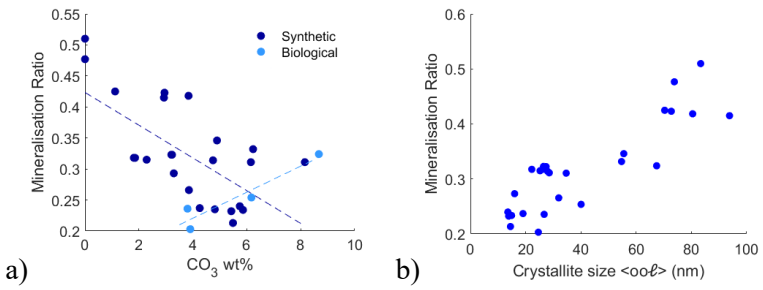

a) b)

Figure 1: a) Correlation between MR and CO_3^{2-} content b) Correlation between MR and crystallite size

[1] M.D. Grynpas, L.C. Bonar, M.J. Glimcher, *Journal of Materials Science* **19** (1984), 723.
[2] GudrunX is available on https://www.isis.stfc.ac.uk/Pages/Gudrun.aspx.
[3] A.S. Posner, F. Betts *Accounts of Chemical Research* **8** (1975), 273.

Corresponding author: e.arnold@cranfield.ac.uk

Synthesis and inelastic neutron scattering investigations of the antiferromagnet $[Cu(\mu\text{-}C_2O_4)(4\text{-aminopyridine})_2(H_2O)]_n$

George Mathew, Deepshikha Jaiswal-Nagar
Indian Institute of Science Education and Research Thiruvananthapuram

States of matter that can be explained only on the basis of quantum mechanics can be best described via the concept of a quantum critical point – a zero-temperature phase transition between quantum ground states. The spin ½ Antiferromagnetic Heisenberg Chain (AFHC) is known to be a quantum critical system in one dimension. Here the magnetic ions possess spin angular momentum of ½, and interact with nearest neighbours through antiferromagnetic Heisenberg exchange couplings in only one crystallographic direction and have spinons as the basic excitations [1].

The main theme of this work is to demonstrate that quantum critical Luttinger liquid (LL) behaviour governs the properties of the title compound over wide ranges in temperature and energy [1]. This will be done by investigating the magnetic excitation spectrum of the title compound, a quasi- 1D, S = ½ Heisenberg antiferromagnet. The magnetic Cu^{2+} ions carrying S = ½ are bridged by oxalate molecules forming chains along the crystallographic c axis (Figure 1). The magnetic susceptibility of the title compound is well described by the model of a spin – ½ AFHC with an intra-chain coupling J/k_B around 3 K [2]. To measure the magnetic excitations in the title compound, we will be using the technique of inelastic neutron scattering (INS). This is a unique, direct probe to study magnetic excitations in complexes of both d- and f-elements.

Prior to INS, synthesis as well as H/D exchange were done on the title compound. Presence of strong incoherent scatterers such as hydrogen in the sample leads to an increase of background in neutron diffraction data [3]. So hydrogen has to be replaced with its heavy isotope deuterium (H/D exchange). This task is accomplished by performing H/D exchange over the two starting reagents potassium bis(oxalato) cuprate(II) dehydrate and 4-aminopyridine. The need for large amount of samples was accomplished by repeating the growth process over 60 times. [This piece of work is not published. We have received a slot for neutron diffraction at ISIS Facility, Rutherford Appleton Laboratory, Oxfordshire, UK on February 18-26, 2019. All the analysis will be done once INS experiment is accomplished].

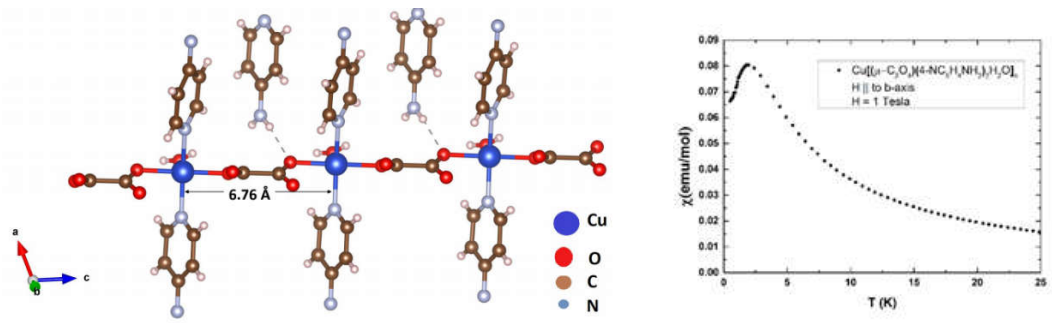

Figure 1: Crystal structure of the title compound and its temperature dependent susceptibility

[1] B. Lake et al, *Nat Mat* **4** (2005), 329.
[2] B. Wolf et al, *PNAS* **108** (2011), 6862.
[3] S. E. Stavretis et al., *Eur. J. Inorg. Chem.* **0000** (2018), 00000.

Corresponding author: deepshikha@iisertvm.ac.in

Application of laboratory X-ray diffraction equipment for Pair Distribution Function (PDF) analysis

G. Nénert, M. Gateshki, M. Sommariva, D. Beckers
Malvern Panalytical, Lelyweg 1, 7602 EA Alemlo, The Netherlands

The increased interest in recent years regarding the properties and applications of nanomaterials has also created the need to characterize the structures of these materials. One of the most promising techniques to study nanostructures is by using the total scattering (Bragg peaks and diffuse scattering) from the samples and the pair distribution function (PDF) analysis. The PDF provides the probability of finding atoms separated by a certain distance. From experimental point of view a typical PDF analysis requires the use of intense high-energy X-ray radiation ($E \geq 15$ KeV) and a wide 2θ range. At present, synchrotron and neutron sources are the preferred choice for PDF analysis, but there is clearly an increasing need for a PDF solution based on laboratory diffraction equipment. Such a solution, though limited, will benefit areas where quick feedback about the materials properties is important and will allow the routine application of PDF analysis for materials characterization in university laboratories as well as industrial R&D departments.

After the initial feasibility studies regarding the use of standard laboratory diffraction equipment for PDF analysis [1,2] this application has been further developed to achieve improved data quality and to extend the range of materials, environmental conditions and geometrical configurations that can be used for PDF experiments. The recent introduction of detectors with improved efficiency for high-energy X-rays [3] has further enhanced the capabilities of laboratory diffractometers for total scattering experiments. This contribution presents several examples of laboratory PDF studies performed on different nanocrystalline and amorphous materials of scientific and technological interest (organic substances, oxides, metallic alloys, materials for battery applications, etc.) and demonstrates that PDF analysis with a laboratory diffractometer can be a valuable tool for structural characterization of nanomaterials.

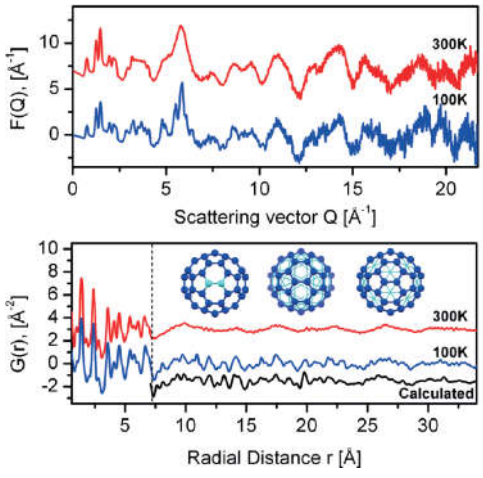

Figure 1: Examples of PDF data collected on Fullerenes at various temperatures.

[1] te Nijenhuis, J. *et al*. *Zeitschrift für Kristallographie*. *Suppl*., **30** (2009) 163A.
[2] Reiss, C. A. *et al*. *Zeitschrift für Kristallographie*, **227** (2012) 257.
[3] G. Confalonieri *et al*. *Powder Diffraction*, **30** (2015) S65.

Corresponding author: gwilherm.nenert@malvernpanalytical.com

Local structural fluctuations in magnetite above the Verwey temperature

G. Perversi[1], J. Cumby[2], E. Pachoud[2], J.P. Wright[3], S. Kimber[4] and J.P. Attfield[2]
[1]University of Montpellier, Institut Charles Gerhardt - UMR 5253, Montpellier, France
[2]University of Edinburgh, Centre for Science at Extreme Conditions (CSEC), Edinburgh, U.K.
[3]European Synchrotron Radiation Facility, Grenoble, France
[4]Laboratoire Interdisciplinaire Carnot de Bourgogne, Université de Bourgogne, Dijon, France

Transition metal oxides can feature mixed valence cations, spin ordering and direct interactions between *d*-orbitals. This makes them intrinsically susceptible to the formation of atomic clusters with direct metal-metal interactions (orbital molecules).

Magnetite (Fe_3O_4) features a very significant example of orbital molecule behaviour in its low temperature phase. At the Verwey transition temperature (T_V ~125 K) the *Fd-3m* high-temperature structure distorts to a monoclinic *Cc* supercell, due to a cooperative bond distortion that brings together three neighbouring Fe sites in a linear Fe(III)-Fe(II)-Fe(III) arrangement. The delocalisation of the extra electron of Fe(II) creates a bonded cluster, or orbital molecule, among three-atoms ('trimeron').[1][2]

The trimeron formation is one of the most complex electronically ordered ground states known, and the origin of the underlying correlations has been an outstanding problem over many decades. Following reports of structural fluctuations persisting above T_V, particularly in single crystal diffuse scattering studies [3], we performed a comprehensive X-ray pair distribution function analysis of a purely stoichiometric magnetite powder ($Fe_{3-\delta}O_4$ with $\delta < 0.0001$). Data with Q_{max} = 31 Å^{-1} were collected at the beamline ID11 of ESRF, from temperatures below the Verwey transition (T = 90 K) to above the Curie temperature of magnetite (T = 923 K) (Figure 1). The challenges related with the data analysis will be discussed.

The results of this study provide new insights on the fate of the characteristics low temperature distortions above the Verwey temperature of magnetite, and unveil the source of the instability driving the Verwey transition.

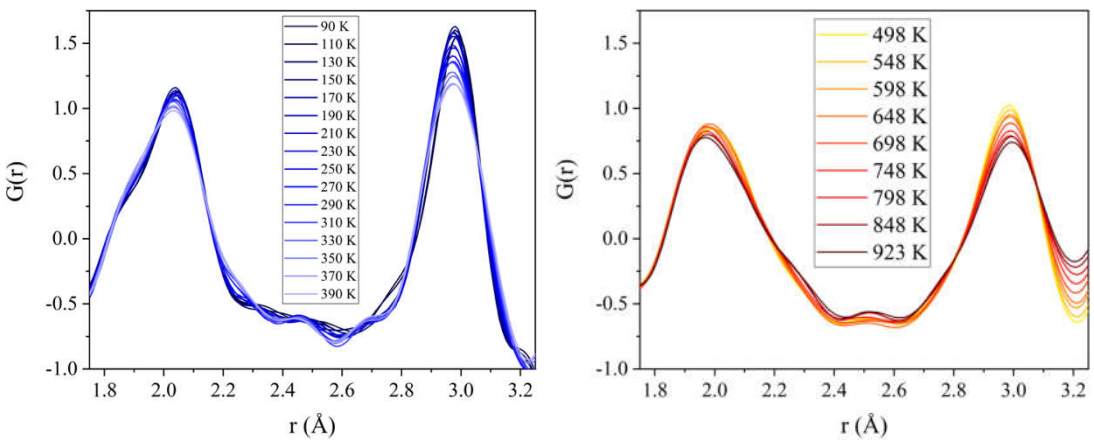

Figure 1: Temperature evolution of the PDFs, displayed in the region of the first and second coordination shells (Fe-O at r ≈ 2.0 Å and Fe-Fe at r ≈ 3.0 Å) for the two different sample environments (low-temperature nitrogen, left, high-temperature hot air blower, right).

[1] E. J. W. Verwey, *Nature* **144**, 327-328. (1939)
[2] M. S. Senn *et al.*, *Nature* **481**, 173-176. (2012)
[3] Bosak, A. *et al.*, *Phys. Rev. X* **4**, 011040 (2014).

Corresponding author: giuditta.perversi@umontpellier.fr

Structural investigation of carbon-based pigments from ancient Egyptian papyri

P.-O. Autran[1,2,3], C. Dejoie[1], P. Bordet[2,3], J.-L. Hodeau[2,3], P. Walter[4], and P. Martinetto[2,3]

[1]European Synchrotron Radiation Facility, F-38000 Grenoble, France

[2]Univ. Grenoble Alpes, Inst NEEL, F-38042 Grenoble, France

[3]CNRS, Inst NEEL, F-38042 Grenoble, France

[4]Laboratoire d'Archéologie Moléculaire et structurale, LAMS, Sorbonne Université, CNRS, F-75005 Paris, France

Starting as early as the fourth millennium B.C., Egyptian writings on papyrus spread knowledge all around the Mediterranean Sea. Carbon-based pigment from Egyptian period were used as a base for ink manufacturing dedicated to writing [1]. Although a large amount of papyri has been preserved, the complexity resulting from the amorphous nature of carbon-based pigments explains our limited understanding of Egyptian writing techniques. Recent studies on papyri fragments from both Herculanum and ancient Egypt showed the presence of metallic element such as copper and lead, their origin remains unanswered [2,3].

The objctive of this study is to get a better understanding of the recipes used in ancient Egypt to elaborate black ink, by tracking the origin of amorphous carbon and other metallic elements. To do so, a series of papyrus from the Champollion museum (Vif, France) have been investigated. Non-destructive X-ray techniques such as X-ray powder diffraction for both Rietveld and pair distribution function analysis and X-ray fluorescence were performed on the ID22 beamline at the ESRF (0.5x0.5mm, Q-range of 24Å^{-1}). X-ray diffraction and fluorescence tomography were also done at the ID11 beamline, ESRF (2x2µm beam, Q-range of 20Å^{-1}). Complementary analyses using scanning electron microscopy, with X-ray microanalysis (Institut Néel, Grenoble) and high-resolution macro photography were also carried out to probe the surface of the papyri.

First results from SEM show similarities between the ink deposited on the papyrus surface and commercial lamp black. In agreement with previous studies, a contrast has been obtained between the ink and the raw papyrus by following particular metallic elements using X-ray fluorescence. A small contrast was also found from 2D and 3D diffraction data and remains to be explained. Combining non-destructive 2D and 3D X-ray analysis with microscopy analyses should help to clarify the heterogeneous nature of these Cultural Heritage materials.

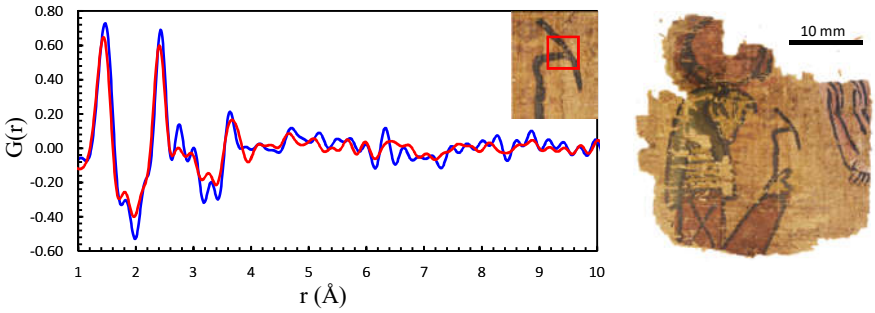

Figure 2: PDF analysis of ink on papyrus (blue) and papyrus (red) – ID22, ESRF

[1] Lucas A. and Harris J. R., Ancient Egyptian materials and Industries, *Dover Publications Inc*., (1962) 338-366.

[2] Brun, E. et al. Revealing metallic ink in Herculaneum papyri. *PNAS* **113(14)**, (2016) 3751–3754

[3] Christiansen et al., The nature of ancient Egyptian copper-containing carbon inks is revealed by synchrotron radiation based X-ray microscopy, *SREP* **7-15346**, (2017).

Corresponding author: pierre-olivier.autran@esrf.fr

Combining a nine-crystal multi-analyser stage with a two-dimensional detector: PDF from a high-resolution powder diffractometer

M. Coduri[1,2], C. Dejoie[1], E. Covacci[1], A. N. Fitch[1]
[1]European Synchrotron Radiation Facility, Grenoble, France
[2]Pavia University, Italy

With the widespread advent of two-dimensional detectors, fast data collection with high counting statistics suitable for pair distribution function (PDF) analysis can be performed routinely. However, the use of a high-resolution setup could bring crucial advantages, such as (i) the possibility to record a diffraction pattern for both Rietveld and PDF analyses with the same experimental conditions, (ii) a negligible instrumental PDF intensity decay or broadening, and (iii) the absence of artefacts arising from the calibration of a two-dimensional detector. The main drawback of using a high-resolution setup is that it is highly time consuming. To overcome this issue, a new detector system was tested and will be implemented at the high-resolution powder diffraction beamline at ESRF (ID22).

ID22 offers routinely the possibility to carry out high-flux, high-resolution powder diffraction above 30 keV. Currently, a bank of nine scintillation detectors is scanned vertically to measure the diffracted intensity as a function of 2θ, each detector being preceded by a Si 111 analyzer crystal. The size of the receiving slit defines the axial acceptance of the detectors and is a compromise between peaks shape at low diffraction angles and statistics at higher angles. The latter is crucial for PDF data collection, as proper counting statistics is achieved by adding more scans in the high 2θ region, thus increasing total collection time.

In order to improve the detection efficiency, a Pilatus3 X CdTe 300K-W was mounted on the arm of the diffractometer behind the 9 analyzer crystals. Continuous scans were acquired on test samples (Si, LaB6, doped ceria) for both conventional Rietveld refinements and PDF analyses. This new detection system allows to vary axial aperture with 2θ selecting different regions of interests: narrow at low angles where the curvature is most marked, wider at higher angles where the curvature is less, thus increasing overall counting efficiency compared to the current fixed 4-mm-wide receiving aperture. This setup allows to reduce the collection time for PDF by a factor of 3 and might further improve with ESRF upgrade to EBS. Combining the high efficiency of a hybrid photon-counting area detector with the high resolution given by analyzer crystals is an effective approach to improving the overall performance of high resolution powder diffraction as well as to collect faster reliable data for PDF.

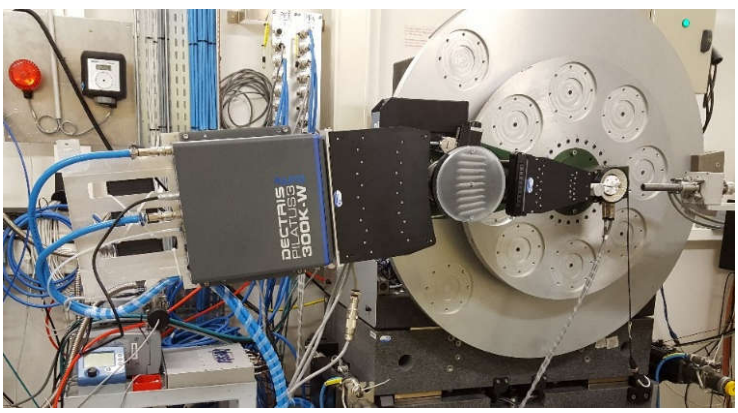

Figure 1: Pilatus detector mounted on the 2θ arm at ID22.

[1] C. Dejoie et al., *J. Appl. Cryst.* **51** (2018), 1721-1733.

Corresponding author: codurimauro@gmail.com

Coherent diffractive Imaging of microtubules using an X-ray laser

G. Brändén, G Hammarin, R. Neutze
University of Gothenburg, Sweden

X-ray free electron lasers (XFELs) have delivered a billion fold increase in peak X-ray brilliance over conventional synchrotron radiation sources. These sources create new possibilities for structural studies of biological objects that go beyond what is possible with synchrotron radiation. Serial femtosecond crystallography is an XFEL method that allows high-resolution structures to be solved from micrometer sized crystals, whereas single particle coherent X-ray imaging requires development to extend the resolution beyond a few tens of nanometres. Here we describe an intermediate approach: the XFEL imaging of biological assemblies with helical (1D translational) symmetry.

We collected X-ray scattering images from samples of microtubules injected across an XFEL beam using a liquid microjet, sorted these images into class averages, merged these data into a 2D diffraction pattern extending to 2 nm resolution, and reconstructed these data into a projection image of the microtubule. 2D electron density projection images were generated using an iterative phase retrieval algorithm implemented in MATLAB. Details such as the 4 nm monomer within the microtubule became visible in this reconstruction. These results illustrate the potential of single-molecule X-ray imaging of biological assembles with helical symmetry at room temperature.

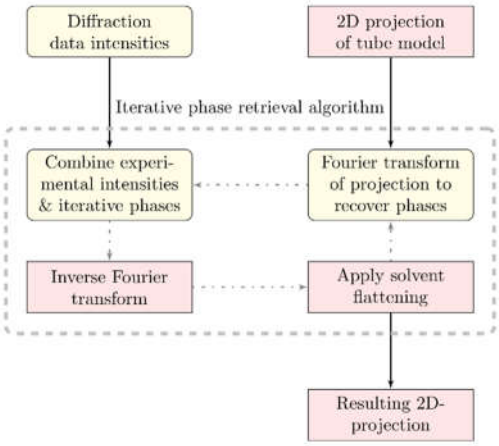

Figure 1: A schematic showing the iterative phase retrieval algorithm.

A total scattering study of the nanoscale structure of iron chalcogenide superconductors

R. J. Koch[1], E. S. Bozin[1], C. Petrovic[1], M. Abeykoon[2], and S. J. L. Billinge[1,3]
[1]Condensed Matter Physics and Materials Science Department,
Brookhaven National Laboratory, Upton, NY 11973, USA
[2]Photon Science Division,
Brookhaven National Laboratory, Upton, NY 11973, US
[3]Department of Applied Physics and Applied Mathematics,
Columbia University, New York, NY 10027, USA

Iron-based superconductors are known for their complex interplay between structure, magnetism and superconductivity. In many of these systems superconductivity is preceded by a nematic phase that persists into the superconducting regime, suggesting that the two share some connection, but the exact nature of this connection remains unclear. The $FeSe_{1-x}S_x$ system offers an opportunity to investigate the underlying relationship, as isovalent substitution allows for tuning both nematic order and superconductivity. The FeSe endmember undergoes an electronically driven structural (tetragonal-orthorhombic) transition at $T_s \sim 90$K [2]. This transition can be systematically suppressed through isovalent sulfur substitution, and T_s decreases as the nematic end-point is approached, where nematic order is absent at $x = 0.17$ (see e.g. Fig. 1). Although nematicity can be suppressed, superconductivity is observed across the whole compositional range. We utilize x-ray total scattering and atomic pair distribution function (PDF) analysis to probe the local structure of the $FeSe_{1-x}S_x$ system across the entire compositional range. We find remnant local nematic fluctuations at temperatures far exceeding T_s. Our results should provide new insights into the origin of nematic order in this system.

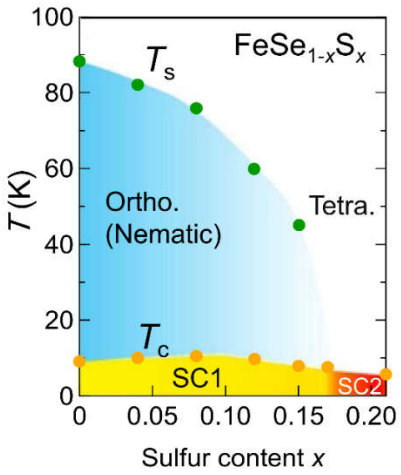

Figure 1 Temperature-composition phase diagram of $FeSe_{1-x}S_x$. Reproduced from Ref. [3].

[1] R. M. Fernandes, A. V. Chubukov, and J. Schmalian, *Nat. Phys.* **10** (2014), 97–104.
[2] K. Matsuura et al., *Nat. Commun.* 8 (2017), 1143.
[3] Y. Sato et al., *Proc. Natl. Acad. Sci.* **115** (2017), 1227–1231.

Corresponding author: rkoch@bnl.gov

Unveiling the magnetic structure in the phase separated quasi-dimensional magnet γ-CoV_2O_6

E. Campillo[1], E. Blackburn[1], L. Shen[1], M. Laver[2], E. Tekin[2], Lucile Mangin-Thro[3].
[1]Lund University
[2]University of Birmingham
[3]Institut Laue-Langevin

Frustrated magnets, in which spins are hindered from reaching an optimal configuration corresponding to the global minimum in the total free energy [1], often develop short-range spin correlations before entering the magnetic ground state [2-4]. As revealed in the quasi-one-dimensional (Q1D) magnet $Ca_3Co_2O_6$ [3], these local spin clusters are of particular importance to understanding the nature of the magnetic ground state. Experimentally, short-range spin correlations are manifested by the diffuse scattering profile in a diffraction pattern [3]. The underlying spin configuration can then be extracted by applying the Reverse Monte Carlo (RMC) algorithm to these data [3].
γ-CoV_2O_6 is a novel frustrated magnet, where spin chains consisting of two inequivalent Co-sited run along the crystallographic b-axis. Using un-polarized neutron powder diffraction, it was established that below T_N = 6.6K, the spin structure consists of two single-k phases in a volume ratio 65(1):35(1) [4]. Also, as it is shown in the inset of Figure 1, there is a commensurate-incommensurate transition in the k2 phase at T* = 5.6K; the k1 phase remains unaffected below this temperature [4].
While RMC is commonly employed to study the short-range spin correlations in single-phase magnets, its capability of dealing with phase-separated systems, however, is yet to be explored. In this project, we have performed polarized neutron powder diffraction measurements on γ-CoV_2O_6 on the D7 diffractometer at ILL and observed an exclusive magnetic diffuse scattering profile at various temperatures above T_N. We aim to use these data to understand the nature of the short-range magnetic phase separation in the paramagnetic region of γ-CoV_2O_6, and more importantly, benchmark RMC in extracting the short-range spin correlations in a phase-separated system.

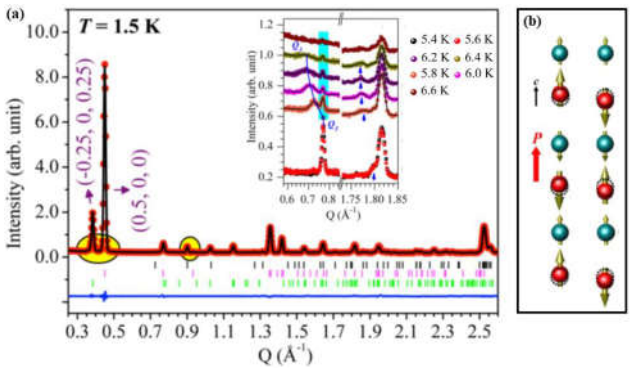

Figure 1: Main panel: Neutron powder diffraction pattern of γCVO (no diffuse scattering). The red solid dots are experimental observations. The black and blue lines are the calculated pattern and the difference using the two-phase model. Black, pink, and green vertical bars mark the nuclear, *k*1- and *k*2-modulated Bragg positions, respectively. Inset: Selected regions of the powder diffraction patterns between 5.4 K and 6.6 K. The arrows mark the shifting reflections (1,0,0) + *k*2 and (−2,0,1) + *k*2, respectively, due to the incommensurate-commensurate lock-in transition [4]. (b) Ising chains with the up-up-down-down spin order and alternating ionic order, in which electric polarization is induced through symmetric exchange striction. The two possible magnetic configurations leading to the opposite polarizations are shown. The atomic positions in the undistorted chains are shown with dashed circles.

[1] J. S. Gardner et al., Rev. Mod. Phys. 82, 53 (2010).
[2] M. Giot et al. Phys. Rev. Lett. 99, 247211 (2007).
[3] J. A. M. Paddison et al. Phys. Rev. B 90, 014411 (2014).
[4] L. Shen et al. Phys. Rev. B. 96, 054420 (2017).

Electronic Structure, Magnetic behaviour and Impedance Spectroscopy of Magnetic ion doped Ferroelectric Ceramics

Anumeet Kaur and Lakhwant Singh
Department of Physics, Guru Nanak Dev University, Amritsar-143005, India.

Ferroelectric ceramics are of technological promise because of their wide range of applications in dynamic random access memories (DRAMS), non-volatile memories, pyroelectric detectors and electro-optic devices, etc. Barium strontium titanate ($Ba_{1-x}Sr_xTiO_3$, hereafter denoted as BST) being ecofriendly material, is considered as one of the most promising candidate for ferroelectric devices due to its excellent properties of high dielectric constant, low leakage current and adjustable Curie temperature (T_C). The doping of magnetic ion 'Fe' at 'Ti' site not only reduces the dielectric loss but also induces magnetism in it. However, very less is known about the magnetic properties and the electronic structures of the Fe-doped BST solid solutions. X-ray absorption spectroscopy especially X-ray absorption near-edge structure (XANES) when invited with Fe doped BST can provide information about the change in the valency of Fe and Ti ions and chemical bonding information. Present investigation focuses on the structural, magnetic and electronic properties of Fe doped BST ceramics [1]. Bulk samples with composition $Ba_{0.7}Sr_{0.3}Fe_xTi_{1-x}O_3$ where x =0, 0.1, 0.2, 0.3 were synthesized via conventional solid state reaction route. X-ray diffraction patterns of all the samples clearly show phase formation with the absence of impurity peaks. The Rietveld refinement confirmed the coexistence of the tetragonal and cubic phase for samples with Fe content x= 0, 0.1 and pure cubic phase for x > 0.1. The M–H hysteresis curves for samples with composition x = 0.1 and 0.2 exhibit paramagnetic behaviour even at low temperatures and the composition with x = 0.3 shows the nature of weak ferro- and ferri-magnetic orderings at about 2K. It is inevitable that presence of Fe^{2+} state is responsible for paramagnetism. However, with increasing Fe content mixed valency seem to be setting in. This strange magnetic behavior is due to the presence of mixed valence states and in particular Fe^{2+} state in the samples, as observed from Fe L_3-edge XANES spectra. The Ti $L_{3,2}$-edges at the XANES spectra confirmed that the doping of Fe in ABO_3 structure leads to the lattice distortion. This doping induced distortion is also evidenced by the Fe K-edge XAS. The Fe L_3-edge XANES spectra revealed that with increasing the Fe concentration, the mixed valence states and presence of Fe^{2+} are observed. The XANES spectra of the Ba L_3-edge and Sr L_3-edge spectra confirmed that the local structure around Ba^{2+} and Sr^{2+} respectively does not show any influence from the dopants in the BST system. The electrical behaviour of the sample has been studied by complex impedance spectroscopy(CIS) as a function of frequency (1 Hz to 1 MHz) at different temperatures (RT to 700K). Two semicircular arcs observed in the Cole-Cole plot confirm the contribution from the grain and grain boundary in overall impedance. Both the electrical as well as ac conduction phenomena take place via correlated barrier hopping (CBH) authenticated by detailed complex modulus analysis and ac fitted conductivity respectively. The values of activation energies calculated from electrical impedance, modulus, and conductivity data clearly reveal that the relaxation and conduction processes in prepared ceramic are induced by doubly ionized oxygen vacancies.

[1] Kaur.A et.al *RSC Adv.***6** (2016) 112363
[2] Anumeet Kaur, Lakhwant Singh and K. Asokan, *Ceramics International* **44**, 4, March (2018) 3751-3759

Corresponding author: anumeetphy@gmail.com

Structure and morphology of star-like polyelectrolytes interacting with hydrophobic or amphiphilic counterions

R. Lunkad, L. Nová, P. Košovan
Department of Physical and Macromolecular Chemistry, Charles University, Prague, Czech Republic

Using computer simulations and coarse-grained polymer models in implicit solvent we demonstrate that star-like polyelectrolytes adopt core-shell morphologies in the presence of relatively small amounts of hydrophobic or amphiphilic counter-ions (oppositely charged small ions). These couter-ions are rather strongly attracted to the star-like polyelectrolyte, and accumulate near the centre of the star. Unlike linear chains, the star-like polyelectrolytes do not phase separate but rather form a collapsed core with accumulated counter-ions, surrounded by a charged shell, which prevents further aggregation. The peculiar density profiles, predicted by our simulations, should be observable by suitable scattering techniques.

Corresponding author: peter.kosovan@natur.cuni.cz

Progress in magnetic PDF-analysis at the Institut Laue-Langevin (ILL)

Henry E. Fischer[1], Joseph A.M. Paddison[2], Simon Riberolles[1,3], Navid Qureshi[1], Oleg A. Petrenko[3], Andrey F. Gubkin[4], Diego G. Franco[5], Silvia Seiro[6], Gabriel J. Cuello[1]

[1]Institut Laue-Langevin, 71 avenue des Martyrs, CS 20156, 38042 Grenoble cedex 9, France
[2]Churchill College, University of Cambridge, Storey's Way, Cambridge CB3 0DS, U.K.
[3]Department of Physics, University of Warwick, Coventry CV4 7AL, U.K.
[4]Russian Acad Sci, MN Mikheev Inst Met Phys, Ural Branch, Ekaterinburg 620137, Russia
[5]División Bajas temperaturas, Centro Atómico Bariloche, 8400 Bariloche, Río Negro, Argentina
[6]Institute for Solid State Physics, IFW-Dresden, Helmholtzstrasse 20, 01069 Dresden, Germany

Fourier transformation of a total-scattering diffraction pattern dσ/dΩ (i.e. including diffuse scattering) into real-space produces a Pair-Distribution Function (PDF) whose amplitude gives the probability of finding scattering centers at a given relative distance. As such, the PDF(r) represents an ensemble-average of quasi-instantaneous local structures within the diffracting sample, and is complementary to the space+time averaged structure gained through Rietveld refinement of elastic scattering at Bragg peak positions. Although atomic PDF(r) have been obtained for several decades using x-ray and neutron diffraction, relatively new is the Fourier transformation of magnetic diffuse neutron scattering to obtain a magnetic PDF(r). The so-called mPDF(r) exhibits positive or negative peaks for ferro- or antiferro-magnetic alignment between spins, respectively, and can be compared quantitatively to results from atomistic simulations that also provide an ensemble average of local structure 'snapshots'. The technique of magnetic PDF-analysis [1] has the additional advantage of revealing not only static spin-spin correlations below T_N, but also dynamic spin-spin correlations above T_N.

The D4 neutron diffractometer for disordered materials at the ILL is well-adapted to PDF-analysis, and has recently been used to produce some mPDF(r) from a variety of magnetic systems including those with magnetic frustration. The magnetic Bragg and diffuse scattering data have been simulated using the Reverse Monte Carlo program Spinvert [2] to obtain a real physical model of spins that is consistent with the data. This poster will present some preliminary results and analysis.

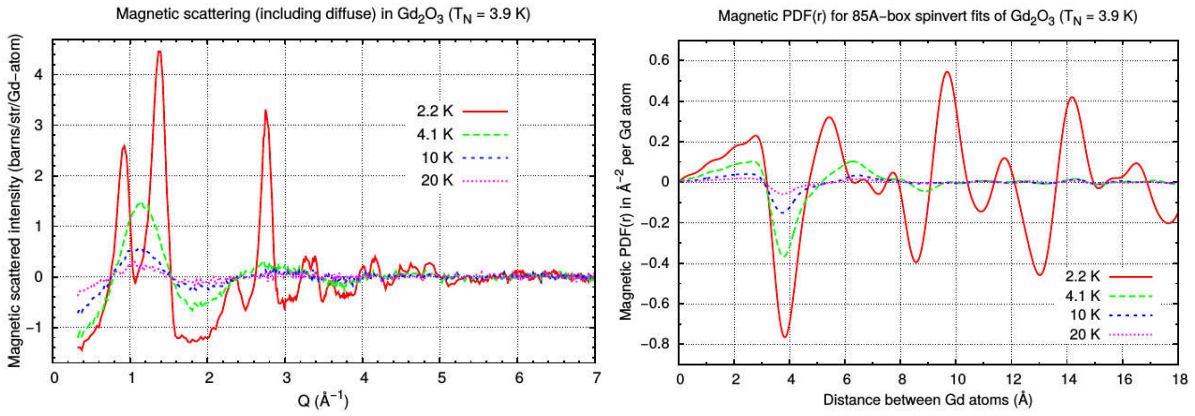

Figure 1: (Left) Magnetic Bragg peaks and magnetic diffuse scattering measured from a powder sample of Gd_2O_3 with the D4c neutron diffractometer (wavelength = 0.5 Å) at the ILL. (Right) The corresponding magnetic Pair-Distribution Function or mPDF(r) obtained via Fourier transformation of the magnetic scattering from an atomistic model of the same data refined using Spinvert. Note the evidence for dynamic spin-spin correlations above T_N that occur at distances distinct from those of the static magnetic structure below T_N.

[1] B.A. Frandsen, X. Yang and S.J.L. Billinge, *Acta Cryst.* (2014) **A70**, 3-11.
[2] J.A.M. Paddison, *J. Phys. Condens. Matter* (2013) **25**, 454220.

Corresponding author: fischer@ill.fr

Modelling liquid and solution structures using X-ray pair distribution function analysis

B. Evans[1], L. H. Al-Madhagi[1,2], A. Pallipurath[1], P. Chater[2], R. B. Hammond[1], B. Mishra[1] and S. L. M. Schroeder[1,2]
[1]University of Leeds, UK
[2]Diamond Light Source, UK

The crystallisation of ionic salts is of particular interest to the pharmaceutical industry, as the number of active pharmaceutical ingredients being marketed as salts is increasing. The salt forms can improve stability, physical and physicochemical properties, and bioavailability of a compound. Control of the crystallisation process is necessary for salt production to be more efficient and reproducible at an industrial scale. The advancement of a molecular-level understanding of the structural evolution of molecular clusters of solutes in solution through to crystal nucleation and growth is therefore crucial. A technique that can identify the short-range atomic interactions that occur during self-assembly is pair distribution function (PDF) analysis. A PDF determines the probability of two atoms in a sample being separated by a distance, r.[1] Most diffraction techniques provide long-range ordering information of a material, but seldom information about local structure. PDF analysis can be used to identify short-range order in materials that are considered to be disordered over the long range (glass, amorphous materials, liquids and solutions). The aim of this work is to develop a computational method to simulate the structure of a solution based on the experimentally-derived PDF analysis.

Experimental method: The total scattering experimental technique uses Bragg and diffuse scattering data to determine the atomic PDF of a material, which is given by the Fourier transform of the corrected and normalised scattered intensity data.[1] Total scattering data for static solid and liquid samples, and temperature-controlled solution samples using a dynamic flow cell has been collected at the X-ray Pair Distribution Function (XPDF) beamline I15-1 at Diamond Light Source. The acquisition of high-resolution data is realised by using a high-energy incident beam (76 keV) and a large detector area to maximise the momentum transfer (Qmax). The processing of the reduced raw scattering data was performed using GudrunX to extract the PDF for each system. Aqueous solutions of guanidinium (Gdm) hydrochloride have been studied. The Gdm ionic species is of biological importance as a protein denaturant and is chemically interesting due to its propensity to form like-charge ion pairs.[2]

Computational modelling: Empirical potential structure refinement (EPSR) is a Monte Carlo-based computational tool that produces a statistically probable structural model. EPSR uses a combination of inter- and intra-molecular forces (the reference potential) to create a structural molecular model that generates a total scattering pattern and therefore PDF similar to that of the experimental data. The model is further refined by an empirical potential to improve the fit.

XPDF analysis and EPSR modelling will probe the formation of Gdm ion dimers in aqueous solutions. A neutron scattering study indicates that the Gdm ions hydrogen bond with the water molecules, allowing water-deficient surfaces to form ion stacks.[3] Reproducing these results could suggest that less intensive XPDF analysis could become a new routine analysis technique.

[1] D. Prill et al. *Acta Cryst.* (2016) **72** 62–72.
[2] M. Vazdar et al. *Accounts of Chemical Research* (2018) **51**(6)1455–1464.
[3] P. E. Mason et al. *Journal of the American Chemical Society* (2004) **126** 11462–11470.

Corresponding author: pmbe@leeds.ac.uk

Catalytic degradation of organic dyes using biosynthesized silver nanoparticles

I. Charti[1], A. Eddahbi[2], Y. Abboud[1], A. El Bouari[1]
[1]Laboratoire de Physico-Chimie des Matériaux Appliqués, Faculté des Sciences Ben M'sik, Université Hassan II Mohammedia-Casablanca Morocco.
[2]Laboratoire de la Physique de la Matière Condensée (LPMC), Mohammedia Faculté des Sciences Ben M'Sik, Université Hassan II Mohammedia-Casablanca Morocco.

Nanoparticles are the basis of nanotechnology and have many applications in a wide variety of areas such as health, the environment and consumer and healthcare products. To fulfill these functions, nanoparticles must be synthesized, passivated to control their chemical reactivity, stabilized against aggregation and functionalized to achieve specific performance objectives [1]. The problem posed by the development of this technology is the use of toxic chemicals in the most traditional chemical methods of nanoparticle synthesis, which limits their applications in the biological, cosmetic, and clinical fields. Therefore, the development of efficient biocompatible, non- toxic and environmentally friendly methods for the synthesis of metallic nanoparticles has become a major concern for researchers. A promising approach to achieving this goal is to exploit all of nature's biological resources. Indeed, in recent years, plants, algae, fungi, bacteria and viruses have been used for the production of low-cost, nontoxic metal nanoparticles and minimizing energy consumption [2,3].

In the present study, silver nanoparticles (AgNPs) were synthesized from palm date wood extract (Phoenix dactiferia L.) in a rapid and eco-friendly microwave-assisted synthesis from silver nitrate solution. Microwave parameters (irradiation time and power), wood extract and silver nitrate concentration were optimized. The UV–visible spectroscopy was used to monitor the silver nanoparticle formation through sampling at time intervals. The formation of silver nanoparticles was apparently displayed within evidence of surface Plasmon bands, photosynthesized silver nanoparticles dimensions 20–60 nm were characterized using X-ray diffraction analysis and transmission electron microscopy (TEM).

This work shows the effect of the concentration of silver nanoparticles on the degradation rate of hazardous dyes, methyl orange and methylene blue by $NaBH_4$. The efficiency of silver nanoparticles as a promising candidate for the catalysis of organic dyes by $NaBH_4$ through the electron transfer process is established in the present study.

[1] Djoumessi Lekeufack, Synthèse et fonctionnalisation des nanoparticules d'or pour des applications en optique: perspective en photocatalys, Université de Lyon 1, 2010
[2] D. Bhattacharya, R.K. Gupta, Crit. *Rev. Biotechnol.* **25** (2005) 199-204.
[3] A.K. Mittal, Y. Chisti, U.C. Banerjee, *Biotechnol. Adv.* **31** (2013) 346–356.

Corresponding author: charti.ibtissam@gmail.com

Structure and Morphology of CdS nanoparticles

B. U. Evtushok[1], S.V. Cherepanova[1,2], E.A. Kozlova[1,2]
[1]Novosibirsk State University
[2]Boreskov Institute of Catalysis, Novosibirsk

The structure and morphology of CdS nanoparticles obtained by the hydrothermal synthesis at temperatures of 80 °C, 100 °C, 120 °C, and 140 °C were studied. The analysis was performed by calculating X-ray diffraction patterns by the Debye formula followed by the optimization of model parameters of nanocrystals using the program DISCUS [1]. It was shown that with increasing temperature the CdS structure gradually transforms from a very defective sphalerite-like structure to very defective wurtzite-like one. At all temperatures the particles are ellipsoids stretched along the perpendicular to stacking faults. An increase in the temperature causes a gradual enlargement of nanoparticles.

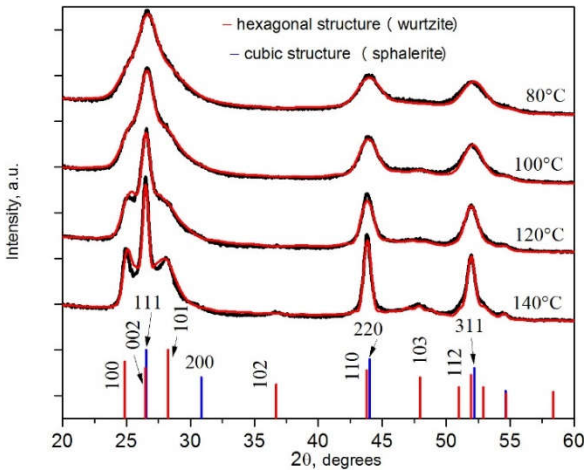

Figure 1: Experimental (black) and calculated (red) XRD patterns

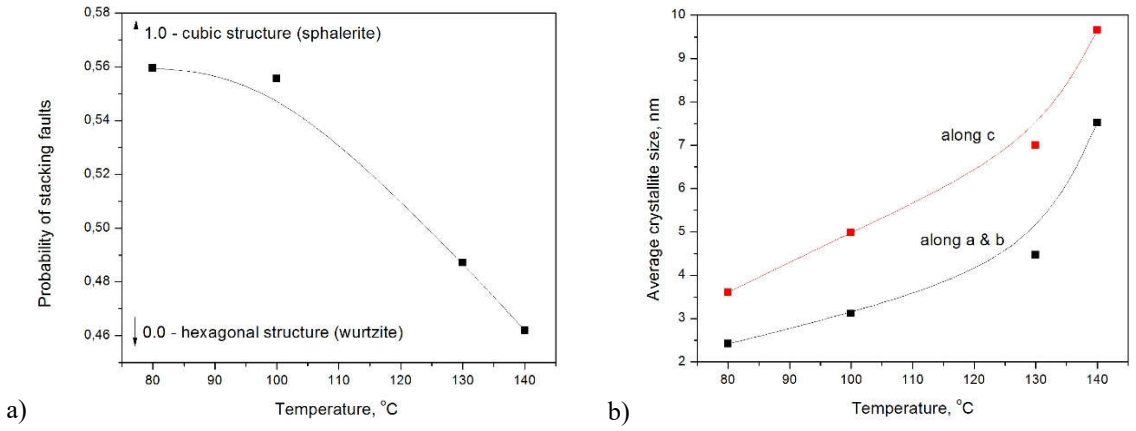

Figure 2: a) Dependence of probability of stacking faults on temperature
b) Dependence of average crystallite size on temperature

[1] Reinhard B. Neder and Thomas Proffen. *Diffuse scattering and defect structure simulations*. 2007. DOI: 10.1093/9780199233694.003.0007.

Corresponding author: evtboyan@mail.ru

Solvothermal synthesis of niobium oxide nanoparticles: Size/structure relations

O. Aalling-Frederiksen, M. Juelsholt, K. M. Ø. Jensen
Department of Chemistry, University of Copenhagen, Universitetsparken 5, 2100 Copenhagen Ø, Denmark

Niobium oxides are of great interest due to their application in various electrochemical devices, e.g. electrochromic displays, batteries and solar cells [1]. The wide range of properties originates in the rich structural chemistry, which has been studied in detail for bulk materials. However, in order to get a deeper understanding of this important material on nanoscale, we here want to map the relation between the particle size and the atomic structure.

In this project, niobium oxide was synthesized using the solvothermal autoclave method. Niobium(V)chloride was used as a precursor and a study of the effect of solvent was carried out, where a range of alcohols were tested as solvent. The study showed that the synthesized crystalline powders all contained the rutile NbO_2 phase, Figure 1.

A further investigation showed a remarkable dependency of NbO_2 particle size on the autoclave material used in the synthesis: When synthesized in steel autoclave, highly crystalline NbO_2 particles formed, whereas small nanoparticles were formed when using Teflon-lined autoclaves. This suggests that the container used in the solvothermal synthesis has an effect on the nucleation process.

The structure of the synthesized niobium oxide particles was determined using X-ray total scattering. For the analyses of the crystalline powder, Rietveld refinement was used. When looking at the nanostructured powder the data was analyzed using Pair Distribution Function method, PDF, which allow detailed structural analysis of the nanostructured samples.

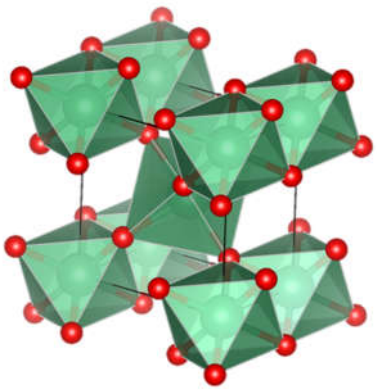

Figure 1: Rutile NbO_2 was synthesized with the solvothermal autoclave method (Green: Nb, Red: O)

[1] R.A. Rani et al., *Journal of Materials Chemistry A* **2** (2014) 15683-15703

Corresponding author: kvt417@alumni.ku.dk

New Cell Design for Operando Total Scattering Battery Studies

Maria Diaz-Lopez[1], Geoff Cutts[1], Phoebe Allan[2], Dean S. Keeble[1], Philip A. Chater[1] and Christine Beavers[1]

[1]Diamond Light Source, Harwell Science and Innovation Campus, Didcot, OX11 0DE, U.K

[2]School of Chemistry. Haworth Building. University of Birmingham, B15 2TT, UK

In situ electrochemical cycling combined with total scattering measurements can provide valuable structural information on crystalline and amorphous phases present during (dis)charging of batteries. *In situ* measurements are particularly challenging for total scattering experiments due to the requirement for low, constant and reproducible backgrounds. Poor cell design can introduce artefacts into the total scattering data or inhomogeneous electrochemical cycling, leading to poor data quality or misleading results. Here we present a new cell design, which is optimised to provide good electrochemical performance and excellent total scattering data quality.

A carefully designed radial geometry cell has been recently commissioned at the XPDF beamline at Diamond Light Source, which builds on previous work on radial geometry cells.[1] The total scattering signal from the component of interest (i.e., cathode or anode) can be isolated by focussing the X-ray beam on that layer of the cell. The cell consists of thin-walled quartz tubes and metal coated polyether ether ketone (PEEK) rods acting as electrodes. Such design minimizes the parasitic scattering from the cell and allows collecting high-quality total scattering and pair distribution function data, even on weakly scattering and amorphous phases, in only a few minutes.

Moreover, this cell design could be equally utilized for operando X-ray Raman Scattering or X-ray Absorption and Emission Spectroscopies. Being able to perform these bulk multi-scale measurements on the same cell, with identical electrochemistry, will provide a deeper insight into the multiple processes happening with a cycling battery.

[1] Stratford, J. M. et al. Investigating Sodium Storage Mechanisms in Tin Anodes: A Combined Pair Distribution Function Analysis, Density Functional Theory, and Solid-State NMR Approach. *J. Am. Chem. Soc*. **139** (2017), 7273.

Corresponding author: maria.diaz-lopez@stfc.ac.uk

Combination of Nanocalorimetry with Synchrotron Nano-focus X-ray Scattering and with Atomic Force Microscopy for studying semirigid-chain polymers

Azaliia Akhkiamova[1,2], Alain Panzarella[1], Marie Capron[1], Pierre Lloria[1], Peter van der Linden[1], Martin Rosenthal[1], Diego Pontoni[1], Dimitri A. Ivanov[2,3]

[1]ESRF – The European Synchrotron Radiation Facility, Grenoble, France
[2]Faculty of Fundamental Physical and Chemical Engineering, Moscow State University, Russia
[3]Institut de Sciences des Matériaux de Mulhouse – IS2M, Mulhouse, France

The complexity of thermal behavior of semirigid-chain semicrystalline polymers has been in the focus of scientific debate for a long time. In order to explain the origin of double, or, in some instances, even multiple, melting events visible in DSC of these polymers several models were put forward.

In the "multiple-crystal-population-model" it is assumed that the structure of typical semirigid-chain polymers such as poly (trimethylene terephthalate) (PTT) contain several distinct crystals populations having different thermal stability. An alternative approach assumes that, due to the thermodynamically metastable structure of such polymers, the crystals can reorganize on heating by melting and recrystallization. With the advent of fast chip calorimetry, also sometimes referred to as nanocalorimetry, it becomes possible to not only study the melting behavior of such system [1], but also the reorganization process as a response to abrupt temperature changes in real time.

In the presented work, we investigate the crystallization behavior of PTT using scanning nano-focus X-ray scattering combined with MEMS-based nanocalorimetry [2] to explore the response of the crystallization process on fast temperature variations during melt crystallization, in-situ. (Fig. 1)

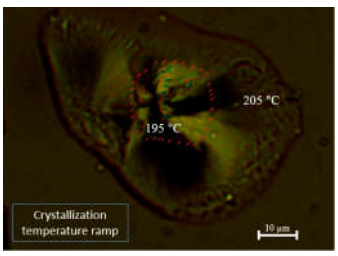

Figure 1: Polarized optical image of PTT spherulites grown from the melt. The central region delimited by the red stripes is crystallized at 195 °C. The temperature was abruptly increased to 205 °C for the crystallization of the outer region.

In a complementary approach we apply scanning force microscopy combined in-situ with nanocalorimetry in order to probe the crystallization and melting of PTT undergoing variable thermal treatment. The high-resolution and non-destructive nature of the AFM technique provides the possibility to examine the morphological organization of PTT down to the lamellar level without altering the structure. [3] Therefore, images of PTT semicrystalline structure were obtained with AFM/ Nanocalorimetry system in order to extract the size distribution of the crystalline and amorphous phases [4]. AFM represents as well a complementary experimental method providing spatial resolution comparable with SAXS and allowing to assess the influence of the X-ray exposure on the sample.

[1] A.P. Melnikov, M. Rosenthal, D.A. Ivanov *ACS Macro Lett.* **7** (12), (2018), 1426–1431
[2] A.P. Melnikov, M. Rosenthal, D.A. Ivanov *European Polymer Journal.* **81,** (2016), 598-606
[3] D.A. Ivanov, G. Bar, M. Dosiere, M. H. J. Koch. *Macromolecules.* **41**, (2008), 23
[4] A.F. Akhkiamova, et al, in preparation (2019)

Corresponding author: azaliia.akhkiamova@esrf.fr, azaliia.akhkiamova@gmail.com

PDF analysis inside a Rietveld refinement paradigm: the MAUD approach

Mauro Bortolotti, Luca Lutterotti, Evgeny Borovin
University of Trento, Department of Industrial Engineering, via Sommarive 9, 38121 Trento, Italy

The analysis of Pair Distribution Functions (PDFs) has become increasingly popular in the field of nanomaterials analysis [1]. For nanocrystalline systems, PDF is a powerful tool to characterize the short range order and is thus complementary to Powder Diffraction analysis, which models the *average* crystal structure. Although many sophysticated and widely adopted software packages exists to perform quantitative PDF analysis [2] [3], the combination of the two modeling approaches is not usually straightforward.

The Maud software [4] is mainly devoted to quantitative powder diffraction analyis by means of the Rietveld Method. Implementing the *combined analysis* approach, the software has been extended over the years to include different physical modeling other than X-Ray Powder Diffraction, namely Neutron and Electron Diffraction, Reflectivity, X-Ray Fluorescence and more recently PDF analysis. Maud approach to PDF modeling is quite different from dedicated software packages, in that the fitting is performed inside a Rietveld framework in which the standard merit function as well as the signal statistics are adjusted in such a way to simulate traditional PDF analysis. In particular, the error function is modified to include the background-subtracted intensities and to take into account the normalization to the total structure factor; error statistics, on the other hand, are also Q corrected to better estimate errors in high-Q regions of the pattern. Compton and multiple scattering, absorption, geometric and other factors are directly taken into account via the default Rietveld modeling, as well as the complete structural description. This approach allows to combine the two techniques in a complementary and even iterative way. Other advantages include the possibility to directly obtain domain size information as well as directly model multi-phase mixtures.

The presentation will report some basic methodological aspects of PDF modeling inside Maud as well as a couple of application examples related to nanocristalline sytems.

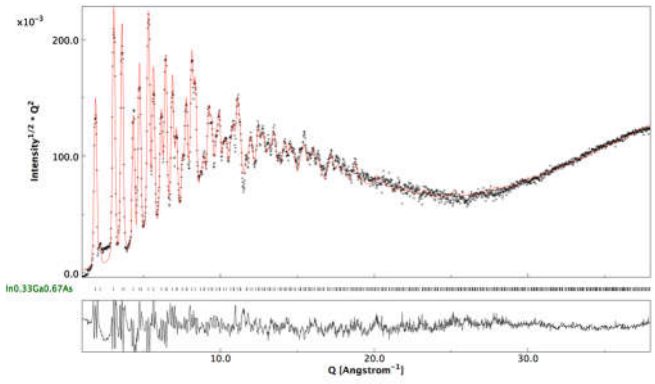

Figure 1: InGaAs PDF modeling in Maud

[1] T. Egami, S.J.. Billinge, *Mater. Today* (2003)
[2] J.N. Louwen, L. Van Eijck, T.C. Vogt, (2018)
[3] Y. Shang, P. Tian, C.L. Farrow, J. Liu, S.J.L. Billinge, W. Zhou, P. Juhas, *Acta Crystallogr. Sect. A Found. Crystallogr.* (2015).
[4] L. Lutterotti, M. Bortolotti (2003) **2** 1.

Corresponding author: mauro.bortolotti@unitn.it

Local structure strong Pt–CeO_2 interaction studied by PDF and EXAFS methods

E. A. Derevyannikova[1], T. Yu. Kardash[1,2], A. I. Stadnichenko[1,2], O. A. Stonkus[1,2], A. I. Boronin[1,2]
[1]Boreskov Institute of Catalysis SB RAS, Novosibirsk, Russia
[2]Novosibirsk State University, Russia

Pt/CeO_2 system is a key component of three-way catalysts for neutralization of exhaust gases. Although these catalysts have been widely studied, the nature of Pt active centre is still debated. In Pt/CeO_2 systems strong metal-support interaction enhances catalytic activity and thermostability substantially.[1, 2] Many researchers point out that the effect of strong metal-support interaction is due to the formation of an ionic forms of Pt.[3] However, how the ionic forms of Pt interact with ceria has not been known yet. The aim of this work was to determine the structural features of the Pt–CeO_2 interactions.

Pt–CeO_2 catalysts with different Pt loading (1-30 wt.%) were prepared by coprecipitation method, followed by calcination in air at 600°C. All the catalysts were studied using set of structural (XRD, EXAFS, PDF and HRTEM) and spectroscopic (XPS and XANES) methods. The Pair Distribution function (PDF) method were obtained at ID22 station of the ESRF. XANES and EXAFS spectra at Pt LIII-edge were collected at XAFS beamline of the ELETTRA Synchrotron.

The XRD and HRTEM data indicate that all samples are single fluorite nanosized phase. The XPS data indicate Pt^{2+} and Pt^{4+} states in the catalysts, but no Pt oxide phases were formed. In the samples with high Pt loading Pt-Pt interactions are presented in distorted phase.

PDF analysis shows the generation of new distances in the local structure of Pt–CeO_2 catalyst with high Pt loading (Figure 1). Using these distances, the models of Pt–CeO_2 local structure were proposed (Figure 1). The EXAFS modeling of the samples with different Pt loading was made. It was shown the formation of Pt single-atom forms on CeO_2 surface in the 1wt.% Pt–CeO_2 catalyst. The increase of Pt loading leads to the formation of additional PtO_x clusters in CeO_2 distorted interphase.[4]

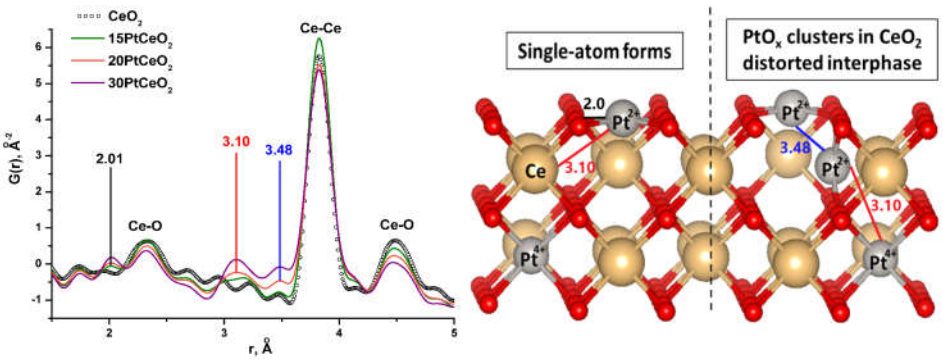

Figure 1: PDF curves and models of Pt–CeO_2 local structure.

[1] S. Gatla et al., *Catal.* **6** (2006), 6151.
[2] Y. Nagai et al., *J. Catal.* **242** (2006), 103.
[3] A. Bruix et al., *Angew. Chem.* **53** (2014), 10525.
[4] E. Derevyannikova et al., *J. Phys. Chem. C* **123** (2019) 1320.

Corresponding author: lizaderevyannikova@gmail.com

This work was supported by RFBR grant № 17-03-00754

Complex structural analysis using Non-negative matrix factorization

H. D. Hutchinson, H. S. Geddes, A. L. Goodwin
Inorganic Chemistry Laboratory, Department of Chemistry, University of Oxford, South Parks Road, Oxford, OX1 3QR

Non-negative matrix factorization (NMF), unlike other statistical analysis methods such as Principal Component Analysis (PCA), does not allow negative values in its matrices leading to a parts-based representation. This approach leads to a more intuitive result with many parts being added together to form a whole providing a more useful for physical interpretation. A good demonstration of the difference between the two uses face recognition as an example [Fig.1]. The current limitation of NMF is that convergence to a global minimum is not guaranteed and the results must be compared to PCA or other methods to check the result is correct. PCA can work out the rank (number of components) for a given data set however NMF requires to be told how many there are in order to work. By employing our own custom implementation we aim to reduce these limitations and thus make NMF a more powerful tool to study a variety of systems.

Our current project has been looking at the process of iron rusting. Although seen everywhere and studied from a industrial perspective heavily, the full structure of rust hasn't been extensively documented. Using NMF of pair distribution function data we have obtained signatures for the different components in the reaction and our working to isolate an interface previously uncharacterised [Fig. 2] along with oxide and interface growth data over the time period of study.

1.

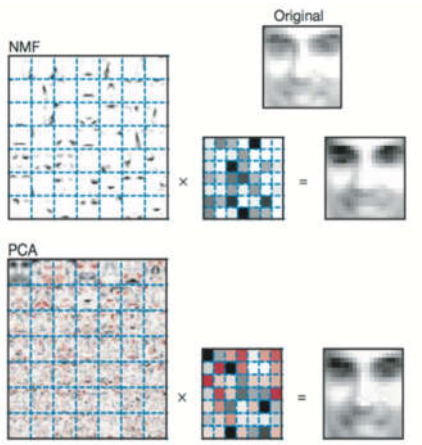

2.

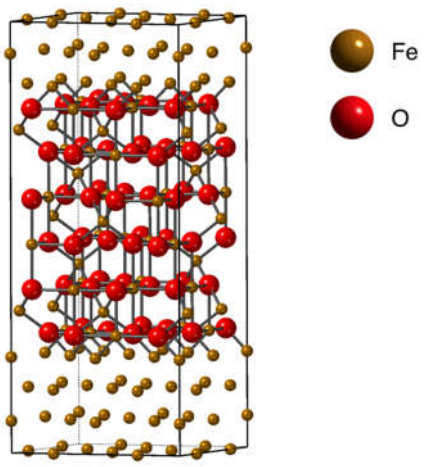

Figure 1: Non-negative matrix factorization (NMF) learns a parts-based representation of faces, whereas principal components analysis (PCA) learns holistic representations. Positive values are illustrated with black pixels and negative values with red pixels. Unlike PCA, NMF learns to represent faces with a set of basis images resembling parts of faces [1].
Figure 2: Potential Iron-Iron Oxide interface during the rusting process [2].

[1] D. D. Lee, H. S. Seung, *Nature* (1999) **401** 788-791.
[2] M. D. Forti et al., *Surface Science* (2016) **647** 55-65

Corresponding author: henry.hutchinson@new.ox.ac.uk

Real-time regeneration of a working zeolite monitored *via operando* X-ray diffraction and X-ray tomography: How coke flees the MFI framework

Georgios N. Kalantzopoulos[1], Daniel Rojo Gama[1], Dimitrios K. Pappas[1], Karl Petter Lillerud[1], Unni Olsbye[1], Pable Beato[2], Lars F. Lundegaard[2], David S. Wragg[1] and Stian Svelle[1,*].

[1]Department of Chemistry, University of Oslo, Sema Sælands vei 26, N-0371, Norway.
[2]Haldor Topsøe A/S, Haldor Topsøes Alle 1, 2800 Kgs. Lyngby, Denmark.

H-ZSM-5 is known to be the archetype zeolite for the **conversion of methanol to gasoline (MTG)** due to its three dimensional structure consisting of **straight** and **sinusoidal channels** that **enhance the diffusion of products**, improving the **resistance towards deactivation**. One of the main hurdles that a zeolite framework inherently exhibits when used as a catalyst in the MTG reaction is the loss of catalytic performance over time. The **loss of activity on H-ZSM-5** during the **MTG reaction** is reported to follow **the "burning cigar" model proposed by Haw**[1,2,3]. Exposure of the catalyst to **suitable oxidative conditions** leads to the burning of the coke, making the **acid sites accessible** for a consecutive MTG cycle. To the best of our knowledge, very little is reported regarding the evolution of the H-ZSM-5 structure during its regeneration. In this work we have used operando X-Ray diffraction and X-Ray tomography to study the local structural transformations of the H-ZSM-5 catalyst during the **removal of coke** under variable temperature oxidative conditions, resulting in **catalyst regeneration**.

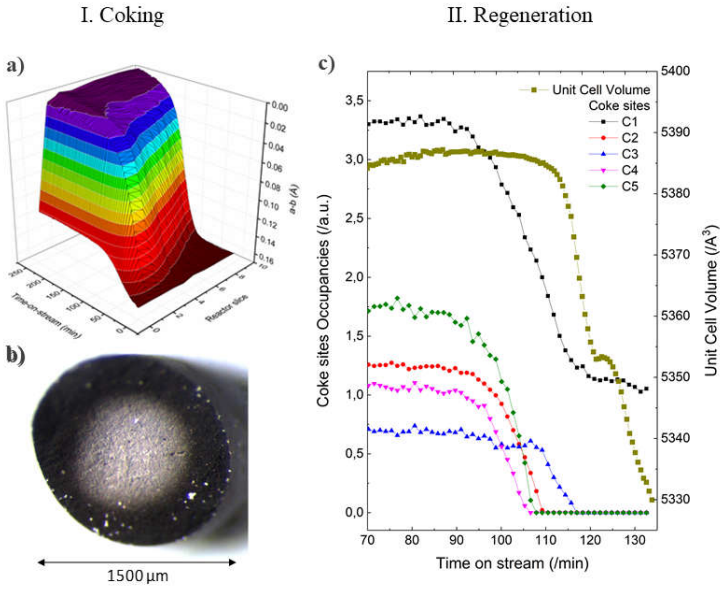

Figure 1: Evolution of the (a-b) parameter of the H-ZSM-5 unit cell over time on stream (TOS) and along the catalyst bed (**a**). Cross-section of partially deactivated zeolite catalyst extrudate (**b**). Evolution of individual coke occupancies within the ZSM-5 framework during regeneration at increasing TOS (**c**).

[1] Catal. Today. 2010, 154, 183-194.
[2] Rojo-Gama, D.; Etemadi, S.; Kirby, E. *et al*, Faraday Discuss. 2017, 197, 421-446.
[3] Haw, J. F.; Marcus, D. M. Top Catal 2005, 34, 41-48.

Corresponding author: stian.svelle@kjemi.uio.no

In situ total scattering studies during growth of thin films by magnetron sputtering

M. Roelsgaard[1,2], A.-C. Dippel[2], Bo B. Iversen[1]
[1]Department of Chemistry, Aarhus University, Aarhus, Denmark
[2]PETRA III, Deutsches Elektronen-Synchrotron DESY, Hamburg, Germany

Total scattering studies of thin films are scarce in the literature, due to experimental difficulties in obtaining satisfactory data quality in such an experiment. Typically very thick films (on the order of 100's of nanometers) are required [1], or exfoliation of the film and subsequently measured in powder-form. With recent developments at the PETRA III synchrotron source, we have successfully demonstrated thin film PDF analysis in grazing incidence geometry, see [2]. We developed a vacuum chamber for physical vapor deposition of polycrystalline thin films by magnetron sputtering [3]. By employing the sputter unit with the surface diffractometer at the P07-EH2 endstation, we show it is possible to obtain PDFs during the very early stages of film deposition with sub-second time resolution. Effectively background-free scattering from the sample is achieved by employing an in-vacuum pinhole and large polyimide X-ray exit window with a beamstop to catch the direct beam close by. Experimental details and recent results from in situ total scattering during sputter deposition will be presented (see fig. 1).

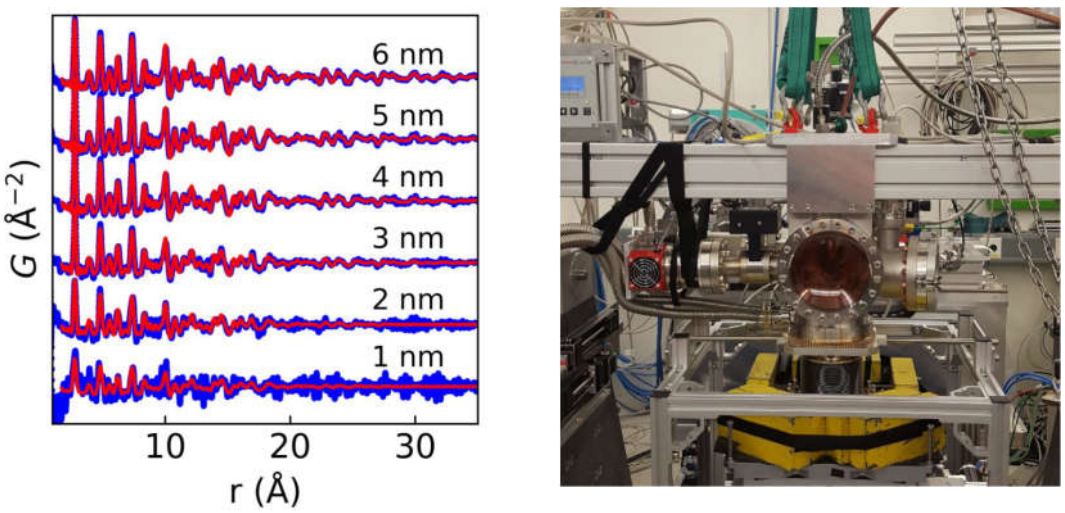

Figure 1: Left: PDFs of a polycrystalline Pt being deposited on fused quartz substrates in 1 nm steps. Right: picture of the RF magnetron sputter unit mounted at the P07-EH2 endstation at PETRA III, DESY, Hamburg, Germany.

[1] K. M. Ø. Jensen, et al, *IUCrJ* **2** (2015), 481.
[2] A.-C. Dippel, et al., *IUCrJ* (2019) accepted.
[3] M. Roelsgaard, et al., *IUCrJ* (2019) accepted.

Corresponding author: m.roelsgaard@chem.au.dk

Synthesis and photoluminescence studies of $KGdF_4:Ho^{3+}/Yb^{3+}$ phosphor

S. K. Maurya, K. Kumar
Optical Materials & Bioimaging Research Laboratory, Department of Applied Physics, Indian Institute of Technology (Indian School of Mines), Dhanbad-826004, Jharkhand (India)

Lanthanide doped/codoped upconversion phosphors have potential applications in temperature sensing, security, bioimaging etc. Fluorides usually exhibit low phonon energies and high chemical stability as compared to oxides and others. Holmium is good dopant with Ytterbium which gives intense green emission on 976 nm excitation. In the present work, $KGdF_4$ codoped Ho^{3+}/Yb^{3+} has been synthesized via hydrothermal method using oleic acid as precursor and then photoluminescence was measured. The phase formation and particle morphology have been confirmed by X-ray diffraction and field emission scanning electron microscopy studies, respectively. Downconversion emission spectra have been measured by using xenon arc lamp as excitation source. Upconversion emission spectra have also been recorded by CCD spectrometer using 976 nm excitation. In both cases emission bands were found at 491, 547 and 664 nm corresponding to the $^5F_3 \rightarrow {}^5I_8$, $^5S_2 \rightarrow {}^5I_8$ and $^5F_5 \rightarrow {}^5I_8$ transitions, respectively. Both the measurements were compared and emission mechanism was identified. Sample has shown high upconversion emission with invariance in CIE color coordinates with excitation power. More details will be discussed during the presentation.

[1] J. Zhou, Q. Liu, W. Feng, Y. Sun, F. Li. Chem. Rev. (2014) **115** 395-465.
[2] X. D. Wang, O. S. Wolfbeis, R. J. Meier. Chem. Soc. Rev. (2013) **42** 7834-69.
[3] A. Kumar, S. P. Tiwari, K. Kumar, and V. K. Rai, Spectrochim. Acta A (2016) **167** 134-141.
[4] G. Liu and J. Bernard, Spectroscopic properties of rare earths in optical materials, Springer Science & Business Media, 2006.
[5] J. E. Sansonetti William Clyde Martin, Handbook of basic atomic spectroscopic data, Journal of Physical and Chemical Reference Data 34, no. 4 1559-2259(2005)

Corresponding author: sachinram.iit@gmail.com

Spin-glass ground-state in defect-fluorite $Er_2Zr_2O_7$ and a comparison with related pyrochlore-structure $Er_2M_2O_7$ compounds

K. Vlášková[1], R.H. Colman[1], P. Proschek[1], J. Čapek[2], M. Klicpera[1]
[1]Charles University, Faculty of Mathematics and Physics, Department of Condensed Matter Physics, Ke Karlovu 5, 12116 Prague 2, Czech Republic
[2]Institute of Physics ASCR, v.v.i., Na Slovance 2, 182 21 Praha 8, Czech Republic

The rare-earth oxides of the general formula $A_2B_2O_7$, with A being a rare-earth ion and B a transition metal, have been extensively studied for their frequently exotic electronic properties. The majority of $A_2B_2O_7$ crystallizes in cubic structure of pyrochlore-type (space-group $F\,d\,{-3}\,m$, 227) and defect-fluorite-type (space-group $F\,m\,{-3}\,m$, 225). In the rare earch zirconates with general formula $A_2Zr_2O_7$, the observed structure is dictated by the size of the rare-earth ion, r_A, with $r_A/r_Z \geq 1.46$ (La - Gd) having the pyrochlore structure at room temperature and pressure, and $r_A/r_Z < 1.46$ (Tb-Lu) having a defect fluorite structure. Materials crystallising in the pyrochlore structure have been intensively studied due to the inherent magnetic frustration of the lattice that often leads to exotic electronic and magnetic properties [1]. The $Er_2M_2O_7$ pyrochlores (M = Pt, Ti, Ge, Sn, Ir) all show signs of a spin-glass-like state at low temperatures, that sometimes gives way to a magnetically ordered state on further cooling.

We recently syntheised a single crystal sample of $Er_2Zr_2O_7$, which crystallises in the defect-fluorite structure. Despite the structural differences between the pyrochlore and defect fluorite sturctures, our measurements show evidence for a spin-glass state on cooling below $T_f \sim 0.62$ K, similar to that observed in (pyrochlore) $Er_2Ir_2O_7$ ($T_f \sim 0.6$ K) [2]. The true structure of defect-fluorite and pyrochlore oxides has recently attracted attention due to discordances between local environment (total scattering) and space-averaged (Rietveld) analysis of diffraction data [3,4].

In this poster I will present our recent measurements (PXRD, dc-magnetisation, ac-susceptibility and specific heat) indicating the spin-glass transition in $Er_2Zr_2O_7$, and present a brief comparison with its pyrochlore-structure cousins. The observed similarities highlight the need for more advanced local structure analysis of this material to confirm that the similar magnetic properties arrise from different origins (geometric frustration in the pyrochlores *vs.* dilution and dissorder effects in the defect-fluorites).

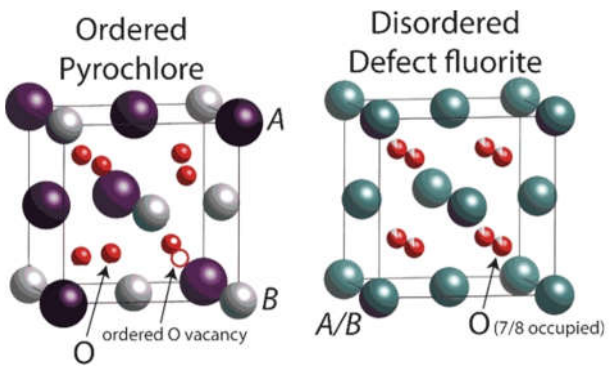

Figure 1: A comparison of the cation ordered pyrochlore structure with the disordered defect fluorite structure.

[1] J. S. Gardner, M. J. P. Gingras, and J. E. Greedan, *Rev. Mod. Phys.* **82** (2010) 53.
[2] E. Lefrançois, V. Simonet, R. Ballou, et al., *Phys. Rev. Lett.* **114** (2015) 247202.
[3] J. Shamblin, M. Feygenson, J. Neuefeind, et al., *Nat. Mater.* **15** (2016) 507.
[4] J. L. Payne, M. G. Tucker, and I. R. Evans, J. Solid State Chem. **205** (2013) 29.

Corresponding author: ross.h.colman@mag.mff.cuni.cz

Thermodynamics and crystallisation of mixed-component zeolitic imidazolate framework-8 (ZIF-8)

K. W. P. Orr, H. H.-M. Yeung, A. L. Goodwin
Inorganic Chemistry Laboratory, Department of Chemistry, University of Oxford, South Parks Road, Oxford, OX1 3QR

Zeolitic imidazolate frameworks (ZIFs) are porous materials that show promise in a range of applications including gas storage, capture, sensing, and separation, as well as medicine delivery and catalysis. [1] In order to optimize a material's use in these fields it is important to be able to tune properties such as pore size to fit a particular guest species. Tunability of pores size in mixed-metal Zn/Cd-ZIF-8 has been displayed previously [2] and work investigating the crystallisation mechanism of pure Zn-ZIF-8 has shed light on the relevant coordination equilibria present during the crystal formation. [3]

Greater understanding of the crystallisation processes governing the formation of these materials is still required, especially when it comes to looking at the crystallization of mixed component ZIFs. As such we conducted an *in situ* XRD experiment at the Diamond Light Source (UK) to study the formation of the mixed Zn/Cd analogue of the prototypical ZIF-8. We observed the presence of two phases growing simultaneously for low temperature syntheses. This was unexpected as previously these mixed Zn/Cd-ZIF-8 samples had only been reported as phase pure. This observation gave us confidence in attributing peak anisotropy of *ex situ* patterns to the presence of these two phases with different lattice parameters that were otherwise identical.

Clustering of Zn and Cd centres was recognised by employing non-negative matrix factorisation (NMF) [4] of IR data and implies a positive enthalpy of mixing for the two metals [2], as does the phase separation described above. As such we investigate the thermodynamics of formation of these materials in variable composition and temperature phase space.

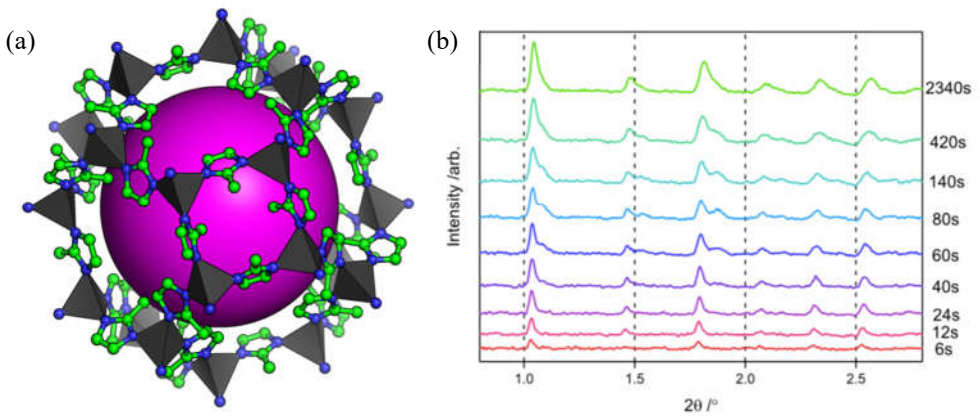

Figure 1: (a) The structure of ZIF-8: grey tetrahedra represent Zn coordinated to four N atoms on imidazolate linkers, blue spheres show N atoms, green spheres show C atoms, H atoms are omitted for clarity. The central pink sphere represents the pore. (b) *In situ* XRD patterns captured during a reaction to form mixed Zn/Cd-ZIF-8 at room temperature. The right-hand labels give the reaction time in seconds. Starting ratio of Zn:Cd was 1:1.

[1] C. Martineau-Corcos, *Curr. Opin. Colloid In.* **33**, (2018), 35-43.
[2] A. Sapnik *et al.*, *Chem. Commun*, **54** (2018), 9651-9654.
[3] H. H.-M. Yeung *et al.*, *Angew. Chem. Int. Ed.* **57** (2018), 1-7.
[4] D. D. Lee, H. S. Seung, *Nature* **401** (1999), 788-791.

Corresponding author: kieran.orr@magd.ox.ac.uk

Index of Authors